DETECTION OF LACTATE AND GLUCOSE USING GLASSY CARBON ELECTRODE COATED WITH MULTI-WALLED CARBON NANOTUBES AND NANO PARTICLES DEPOSITED ON MULTI-WALLED CARBON NANOTUBES

by
Khanh Thanh Quynh Tran

A Major Qualifying Project submitted to the Faculty of
Worcester Polytechnic Institute
in partial fulfillment of the requirements
for the Bachelor of Science Degree
in Chemical Engineering

January, 2015

Approved by

Professor Susan Zhou, Advisor

Abstract

This Major Qualifying Project aims to investigate the stability and sensitivity of modified glassy carbon electrode as well as its performance in the detection of glucose and lactate. Two types of modification are applied to the electrode. First, the glassy carbon electrode is coated with multi-walled carbon nanotubes. Second, the glassy carbon electrode is coated with Pt nanoparticles deposited on multi-wall carbon nanotubes. Voltammetry and amperometry are used to study the electrodes' performance.

Acknowledgement

Upon the completion of this Major Qualifying Project, I would like to give special thanks to individuals to whom I am greatly thankful. The two most important persons who have enormously contributed to the success of this project are Professor Susan Zhou and Ms. Zanzan Zhu.

Special thanks to Professor Susan Zhou for her excellent advising from the very first to the final steps in conducting the work leading to this project. She is an excellent project advisor in many aspects and a warm and cheerful supporter. Moreover, Ms. Zanzan Zhu, with her vast knowledge and experience on the subject, has taught me lab techniques and given me prompt instructions throughout the course. During the process of the research, her pertinent and useful advice has helped me to work, focus on the key issues, sharpen my perspectives, improve the experiment results, and greatly enhance the quality of the project overall. I really appreciate Professor Zhou's as well as Ms. Zhu's help for giving me the necessary guidance and unwavering support during the entire project.

Again, had it not been for the aforementioned individuals, this MQP would have never been possible.

Contents

List of Figures

Part I. Introduction

With the number of diabetes cases increasing at an alarming rate, it is extremely necessary and urgent to develop a functional blood glucose sensor so that diabetic patients can continuously and constantly monitor their sugar levels. Enzymatic glucose sensor has been developed to fulfill this purpose. Despite its great advantages, there are still significant drawbacks due to the presence of enzyme, which obstruct this device from performing as expected. Because the activity of enzyme is easily influenced by temperature, humidity and chemical environment, stability and reproducibility are the greatest concerns. In order to overcome these disadvantages, researchers are becoming more interested in developing glucose sensors without the presence of enzyme.

Non-enzymatic biosensors exploit electrochemical method to directly oxidize glucose. The electrochemical sensor creates a current proportional to the glucose concentration and a control circuit creates a voltage proportional to the current. Thus, scanning the resulting voltage at different currents can specify the blood glucose concentration. Direct non-enzymatic electrochemical oxidation of glucose varies considerably depending on electrode material used. In this Major Qualifying Project, glassy carbon electrodes modified with a variety of nanomaterials are experimented on to determine whether they are capable of detecting glucose. Specifically, in the first half of the project, glassy carbon electrode is coated with multi-walled carbon nanotubes and in the latter experiments, the electrode is coated with nanoparticles deposited on multi-walled carbon nanotubes. Each modified electrode is tested using 0.1M PBS solution in which the glucose concentration ranges from 0.1mM to 10mM. Voltammetry is used to measure the current resulted from corresponding potential. The Randle-Sevcik relationship states that higher bulk concentration yields higher current, which is the expected result from the voltammogram. Moreover, if the electrode is successful in detecting glucose, observable peak should be present in the voltammogram as well. Many other experiments are also carried out to confirm the results.

In the second part of the project, electrode coated with nanoparticles deposited on multi-walled carbon nanotubes is used to determine its sensitivity toward glucose and lactate individually. Two distinct methods, electrical and chemical, are applied to coat the electrode. Surprisingly, each method yields completely dissimilar performance of electrode. Similarly,

different solutions with various concentrations of the analyte are used to test the performance of the electrode. Then, the sensitivity of the two modified electrode toward glucose and lactate is compared. From the comparision, it can be determined that which modification provides better performance or what can be done to the electrode to improve its performance.

Part II. Background

1. Diabetes mellitus

Diabetes mellitus, a lifelong disease in which the level of sugar in the blood is high, is growing at an alarming rate not only in the United States but all over the world. It was estimated that 2.8% of the world population was affected by diabetes in 2000, approximately 171 million people. By 2030, however, this number is projected to more than double, with 336 million people suffering from diabetes globally **Invalid source specified.**. Figure 1 portrays that here is a significant increase in diabetes cases over the past few years. With serious effects of diabetes on patients such as blurred vision, strokes, high blood pressure, it is crucial for diabetes patients to be able to self-test and monitor blood glucose continuously in order to adjust their diets accordingly. Thus, glucose sensors are gaining more and more of researchers' interest due to the escalation in diabetes cases.

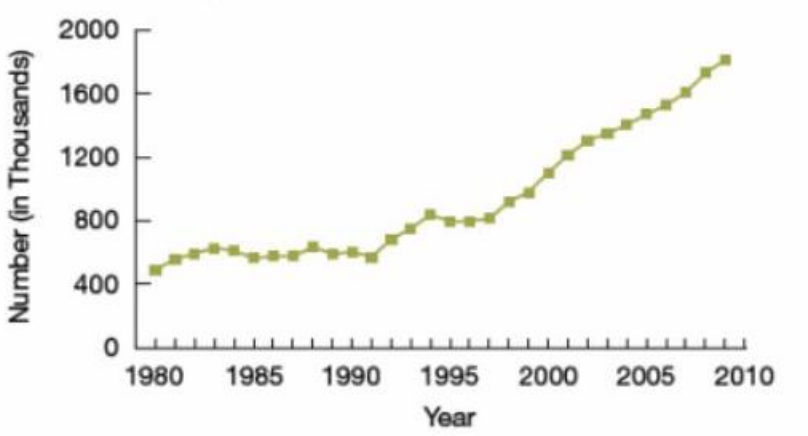

Figure 1. New cases of diagnosed diabetes among U.S. adults, aged 18-79 years, 1998-2009 (Prevention)

2. Enzymatic Biosensors

Enzymatic biosensor is an analytical device that uses enzyme as a biological element with an analyte. A physicochemical detector implemented in the device then transfers the signal resulting from the interaction into another signal that can be more easily measured and quantified. In glucose sensor, enzyme is incorporated on an electrode surface and the electrochemistry functions based on the immobilization of glucose oxidase enzyme (GOx) (Zhao and Jiang). This enzyme has relatively high selectivity, sensitivity and stability, compared to other enzymatic materials. The key component of the large protein molecule is the redox center, which is located deep within the enzyme, however, protected by a thick

protein layer. This thick protein layer in which the redox active center is embedded hinders direct electron transfer between the electrode and enzyme. In recent years, rapid advancement in development of nano and porous materials offers an electrode surface that entraps and encompasses the enzyme. As such direct electron transfer from enzyme to electrode can occur, a current corresponding to enzyme oxidation may be directly observed (Newman and Setford).

Overall, enzymatic glucose sensors remain a balance of advantages versus disadvantages of which both are significant. Stability issues that surround enzymatic systems in all fields of science greatly obstruct the development and application of enzymatic glucose sensors. Despite numerous attributes with respect to relative stability, GOx is still constrained to pH ranges of 2-8, temperatures below 44C, and ambient humidity levels (Toghill and Compton). Despite these problems, enzymatic glucose sensors are highly reliable and remain commercially unchallenged. Fabrication by mass production has been possible, allowing for single-use disposable electrodes.

3. Non-enzymatic Biosensors

Since enzymatic biosensors are frequently unstable because the activity of enzyme is easily influenced by temperature, humidity and chemical environment, non-enzymatic glucose (NEG) sensors have recently become a promising alternative candidate. With the use of non-enzymatic electrodes as glucose sensors, the oxidation of glucose in the sample is more effective as non-enzymatic electrodes strive to directly oxidize glucose through electrochemical method. Its potential has aroused an enormous amount of NEG sensor research.

The electrochemical sensor creates a current proportional to the glucose concentration and a control circuit creates a voltage proportional to the current. Thus, scanning the resulting voltage at different currents can specify the blood glucose concentration. Direct non-enzymatic electrochemical oxidation of glucose varies considerably depending on electrode material used (Bianchi, Rodrigo da Silva and Ferreira).

Thus, non-enzymatic biosensors, the fourth generation glucose sensors, have become a more ideal system. Figure 2 illustrates the development of the first three generations of enzymatic biosensors regarding the enzymatic glucose oxidation mechanisms.

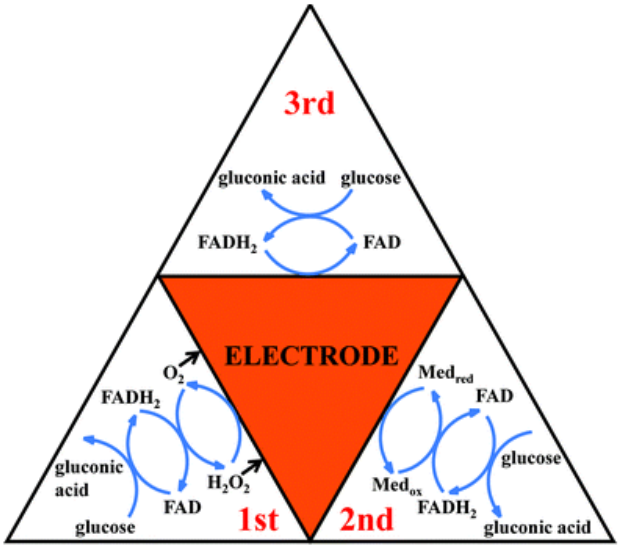

Figure 2. Summary of enzymatic glucose oxidation mechanisms, presented as first, second and third-generation sensors

The most common and serious problem of enzymatic sensors is insufficient stability originated from the nature of the enzymes, which is now overcome by using non-enzymatic biosensors instead. Moreover, for an enzyme electrode, one or more enzyme layers should be placed on the bare electrode through carefully optimized process. Because the sensitivity of these glucose sensors essentially depends on the activity of the enzymes immobilized, the reproducibility is still a critical issue in quality control. In this respect, the non-enzymatic sensor is an attractive alternative. Additionally, low oxygen concentration regulates the responses of most enzyme electrodes while NEG sensors are free from oxygen limitation. On the other hand, there are several key issues associated with NEG sensors as well. One is the mechanism of the glucose oxidation on bare platinum surface and the other is the electrocatalytic oxidation of glucose (Babu). The mechanism studies, which still need lots of further work, showed the overall kinetics of glucose oxidation is too slow to produce significant current that is resulted from electrical induction. Moreover, the fouling of the electrode contributes to the impracticality of this approach as well (Toghill and Compton). In recent advances of both enzymatic and non-enzymatic glucose sensors development, synthesis of nanomaterials seems to help to amount deficiencies of glucose sensors mentioned above.

Since porous materials offer surfaces with a high surface to volume ratio, microporous and nanoporous materials are in particular interest. It is noted that the electrochemical activity is proportional to the surface roughness. Additionally, nanoscopic electrode materials introduce surface area that is highly active for a kinetically controlled, surface bound reaction such as glucose oxidation. Indeed, this surface area is much greater than the geometric surface area of the electrode. The introduction to carbon nanotubes to enhance electrocatalysis also demonstrates the advantages posed by increasing surface area. Non-enzymatic glucose sensors consisting of metal nanoparticles/carbon nanotubes have attracted tremendous attention among scientists to explore their full potential in the industry. While carbon nanotubes provide excellent electrode transfer rate and electrocatalytic activities, metal nanoparticles enhance mass transport, offer high catalysis and increase surface areas. More details about these nanostructured materials are mentioned in the following sections.

This Major Qualifying Project aims to investigate the performance of Glassy Carbon Electrode modified with nano materials in glucose detection. It is hoped that after being modified with carbon nanotubes and/or nano particles, such drawbacks of NEG sensors mentioned above can be overcome. If successful, non-enzymatic glucose sensors would certainly be a major development in the society. Diabetic patients would be able continuously monitor their blood sugar using a device that is much more stable and reliable than enzymatic glucose sensor.

4. Glassy Carbon Electrode (GCE)

Carbon has been widely used as an electrode material in electrochemistry; yet, a new form of carbon known as "glassy" carbon has been proven to be a good indicator electrode in voltammogram. Generally carbon substrates are used due to their electronically conductive, yet electro-catalytically inert properties (Toghill and Compton). Glassy carbon is a gas- as well as liquid-impermeable material with high temperature resistance, hardness, low density, low electrical resistance, low friction, low thermal resistance and extreme resistance to chemical attack. Moreover, the low porosity characteristic of glassy carbon helps to produce a smooth surface after the electrode is polished, thus, giving rise to minimized substrate double layer current (Zittel and Miller). According to investigation by Vasil'ev et al in 1985, glassy carbon

electrodes produce a slight anodic current in response to glucose (Vasil'ev, Khazova and Nikolaeva).

5. Carbon Nanotubes (CNTs)

CNTs are tubular cylinders of carbon atoms that have extraordinary mechanical, electrical, thermal, optical and chemical properties. The cylindrical graphene sheets of nano dimensions are highly conductive, and substantially increase the surface area of a planar electrode whilst retaining high chemical and physical stability. Carbon nanotubes (CNTs) are promising materials for sensing applications due to several intriguing properties. In particular, their large length-to diameter aspect ratios provide for high surface-to-volume ratios. Moreover, CNTs have an outstanding ability to mediate fast electron-transfer kinetics for a wide range of electroactive species (Balasubramanian and Burghard).

CNTs are classified in following two types: single-walled CNTs (SWCNTs) and multi-walled CNTs (MWCNTs). Comprised entirely of carbon, the structure of pure SWCNT can be visualized as rolled-up tubular shell of graphene sheet which is made up of benzene type hexagonal rings of carbon atoms. A MWCNT is a stack of graphene sheets rolled up into concentric cylinders. Each nanotube is a single molecule composed of millions of atoms and the length of this molecule can be tens of micrometers long with diameters as small as 0.7 nm (Meyyappan, Delzeit and Cassell). Figure 3 illustrates molecular representations of SWCNT and MWCNT.

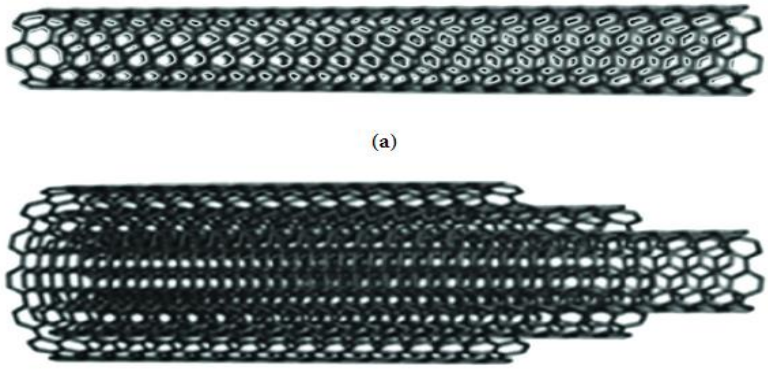

Figure 3. Molecular representations of (a) SWCNT and (b) MWCNT (Donaldson, Aitken and Tran)

Comparison between SWCNTs and MWCNTs is presented in Table 1 (Abrahamson, Wiles and Rhoades) (Hrlekar, Yamagar and Garse).

Table 1. Comparison between SWCNT and MWCNT

SWCNTs	MWCNTs
• Single layer of graphene. • Catalyst is required for synthesis. • Bulk synthesis is difficult as it requires proper control over growth and atmospheric condition. • Not fully dispersed, and form bundled structures. • Resistivity usually in the range of 10^{-4} – 10^{-3} Ωm. • Purity is poor. Typical SWCNT content is as-prepared sample by chemical vapor deposition (CVD) method is about 35-50 wt%. However high purity up to 80% has been reported by using arc discharge synthesis method. • A chance of defect is more during functionalization. • Characterization and evaluation is easy. • It can be easily twisted and are more pliable.	• Multiple layer of graphene. • Can be produced without catalyst. • Bulk synthesis is easy. • Homogeneously dispersed with no apparent bundled formation. • Resistivity usually in the range of 1.8 * 10^{-5} – 6.1*10^{-5} Ωm. • Purity is high. Typical MWCNT content in as-prepared samples by CVD method is about 35-90wt%. • A chance of defect is less, especially when synthesized by arc-discharged method. • It has very complex structure. • It cannot be easily twisted.

'Bare' or unmodified glassy carbon electrodes have a series of disadvantages, such as poor stability and sensitivity, large response time, low reproducibility and a high overpotential for electron transfer reactions. Yet, CNTs can overcome most of these disadvantages owing to their ability to undergo fast electron transfer and the resistance of CNT-modified electrodes to surface fouling. Furthermore, the CNT modified electrodes have shown greater long term stability than is observed on a modified GCE, due to the strong adherence of the enzyme to the carboxylated open ends of the nanotubes.

The simplest route to CNT-modified electrodes is to cast a solution of CNTs onto a GCE. Since CNTs are insoluble in most solvents, ultrasonication is required during preparation in order to effectively disperse the tubes. Electrodes have been fabricated by dispersing CNTs in a phosphate buffer or concentrated sulfuric acid, and subsequent spin-casting onto a polished GCE. The dispersion of CNTs in aqueous solution can be facilitated by an appropriate surfactant (Wang, Deo and Musameh).

The direct growth of CNTs onto GCE has been proven to be an effective method for the fabrication of CNT-modified electrodes. This approach not only improves the electrical contact between the active sensing material (CNTs) and the conducting substrate, but also ensures that the sensor is free of impurities originating from the surfactant or the binder (Tang, Chen and Yao). Another advantage of direct growth is the ability to fabricate arrays of CNT nanoelectrodes (Li, Ng and Cassel). Since the edges of the nanotubes are exposed, electrodes with vertically aligned CNT arrays exhibit the highest electrocatalytic activity coupled with fast electron transfer (Li, Cassell and Delzeit) (Gao, Dai and Wallace).

6. Metallic Nanoparticles

Nanoparticles are particles between 1 and 100 nanometers in size. Metallic nanoparticles have fascinated scientist for over a century and are now heavily utilized in biomedical sciences and engineering. They are a focus of interest because of their huge potential in nanotechnology. Today these materials can be synthesized and modified with various chemical functional groups which allow them to be conjugated with antibodies, ligands, and drugs of interest and thus opening a wide range of potential applications in biotechnology, magnetic separation, and preconcentration of target analytes, targeted drug delivery, and vehicles for gene and drug delivery and more importantly diagnostic imaging. Transition metals such as gold, platinum, palladium, copper, silver and nickel are well-known for their high catalytic activity. They have been widely utilized to enhance the performances of electrodes made of carbonaceous materials, and, in particular, to increase their sensitivity towards a specific analyte. However, electrode coatings made of thin metallic films are disadvantageous due to the complicated interplay between the thickness of the film and the sensor response. In addition, such electrodes are prone to severe poisoning or corrosion. A promising alternative is the use of metallic nanoparticles, which help to increase the catalytic activity and provide a larger surface area, thereby imparting a higher sensitivity to the sensing electrode. Furthermore, because nanoparticles can be easily modified with a wide range of biomolecules, they enable the fabrication of biosensors with a plethora of sensing possibilities.

Biosensing electrodes composed of CNTs have been modified with metallic nanoparticles via the adsorption of preformed nanoparticles, or via electro-deposition from metal salt solutions. The latter method is especially attractive since it allows precise control over the

degree of modification in a reproducible manner (Balasubramanian, Burghard and Kern) (Day, Unwin and Wilson).

7. Cyclic Voltammetry (CV)

7.1 Introduction

Cyclic voltammetry is an electrochemical technique which measures the current that develops in an electrochemical cell under conditions where voltage is in excess of that predicted by the Nernst equation. CV is performed by cycling the potential of a working electrode, and measuring the resulting current.

The potential of the working electrode is measured against a reference electrode which maintains at a constant potential, and the resulting applied potential produces an excitation signal such as that of Figure 3 (Kissinger and Heineman).

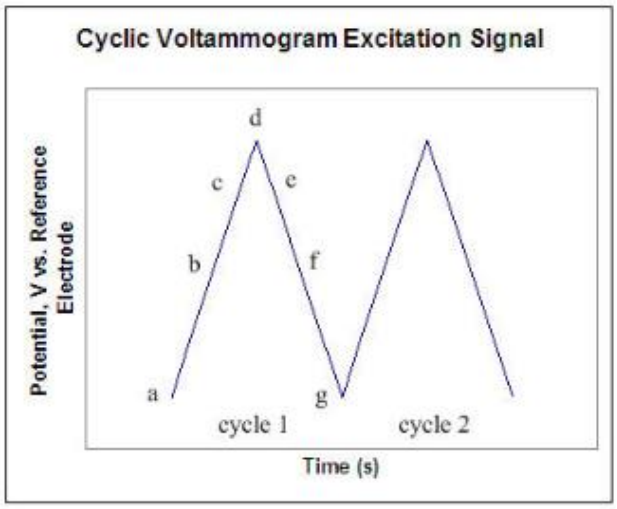

Figure 4. CV excitation signal

In the forward scan of Figure 3, the potential first scans negatively, starting from a greater potential (a) and ending at a lower potential (d). The potential extrema (d) is call the switching potential, and is the point where the voltage is sufficient enough to have caused an oxidation or reduction of an analyte. The reverse scan occurs from (d) to (g), and is where the potential scans positively. Figure 1 shows a typical reduction occurring from (a) to (d) and an oxidation occurring from (d) to (g). It is important to note that some analytes undergo oxidation first, in

which case the potential would first scan positively. This cycle can be repeated, and the scan rate can be varied. The slope of the excitation signal gives the scan rate used.

A cyclic voltammogram is obtained by measuring the current at the working electrode during the potential scans (Kissinger and Heineman). Figure 4 depicts a cyclic voltammogram resulting from a single electron reduction and oxidation. Consider the following reversible reaction:

$$M^+ + e^- \leftrightarrow M$$

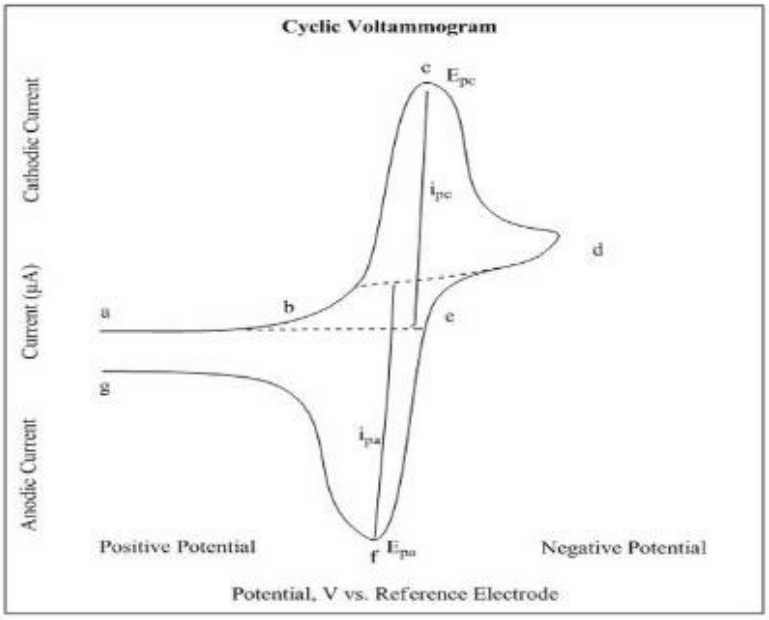

Figure 5. Cyclic voltammogram of single electron oxidation-reduction

In Figure 4, the reduction occurs from (a) the initial potential to (d) the switching potential. In this region the potential is scanned negatively to cause a reduction. The resulting current is called cathodic current (I_{pc}). The corresponding peak potential occurs at (c), and is called the cathodic peak potential (E_{pc}). The E_{pc} is reached when all of the substrate at the surface of the electrode has been reduced. After the switching potential has been reached (d), the potential scans positively from (d) to (g). This results in anodic current (I_{pa}) and oxidation to occur. The peak potential at (f) is called the anodic peak potential (E_{pa}), and is reached when all of the substrate at the surface of the potential has been oxidized.

7.2 Concentration Profiles at the Electrode Surface

In an unstirred solution, mass transport of the analyte to the electrode surface occurs by diffusion alone (Skoog, Holler and Crouch). Fick's Law for mass transfer diffusion relates the distance from the electrode (x), time (t), and the reactant concentration (C) to the diffusion coefficient (D).

$$\frac{\partial C}{\partial t} = D\,\frac{\partial^2 C}{\partial x^2}$$

During a reduction, current increases until it reaches a peak: when all M+ exposed to the surface of an electrode has been reduced to M. At this point, additional M+ to be reduced can travel by diffusion alone to the surface of the electrode, and as the concentration of M increases, the distance M+ has to travel also increases. During this process the current which has peaked, begins to decline as smaller and smaller amounts of M+ approach the electrode. It is not practical to obtain limiting currents I_{pa}, and I_{pc} in a system in which the electrode has not been stirred because the currents continually decrease with time (Skoog, Holler and Crouch).

In a stirred solution, a Nernst diffusion layer about 10^{-2} cm thick lies adjacent to the electrode surface. Beyond this region is a laminar flow region, followed by a turbulent flow region which contains the bulk solution (Skoog, Holler and Crouch). Because diffusion is limited to the narrow Nernst diffusion region, the reacting analytes cannot diffuse into the bulk solution, and therefore Nernstian equilibrium is maintained and diffusion-controlled currents can be obtained.

Regarding to the peak current, the Randle-Sevcik relationship states that:

$$I_p = k\,n^{3/2}\,A\,D^{1/2}\,C^b\,v^{1/2}$$

where k = 2.72 x 10^5; n is the number of moles of electrons transferred per mole of electroactive species (e.g., ferricyanide); A is the area of the electrode in cm^2; D is the diffusion coefficient in cm^2/s; Cb is the solution concentration in mole/L; and υ is the scan rate of the potential in V/s (Skoog, Holler and Crouch). In latter experiments, as other variables are held constant, the peak current solely depends on the bulk concentration (Cb) of the analyte in solvent and the square root of the scan rate ($v^{1/2}$).

Part III. Methodology

1. Working electrode polishing

1.0 µm alumina polish is mixed with deionized water on a texmet pad and the glassy carbon electrode surface is moved in this mixture in a circular motion to ensure uniform polishing (Figure 5). After the defects have been removed, the polishing continues with successively smaller particle size polish – 0.3 µm alumina powder. Each stage usually takes several minutes, depending upon the state of the electrode. Once polishing has been completed, the electrode surface must be rinsed thoroughly with deionized water to remove all traces of the polishing material. The water should be sprayed directly onto the electrode surface. After the surface has been rinsed, electrode polished with alumina is sonicated subsequently in ethanol, acetone and finally deionized water for about 10 minutes each to ensure complete removal of the alumina particles (Figure 6).

Figure 7. GCE is being polished using alumina polish.

Figure 6. GCE is being sonicated.

2. Glassy carbon electrode coated with multi-walled carbon nanotubes

2.1 Synthesis of multi-walled carbon nanotubes

12M HCl solution is added to fullerene CNT (multi-walled, 3-20 nm OD, 1-3nm ID, 0.1-10 µm long, 95%) and this mixture is sonicated for about 20 minutes. Next, vacuum suction

filtration is applied to separate the powder from the acid. After all of the powder has been filtered out, it is rinsed with deionized water multiple times (while filtration still goes on) until the pH of the leaving water is the same as that of deionized water. This step is to ensure that no acid remains in the powder. The filter paper with MWCNTs on it is put in cubicle which is then placed in the oven at 85℃ for at least one hour so that the MWCNTs powder is dried. After the powder is dry, the cubicle is taken out of the oven and placed in the burner at 350℃ for two hours. Finally, collect MWCNTs powder from the cubicle and store it properly for future use.

2.2 Preparation of glassy carbon electrode modified with multi-walled carbon nanotubes

Mix 5mg of the prepare MWCNTs with 2mL of CHI solution (1% CH3COOH). This mixture is then sonicated for about 20 minutes to ensure that it is well-mixed. Use a pipette to add a few drops of the mixture on the polished surface of GCE; the glassy carbon area on the surface of the GCE has to be completely covered with the MWCNT mixture. Let the GCE dry (overnight preferably) before it is used for experiment.

3. Deposition of Pt nanoparticles on multi-walled carbon nanotubes (PtNPs-MWCNTs)

3.1 Electrochemical method

The GCE surface coated with MWCNTs (step 2.2) is placed in 0.3mM K_2PtCl_6 in 0.5M H_2SO_4 and cyclic voltammetry is run.

3.2 Chemical method

3.2.1 Synthesis of Pt nanoparticles

5mg of nitrogen-doped carbon nanotubes (NCNTs) is dispersed in 10mL deionized water by ultrasonic vibration for 0.5h. Then 0.5mL of 0.0386M H_2PtCl_6 is added to the NCNTs suspension with continuous stirring for 2h. During this period, the charged $PtCl_6^{2-}$ is anchored on the surface of NCNT through electrostatic interaction. Next, 1.0 mL of 0.07M $NaBH_4$ aqueous solution is slowly dropped into this mixture and vigorously stirred at room temperature for 12h. Vacuum suction filtration is performed to filter out the NCNTs and the powder is rinsed with deionized water until the pH of the water that has passed through the filtered powder is the same as that of the pure water. After the powder is dried in heater at 80℃, it is collected and stored properly for future use.

3.2.2 Preparation of glassy carbon electrode modified with Pt nanoparticles deposited on multi-walled carbon nanotubes

The powder synthesized and collected from previous step is mixed with ethanol. The mixture is sonicated for 5 minutes to make sure it is well-mixed. Use a pipette to add a few drops of the mixture on the polished surface of GCE; the glassy carbon area on the surface of the GCE has to be completely covered with the PtNPs-MWCNTs mixture. Let the GCE dry (overnight preferably) before it is used for experiment.

Part IV. Results and Discussion

First of all, each glassy carbon electrode is polished carefully to remove adsorbed species from the working electrode surface, which is then capable of generating reproducible results. It is critical that the transfer of electrons between the electrode surface and molecules in the interfacial regions is not hindered by the microstructure and roughness of the electrode surface. Hence, multiple trials of polishing are performed to ensure that best results are achieved. After the electrodes are polished, cyclic voltammetry of each electrode is run with the analyte being potassium ferricyanide and the solvent being 0.1M potassium chloride. As shown in Figure 8, the more the electrodes are polished, the closer the separation of the peak potentials in the

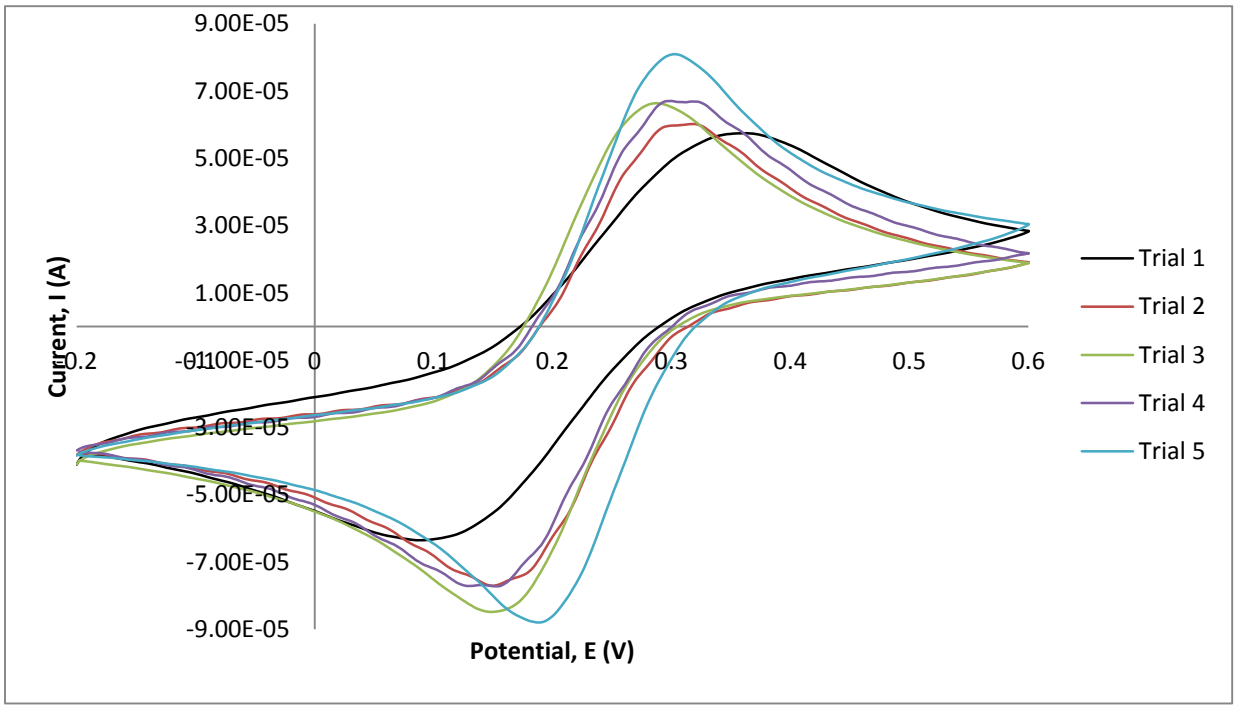

Figure 8. Cyclic voltammogram of unmodified GCE #1 in $K_3Fe(CN)_6$

cyclic voltammogram are. After five trials of polishing, the separation between the reduction and oxidation peaks of both electrodes is less than 0.1V; therefore, the glassy carbon electrode is ready to be experimented on.

Next, each electrode is coated with multi-walled carbon nanotubes (MWCNTs) and cyclic voltammetry is run on each electrode with the analyte being glucose and the solvent being 0.01M phosphate buffered saline (PBS). This process serves to assess whether and how well glassy carbon electrode coated with carbon nanotube is able to detect the presence of glucose in the solution. The experimental potential window is from -0.2V to 1.2V and the scan rate is 0.1V/s. The optimal number of cycles is determined to be 10 considering the stability of the voltammograms after 10 scans. Various concentrations of glucose in 0.01M PBS are used, specifically 1mM, 5mM and 10mM of glucose in 0.01M PBS. As suggested by the Randle-Sevcik relationship mentioned in the background section, the peak current increases as the concentration of the analyte in solvent increases (if the remaining variables are held constant).

According to Figure 9, as the scan rate is constant at 0.01V/s, the corresponding current increases as the concentration of glucose is increases from 1mM to 5mM and then 10mM. Moreover, it is observed that with the experimental potential window ranging from -0.2V to 1.2V, the minimum and maximum points occur at -0.2V and 1.2V, respectively, which are the

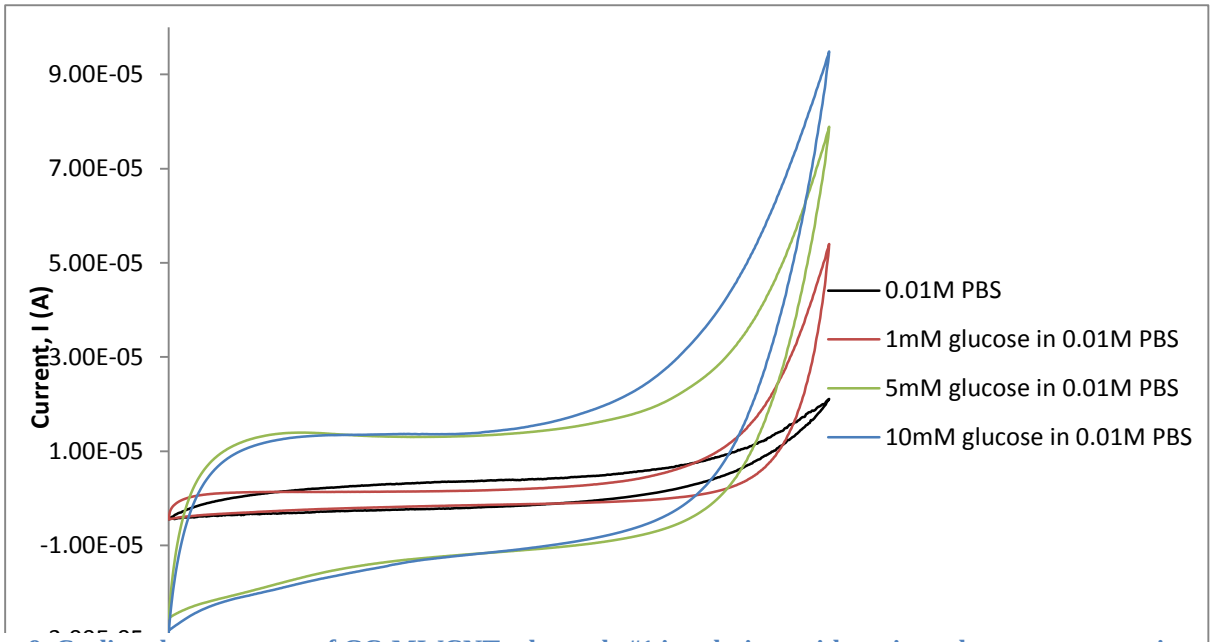

Figure 9. Cyclic voltammogram of GC-MWCNTs electrode #1 in solutions with various glucose concentrations in 0.01M PBS, scanned at 0.01V/s

two ends of the potential window. Same conditions are applied on both GCEs and they both show the same results.

However, there are no peaks (as described in Figure 4) occurring in the given range of the above graph. Several trials are repeated and the resulting graphs are shown in the Appendix. Yet, same results are obtained; no peaks are observed. This unexpected result may be due to several reasons:

- Concentration of glucose is not significant enough to be detected.

- Scan rate is too low.

Nevertheless, the concentration of glucose in solutions ranges from 0 to 10mM, and for each of the concentration, no observable peak is present. As a result, the assumption that low glucose concentration leads to the failure of the electrode is eliminated. Hence, different scan rates will be applied to test the effect of scan rate of the resulting current. Moreover, from the first experiment, it is confirmed that while other variables are held constant, the current is proportional to the bulk concentration. Moreover, the two modified electrodes also function properly as expected. In latter experiments, the scan rate is varied. Specifically, cyclic voltammetry is run on the two multi-walled carbon nanotubes coated GCEs in solutions with various concentrations of glucose (1mM, 5mM and 10mM) in 0.01M PBS at different scan rates (0.03V/s, 0.05V/s, 0.07V/s and 0.09V/s). Figures 9 shows cyclic voltammogram of the modified GCE in electrolyte solutions scanned at 0.03V/s. The trend is similar to the previous voltammogram, that is, the current is higher if the bulk concentration of glucose in solvent is higher. Yet, since the scan rate is increased from 0.01V/s to 0.03V/s, the range of the peak current also expands, which agrees with the Randle-Sevcik relationship. Again, no peak is observed.

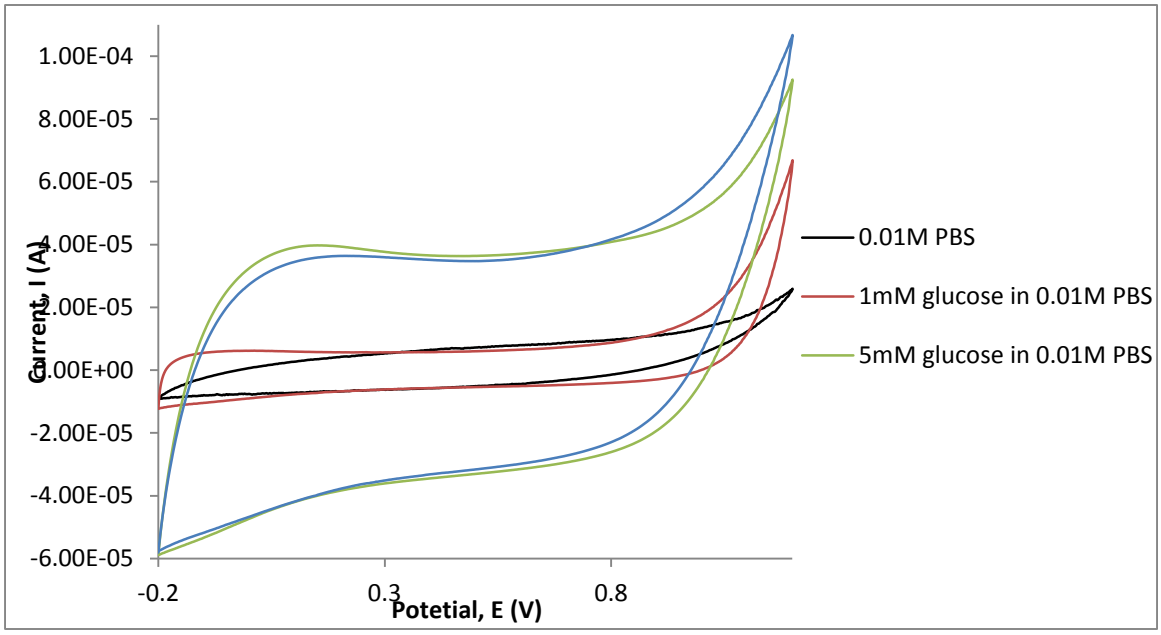

Figure 11. Cyclic voltammograms of GC-MWCNTs electrode #1 in solutions with various glucose concentrations in 0.01M PBS, scanned at 0.03V/s

Correspondingly, figures 12 shows cyclic voltammogram of the modified GCE in solutions with various concentrations of glucose scanned at 0.05V/s. Figures 13 displays similar content with the scan rate being 0.07 V/s and the scan rate in figure 14 is 0.09V/s. With the difference in scan rate, it is expected that the range of the current in the voltammograms differ between figures; yet, the location of the minimum and maximum points as well as the relationship between the current and the concentration of the analyte should remain the same.

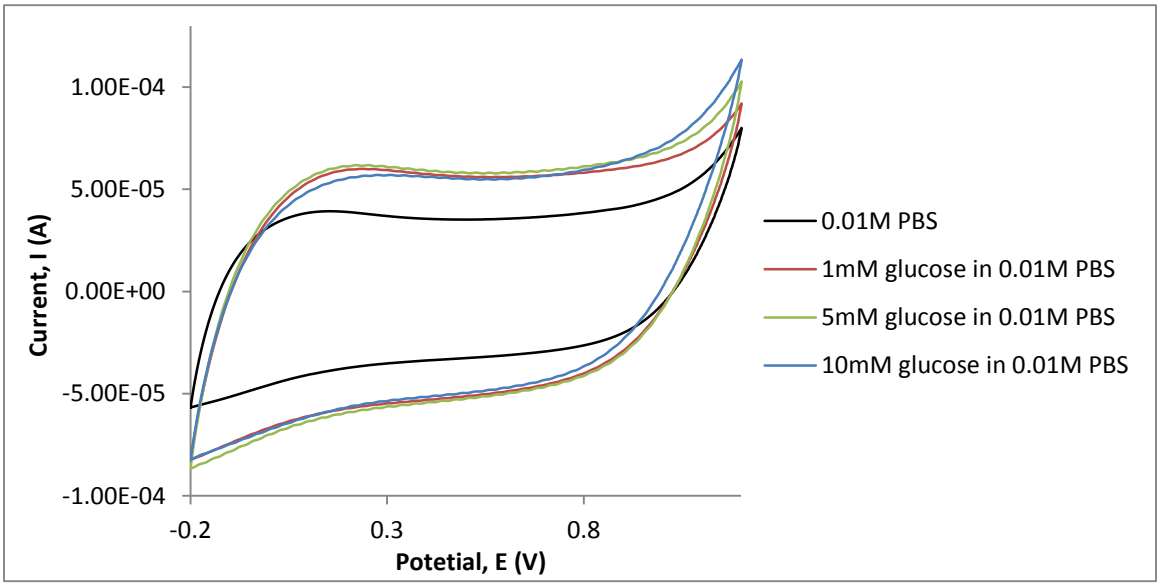

Figure 10. Cyclic voltammogram of GC-MWCNTs electrode #1 in solutions with various glucose concentrations in 0.01M PBS, scanned at 0.05V/s

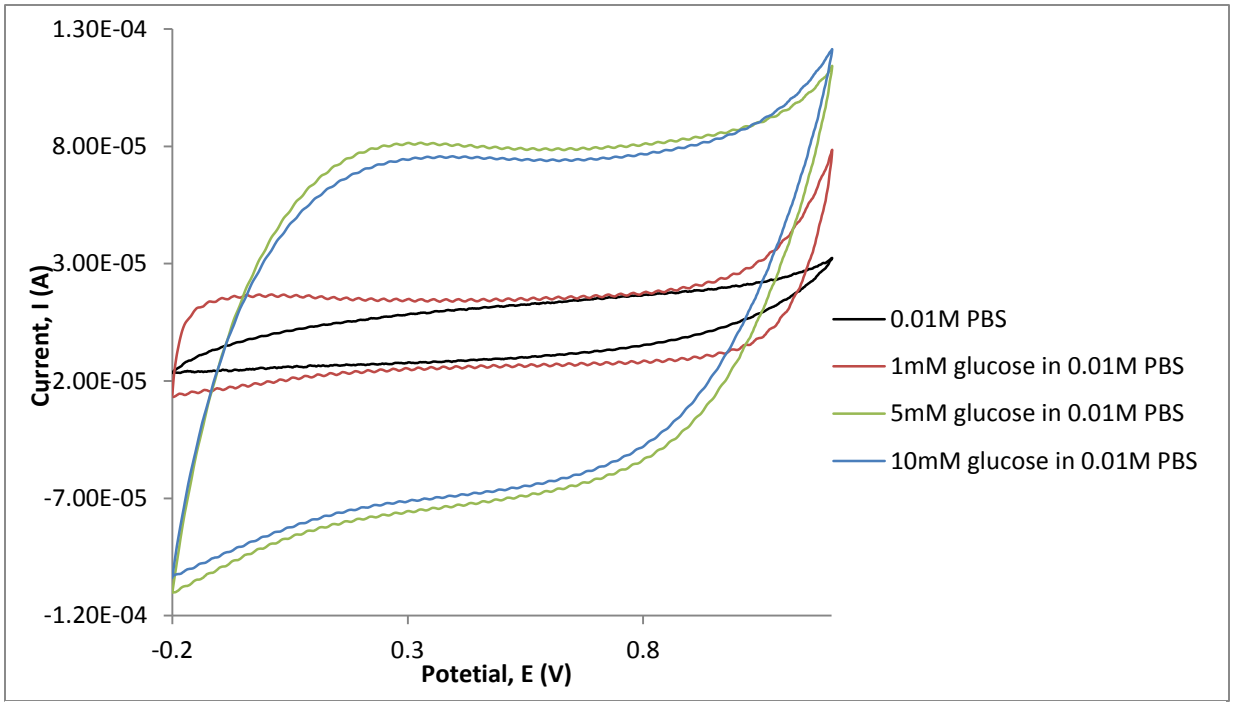

Figure 12. Cyclic voltammogram of GC-MWCNTs electrode #1 in solutions with various glucose concentrations in 0.01M PBS, scanned at 0.07V/s

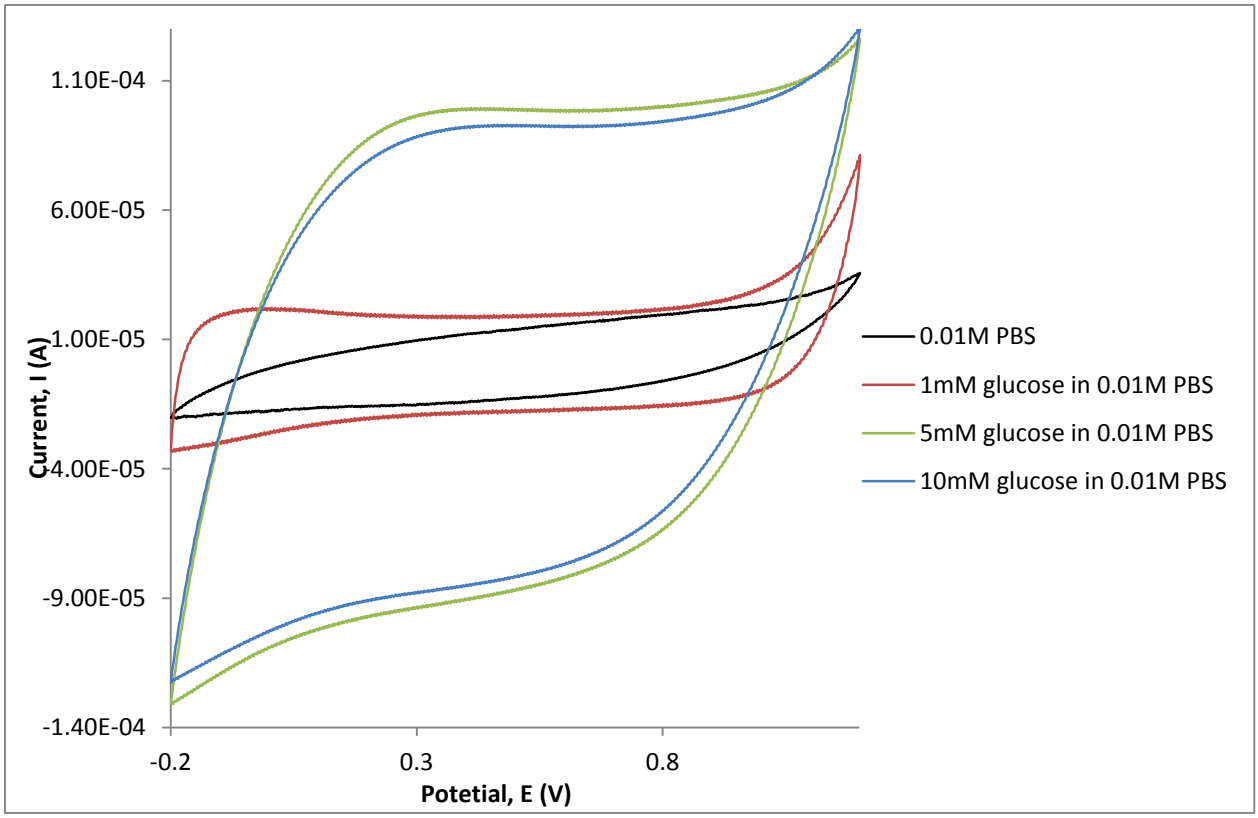

Figure 13. Cyclic voltammogram of GC-MWCNTs electrode #1 in solutions with various glucose concentrations in 0.01M PBS, scanned at 0.09V/s

Figures 9 – 13 all portray a unified trend, which is that as the bulk concentration increases, the current increases. The oxidation process occurs from the initial potential (-0.2V) to the switching potential (1.2V) and in this region, the potential is scanned positively to cause an oxidation and the anodic peak potential occurs at 1.2V. This potential is reached when all of the substrate at the surface of the electrode has been oxidized. After the switching potential is reached, the potential scans negatively from 1.2V to -0.2V and the cathodic minimum potential occurs at -0.2V. In other words, the minimum and maximum potentials occur at the two ends of the potential window.

Again, no peak is observed in any of the above experiments, which indicate that glassy carbon electrode modified with carbon nanotubes failed to detect the presence of glucose in solutions. Though the electrode is not successful in glucose detection, lactate is now used as an analyte in 0.1M PBS solution.

Next, similar procedures are applied to the subsequent experiment; the only difference is that the analyte in the solvent is changed from glucose to lactate. This procedure is meant to test whether as well as how well the glassy carbon electrode coated with multi-walled carbon nanotube is capable of detecting lactate in the solution. The concentrations of lactate in 0.01M PBS are 1mM and 5mM, and scan rate of the cyclic voltammetry also ranges from 0.01V/s to 0.09V/s. It is expected that as lactate concentration increases, the current also increases and there are cathodic and anodic peaks observed in the given range. However, it remains unknown where in the potential window the peaks will occur.

Figures 14 shows the cyclic voltammograms of the modified GCE in solutions with various lactate concentrations, and they agree with some of the predictions. The resulting current is higher if the lactate concentration is higher. It is also observed in both cases that the minimum and maximum potentials occur at the two ends of the potential window (-0.2V and 1.2V), which is similar to the previous case when the analyte is glucose. This result is again confirmed when the scan rate ranges from 0.01V/s and 0.09V/s (Figures are shown in Appendix). However, the biggest goal is that the graph can show whether there is lactate

present in the solution or not. Since there is no peak occurring in the range, no conclusion regarding the presence of lactate can be made.

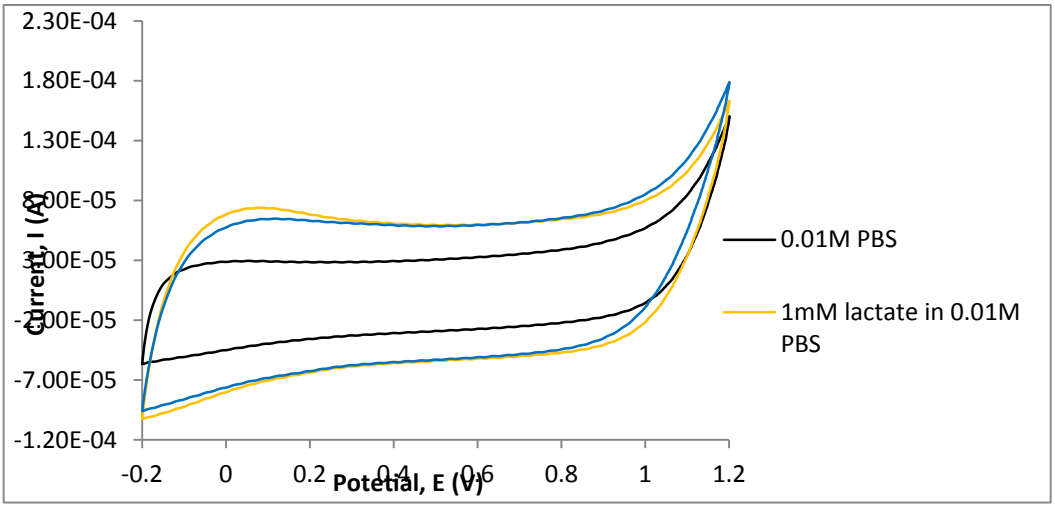

Figure 14. Cyclic voltammogram of GC-MWCNTs electrode #2 in solutions with various lactate concentrations in 0.01M PBS, scanned at 0.03V/s

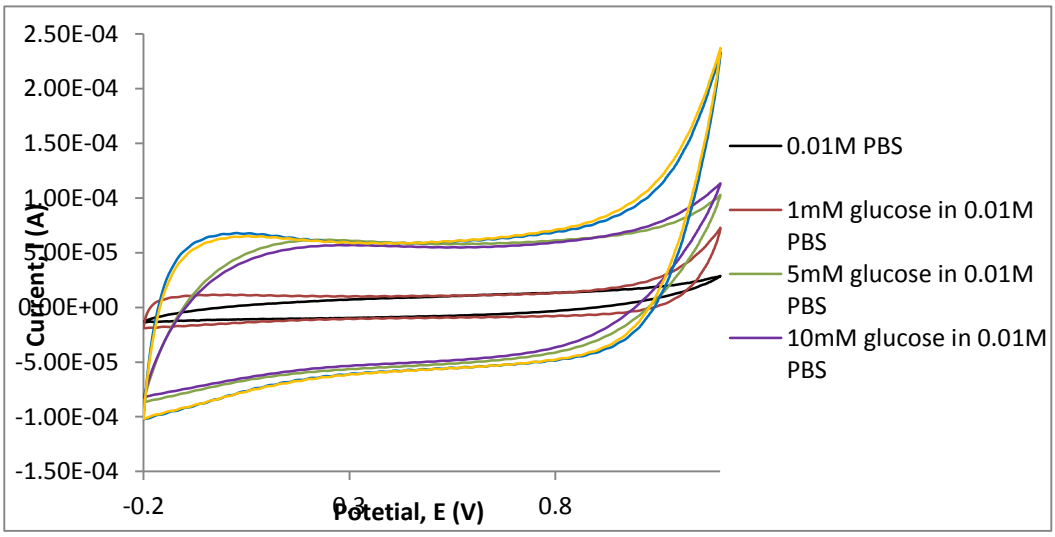

Figure 15. Cyclic voltammogram of GC-MWCNTs electrode #1 in solutions with various glucose and lactate concentrations, scanned at 0.05V/s

In previous figures, it is concluded that the current is directly proportional to the concentration of the analyte in the solvent. Moreover, when the analyte in the solvent is lactate, the locations of the peaks are also found, which are at potentials of -0.2V and 1.2V. Nevertheless, although two different analytes, glucose and lactate, are used, the minimum and maximum potentials occur at the same positions, which are at -0.2V and 1.2V. Figures 15 and 16 combine the cyclic voltammograms scanned at 0.05V/s of glassy carbon electrode 1 and 2 coated with multi-walled carbon nanotubes in both glucose and lactate solutions, respectively.

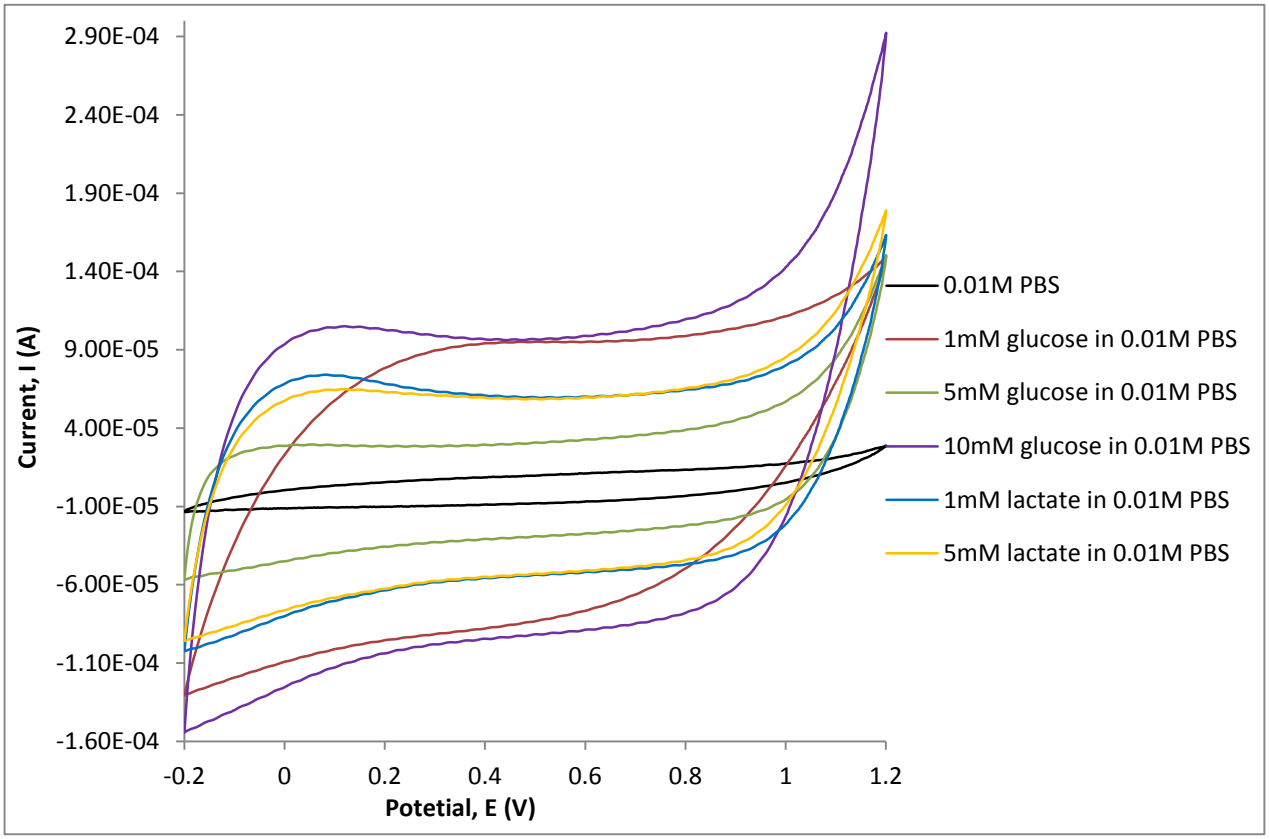

Figure 16. Cyclic voltammogram of GC-MWCNTs electrode #2 in solutions with various glucose and lactate concentrations, scanned at 0.05V/s

It is observed from both figures that the current when the analyte being lactate is much higher than that when the analyte being glucose, regardless of the bulk concentration. However, despite the significant difference in current, all of the minimum and maximum potentials occur at the same position; therefore, it is not possible to detect glucose or lactate individually, let alone simultaneously detect lactate and glucose using glassy carbon electrode coated with multi-walled carbon nanotubes. If the glassy carbon electrode coated with multi-walled carbon nanotube is to simultaneously detect if glucose, lactate or both is present in a solution, it would fail to do so. First of all, when the glassy carbon coated with multi-walled carbon nanotube is placed in the solution in which both lactate and glucose are present and cyclic voltammogram is run, no peak occurs. Only minimum and maximum potentials are observed, one at each end of the potential window. Nonetheless, it is impossible to tell that the minimum and maximum points represent which substance, lactate or glucose, because as

determined from previous experiments, these points when the analyte being glucose or lactate occur at the same location.

Amperometry is also run on both modified electrodes. This method is to test if the modified glassy carbon electrodes function properly. Since amperometry is the detection of ions in a solution based on electric current or changes in electric current, as the concentration of the analyte increases, the current also increases.

Figure 17 displays the amperometry of modified glassy carbon electrode #1 in solutions with various concentrations of glucose in 0.01M PBS. As shown in figure 17, the current is negative, which indicates the direction of the current. Hence, the graph of the magnitude of the current versus time is actually the mirror image of the below graph over the x-axis. Therefore, with the line representing the current when the GCE is in the solution of 10mM glucose in 0.01M PBS (the blue line in figure 25) being the lowest, its current is actually the largest. Similarly, when the concentration of glucose in the solvent is 1mM, which is the lowest concentration, the current is also the lowest.

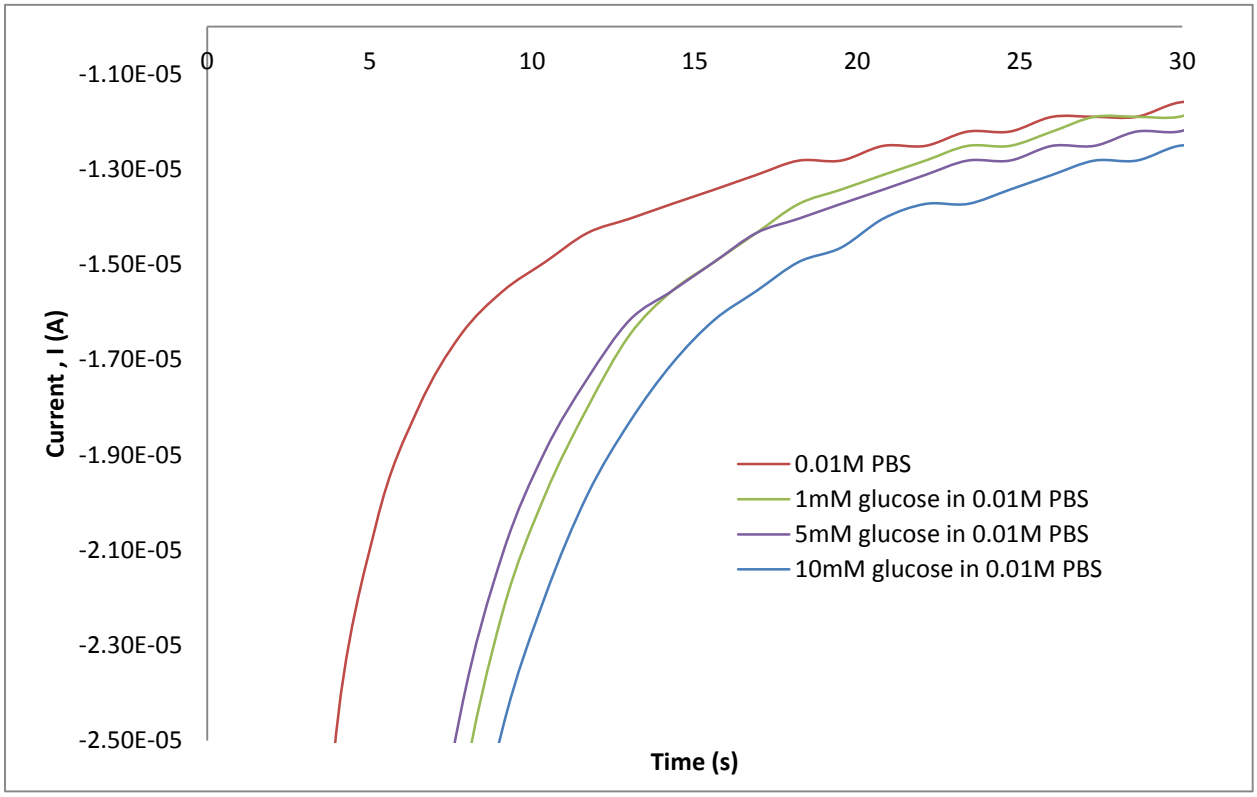

Figure 17. Amperometry of GC-MWCNTs electrode #1 in solutions with various glucose concentrations in 0.01M PBS

Figure 18 depicts the amperometry of modified glassy carbon electrode #2 in solutions with various concentrations of glucose in 0.01M PBS. Again, the trend is as expected. The line representing the current when the bulk concentration is 10mM (the blue line in figure 18) is the lowest and the line representing the current when the bulk concentration is 1mM (the red line in figure 18) is the highest. Hence, when these lines are flipped over the x-axis due to the negative current, the current when the bulk concentration is 10mM is actually the highest and the current when the bulk concentration is 1mM is the lowest

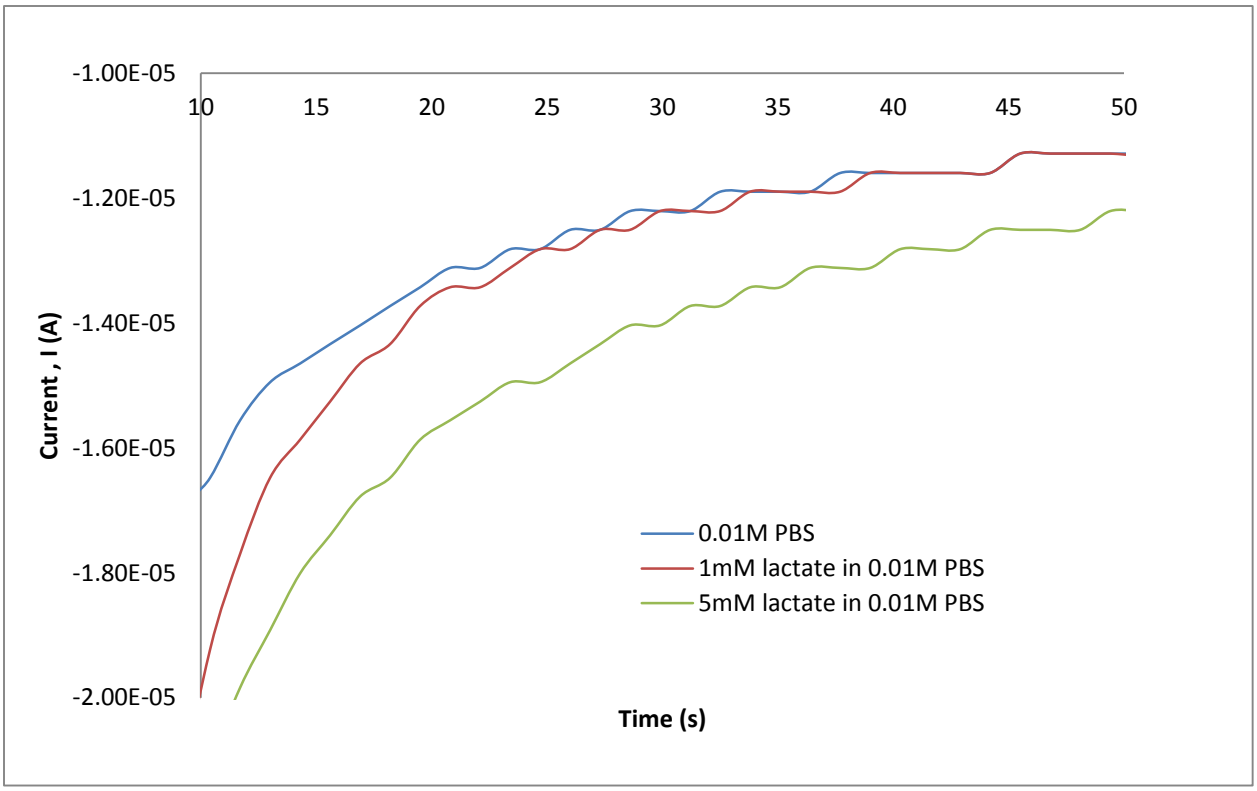

Figure 18. Amperometry of GC-MWCNTs electrode #2 in solutions with various glucose concentrations in 0.01M PBS

Similarly, figures 19 and 20 show amperometry of modified glassy carbon electrodes #1 and #2 in solutions with various concentrations of lactate in 0.01M PBS.

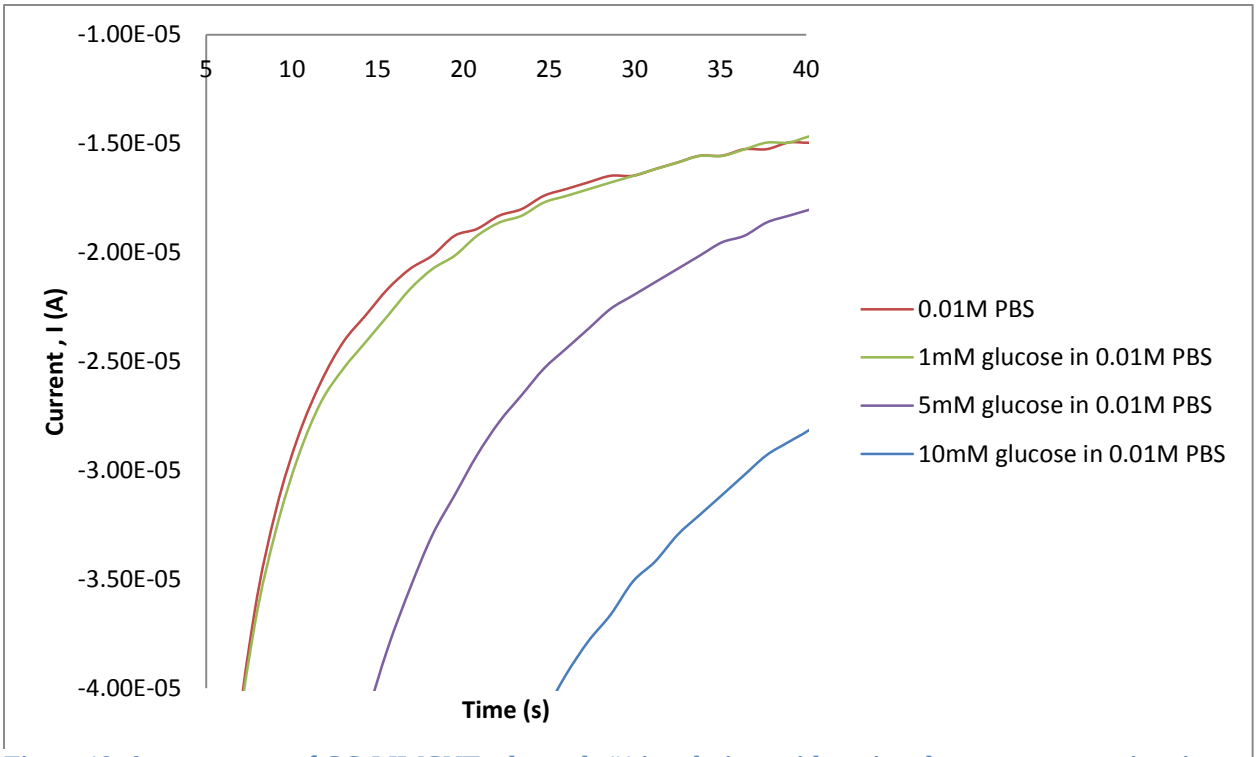

Figure 19. Amperometry of GC-MWCNTs electrode #1 in solutions with various lactate concentrations in 0.01M PBS

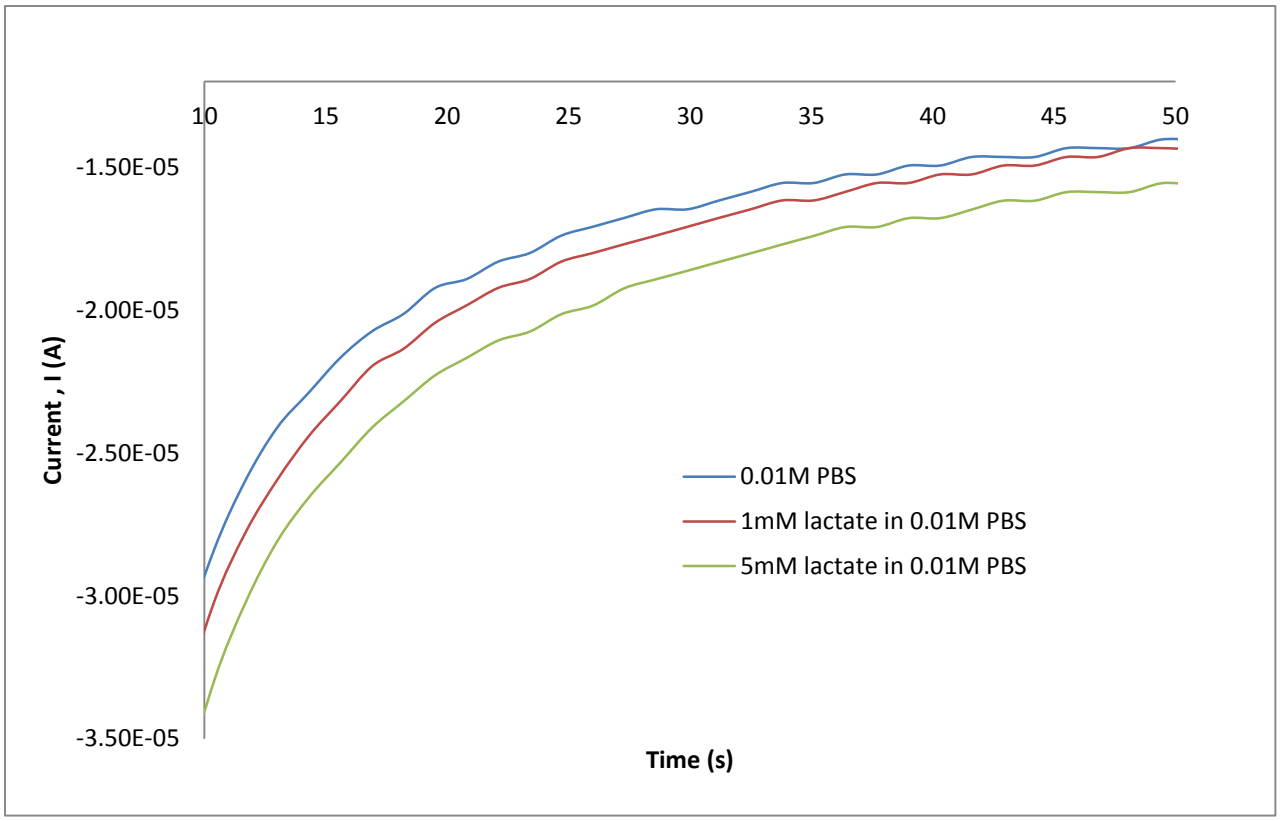

Figure 20. Amperometry of GC-MWCNTs electrode #2 in solutions with various lactate concentrations in 0.01M PBS

Both the various voltammetry and amperometry data set show that the two glassy carbon electrodes coated with carbon nanotubes function properly. For instance, as the bulk concentration increases, current increases as well. However, it does not meet the ultimate goal which is the detection of glucose. Although the electrodes fail to detect glucose, the next experiment will test its sensitivity toward the presence of glucose. In the next experiment, the amperometric response of GCE #1 towards 0.5mL of 50mM glucose additions in 0.1M PBS is recorded. This study is to investigate the stability of the GCE. As the glucose concentration gradually increases as 0.5mL of 50mM glucose in 0.1M PBS is added each time to the initial 0.1M PBS solution. Because each time 0.5mL of 50mM glucose in 0.1M PBS is added, the bulk concentration increases, thus, increases the current. Hence, a graph showing step function behavior is expected. However, figure 21 fails to display so.

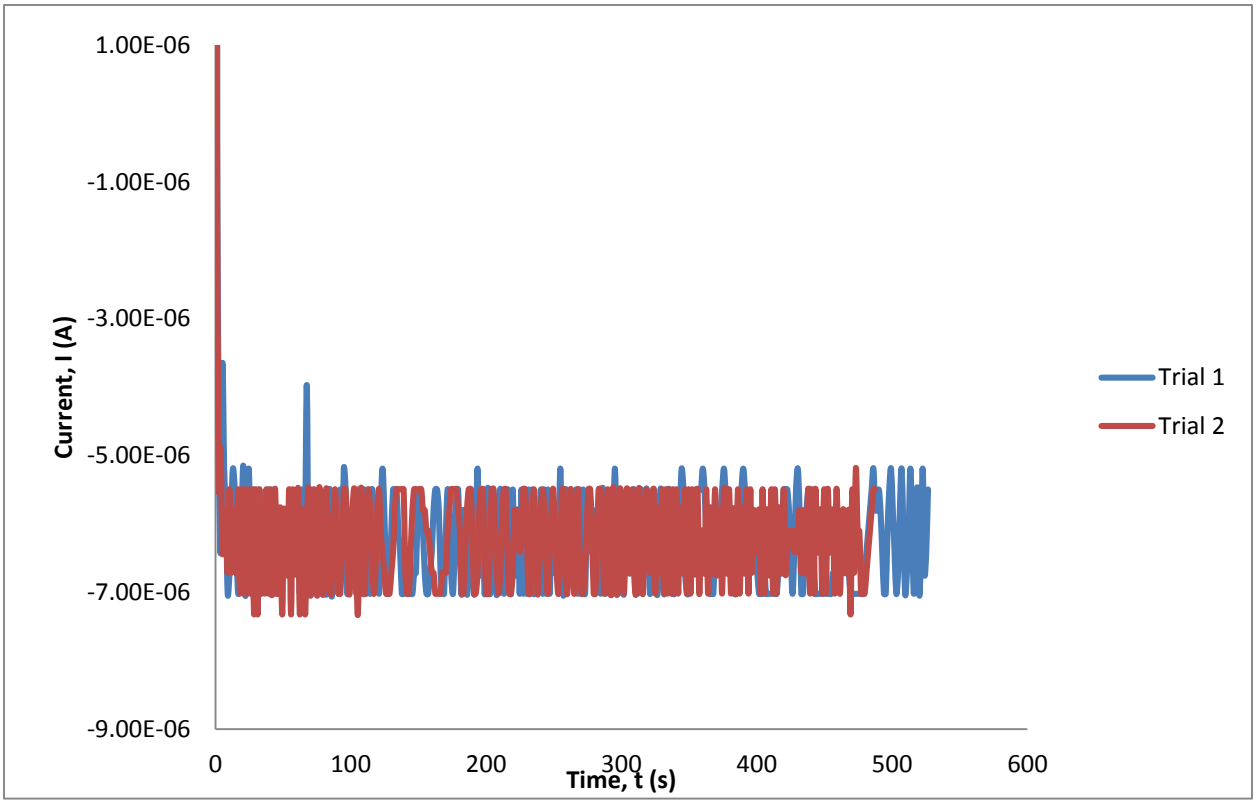

Figure 21. Amperometry of GCE #1 in 0.01M PBS solution initially, then 0.5mL of 50mM glucose in 0.01M PBS solution is gradually added

Now, it is sufficient to conclude that glassy carbon electrode modified with carbon nanotube is not sensitive toward glucose, thus, making it fail to detect the presence of glucose, even at large concentrations. The next approach is to use glassy carbon electrode coated with carbon nanotubes deposited with Pt nanoparticles. High deposition of Pt nanoparticles on CNTs is carried out by two methods, one of which seems to be much more effective. First, after electrochemistry method is used, the cyclic voltammetry of GCE #1 submerged in 0.5M H_2SO_4 is run to test whether the nanoparticles are successfully deposited on the electrode. The performance test is displayed in Figure 22 below.

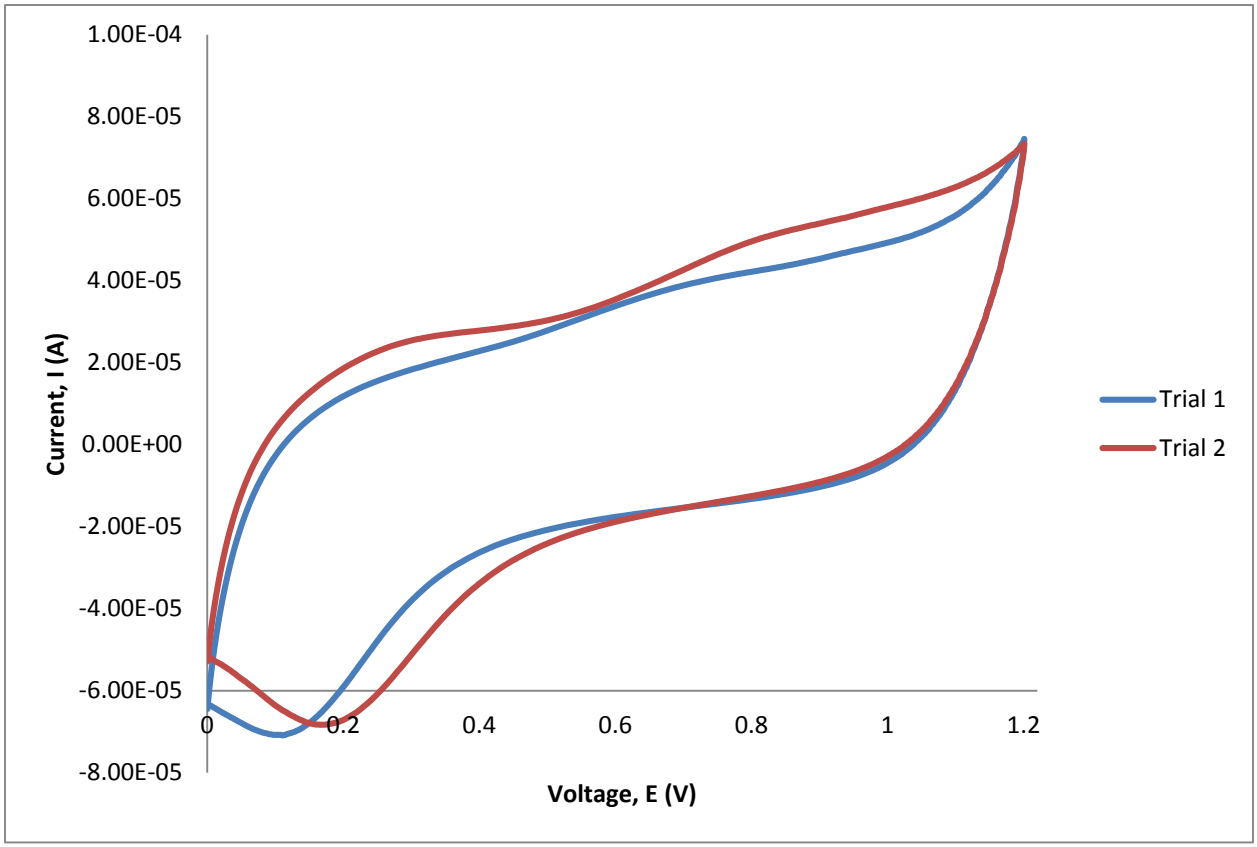

Other performance tests are also carried out; specifically, 0.1M PBS solution and 40mM glucose in 0.01M PBS solution are used as solvents in the subsequent tests.

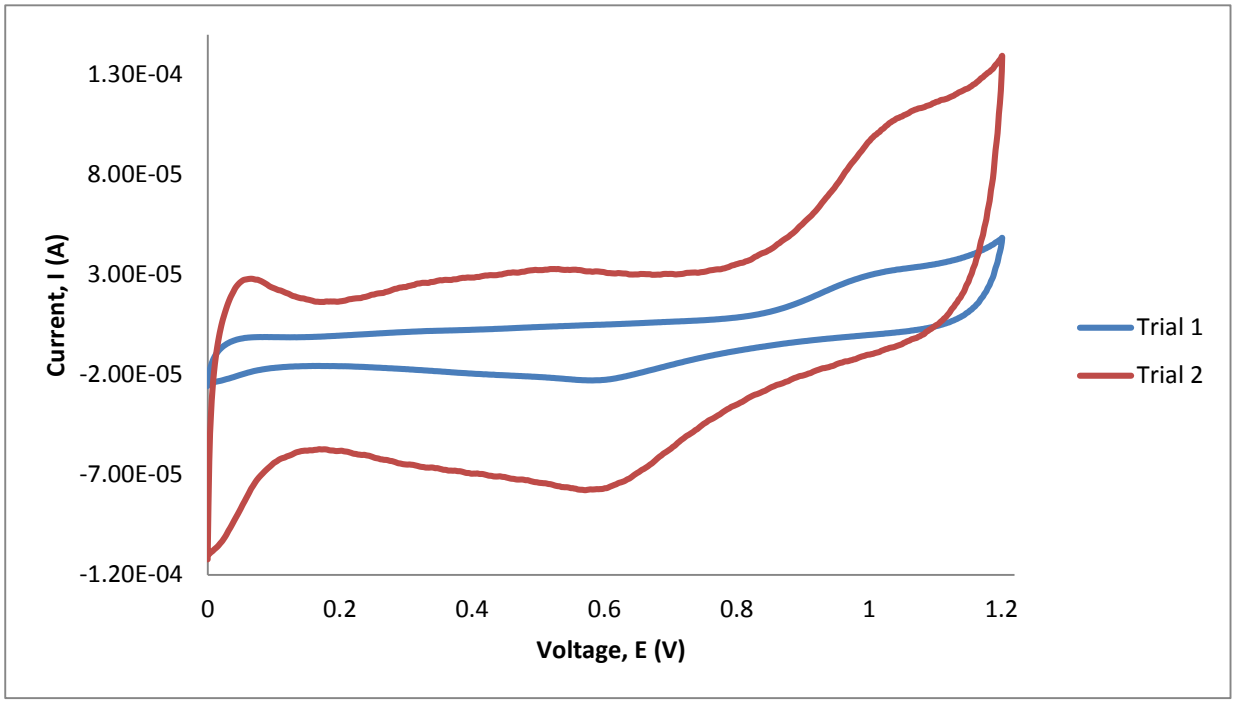

Figure 24. Cyclic voltammetry of GCE #3 in 0.5M H2SO4 after electrodeposition of Pt nanoparticles is performed

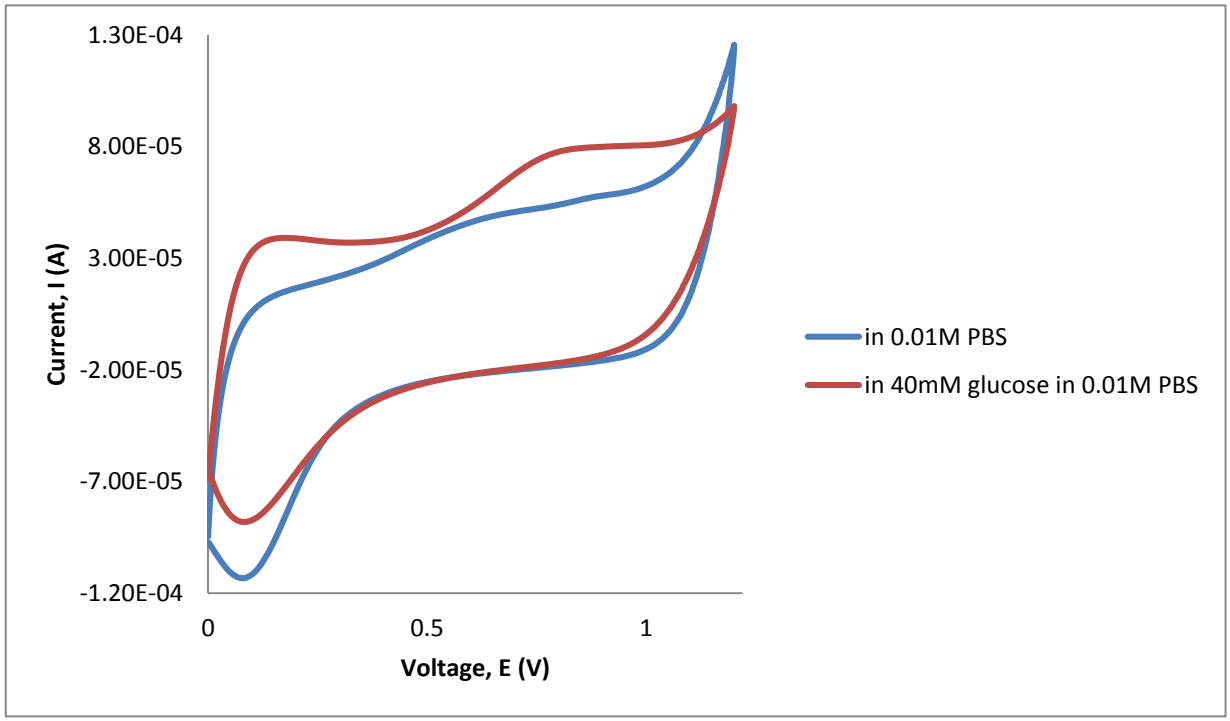

Figure 23. Cyclic voltammetry of GCE #3 in other electrolytes after electrodeposition of Pt nanoparticles is performed

From the data above, it is seen that Pt nanoparticles are not successfully deposited on CNT via the electrochemistry method. Hence, the chemical method is used. Yet, after Pt nanoparticles are synthesized, there are also two approaches on how to coat the GCE with CNTs and nanoparticles. First, CNTs are coated directly on the electrode. After this layer is dry, nanoparticles are coated as the next layer on top of the CNT layer. The performance tests are shown in Figures below.

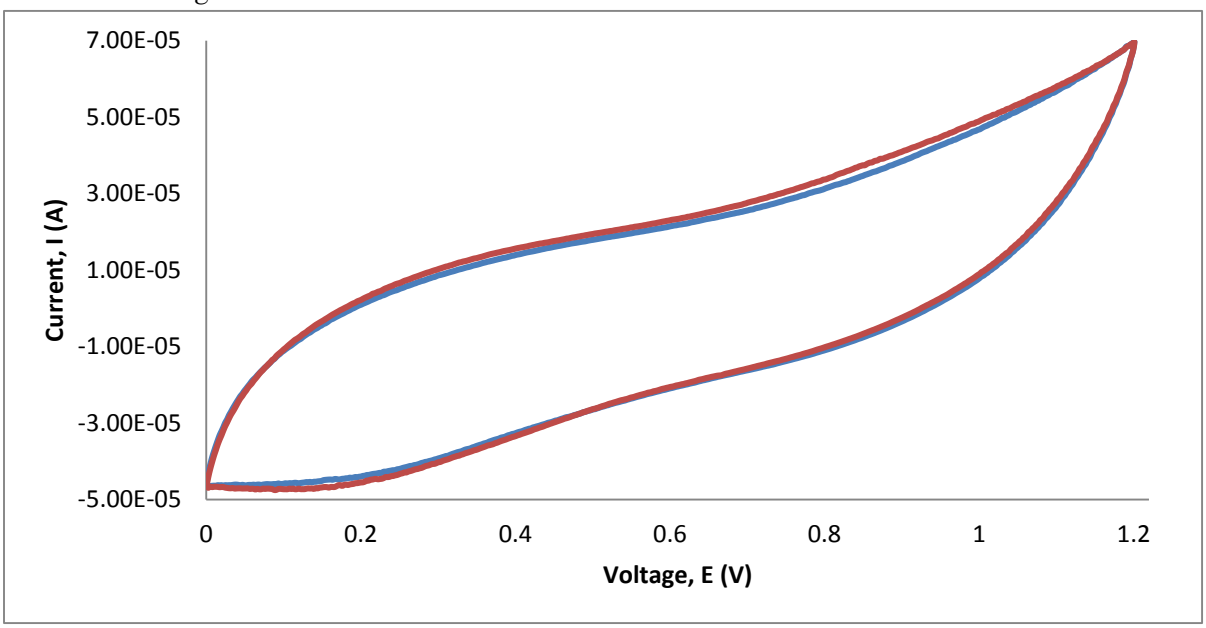

Figure 26. Cyclic voltammetry of GCE #1 with two distinct layers in 0.05M H2SO4 after chemical deposition of Pt nanoparticles is performed

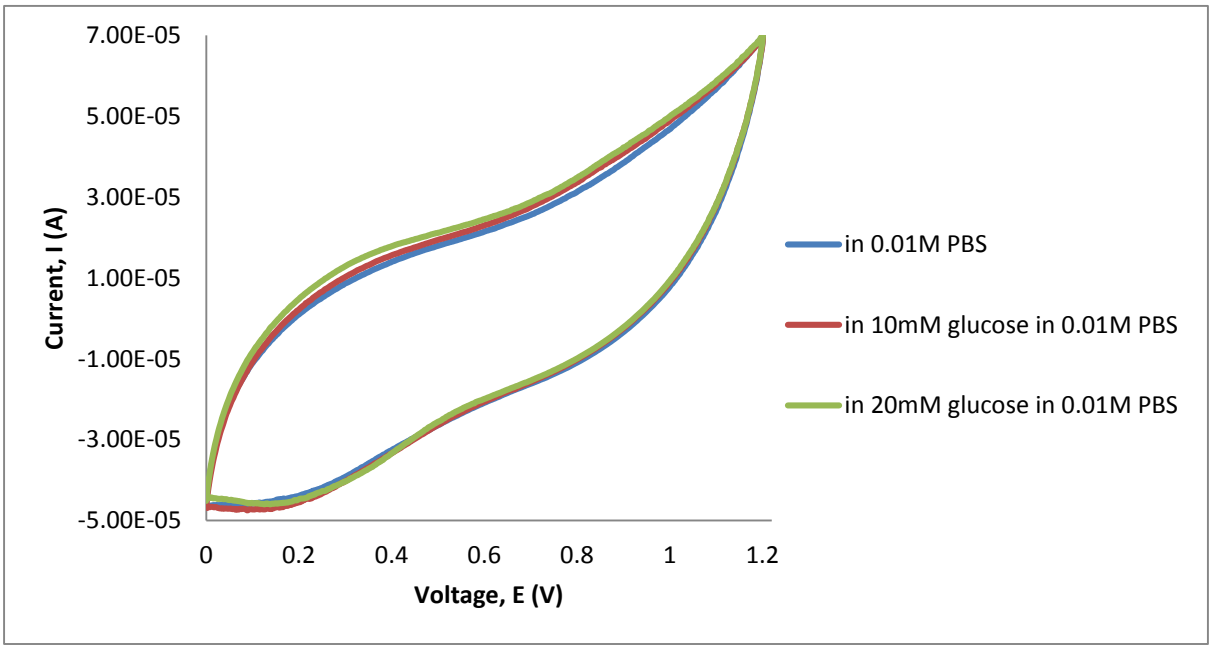

Figure 25. Cyclic voltammetry of GCE #1 with two distinct layers in other electrolytes after chemical deposition of Pt nanoparticles is performed

Again, the data show that GCE coated with CNT as the first layer and NP as the second layer, where NP are synthesized using chemical method, does not perform as expected. The next approach is to mix CNT and NP together and coat hem on the surface of the GCE.

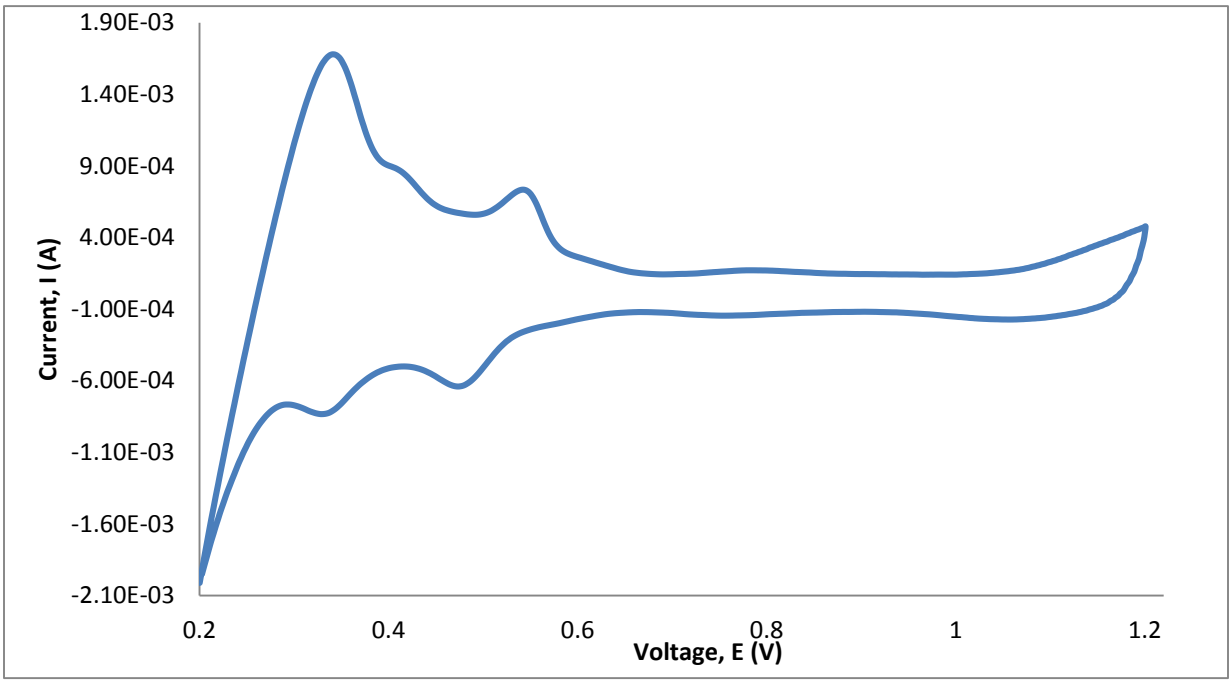

Figure 28. Cyclic voltammetry of GCE #3 in 0.05M H2SO4 after chemical deposition of Pt nanoparticles on MWCNT is performed

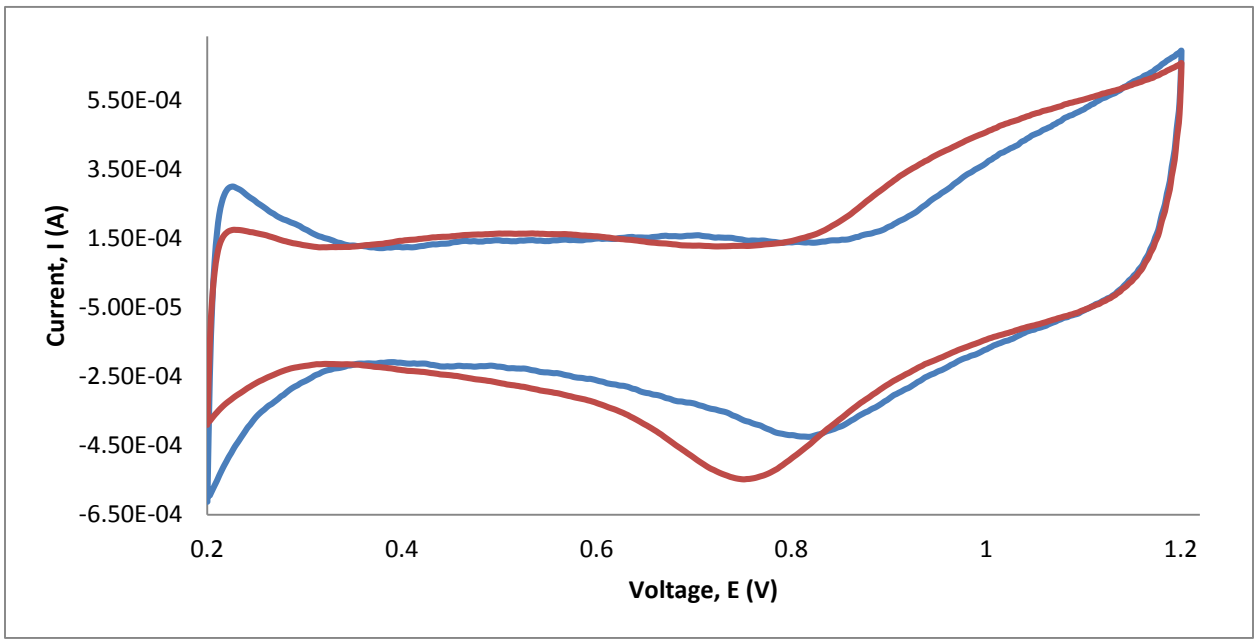

Figure 27. Cyclic voltammetry of GCE #1 in 0.05M H2SO4 after chemical deposition of Pt nanoparticles on MWCNTS is performed

After it has been confirmed that chemical deposition of Pt nanoparticles on MWCNTs is successful, the modified GCEs are now used for further experiments. First of all, cyclic voltammetric response of the two GCEs coated with Pt nanoparticles deposited on multi-walled carbon nanotubes towards solutions of different concentrations of glucose in 0.01M PBS. The expected trend is that the higher concentration of glucose should produce the higher current and the experiment results, shown in Figures 29, 30 and 31, do coincide with the expectations.

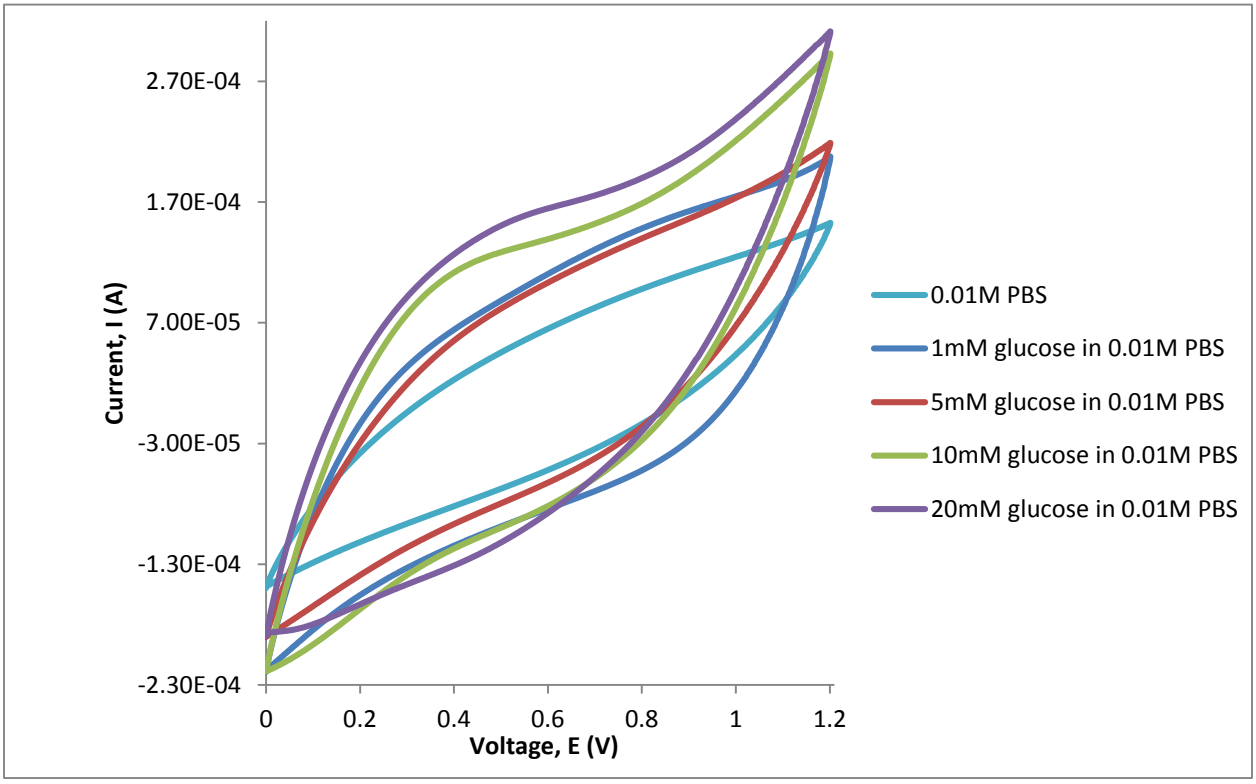

Figure 29. Cyclic voltammetry of GCE #3 modified with PtNPs-MWCNTs in different concentrations of glucose in 0.01M PBS

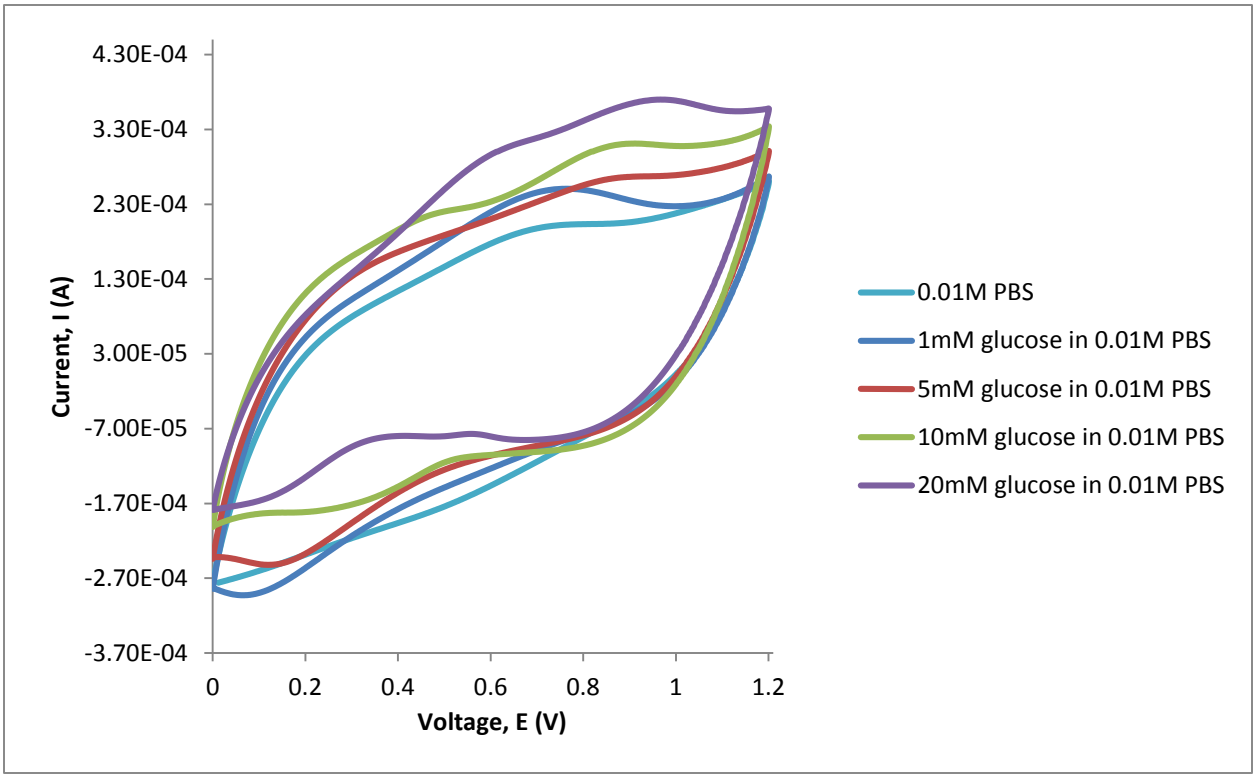

Figure 31. Cyclic voltammetry of GCE #1 modified with PtNPs-MWCNTs in different concentrations of glucose in 0.01M PBS, trial 1

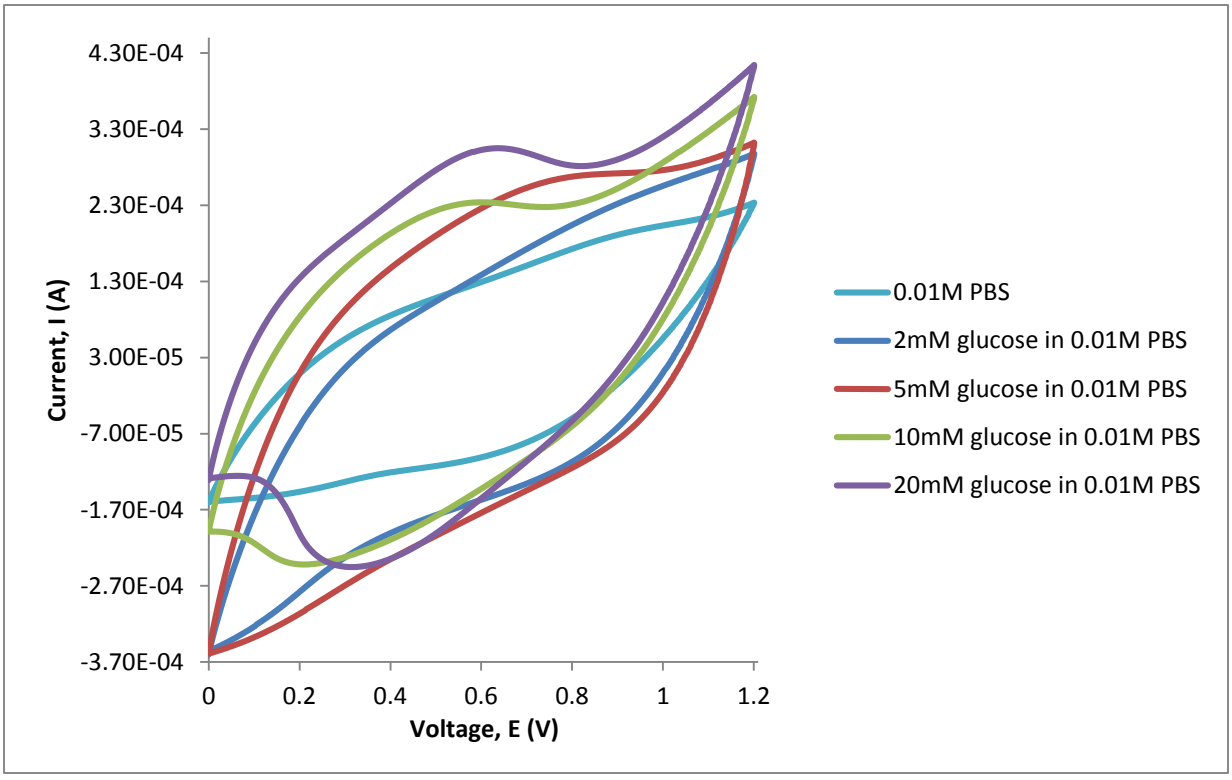

Figure 30. Cyclic voltammetry of GCE #1 modified with PtNPs-MWCNTs in different concentrations of glucose in 0.01M PBS, trial 2

Nevertheless, though the voltammogram shows that higher bulk concentration produces higher current, no peaks are observed. The relationship between concentration and current only proves that the electrode is functioning properly as expected. Yet, the fact that no peak is present in the potential range indicates that this modified electrode, again, does not succeed in detecting glucose, even at high concentration (20mM). Many other trials are carried out to confirm this result (see Appendix), and it is confirmed. The following experiment serves to test the electrode's sensitivity toward glucose. The amperometric response of GCE #1 towards 0.5mL of 50mM glucose additions each time in 0.1M PBS is recorded. This study is to investigate the stability of the GCE. As the glucose concentration gradually increases as 0.5mL of 50mM glucose in 0.1M PBS is added each time to the initial 0.1M PBS solution. Because each time 0.5mL of 50mM glucose in 0.1M PBS is added, the bulk concentration increases, thus, increases the current. Hence, a graph showing step function behavior is expected. Successfully, figure 30 and 31 do display so.

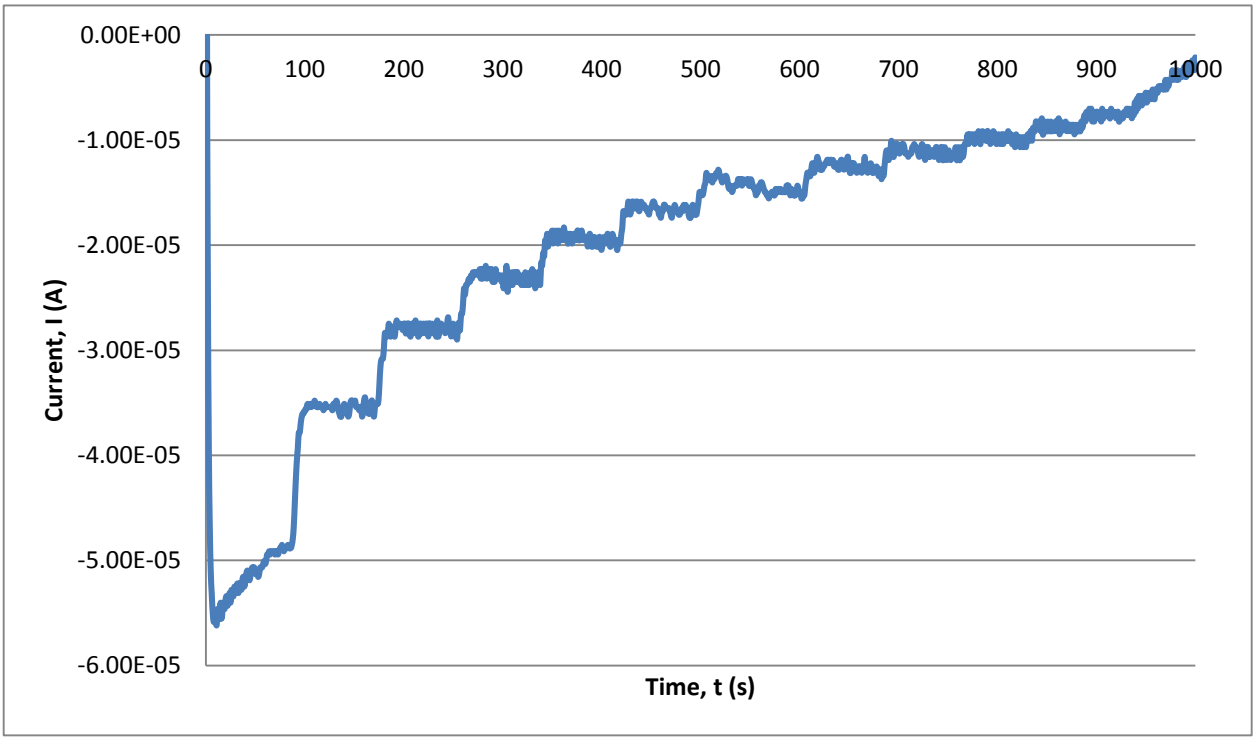

Figure 32. Amperometry of GCE #1 in 0.01M PBS, then 0.1mL of 1M glucose in 0.01M PBS is gradually added to the solution, trial 1

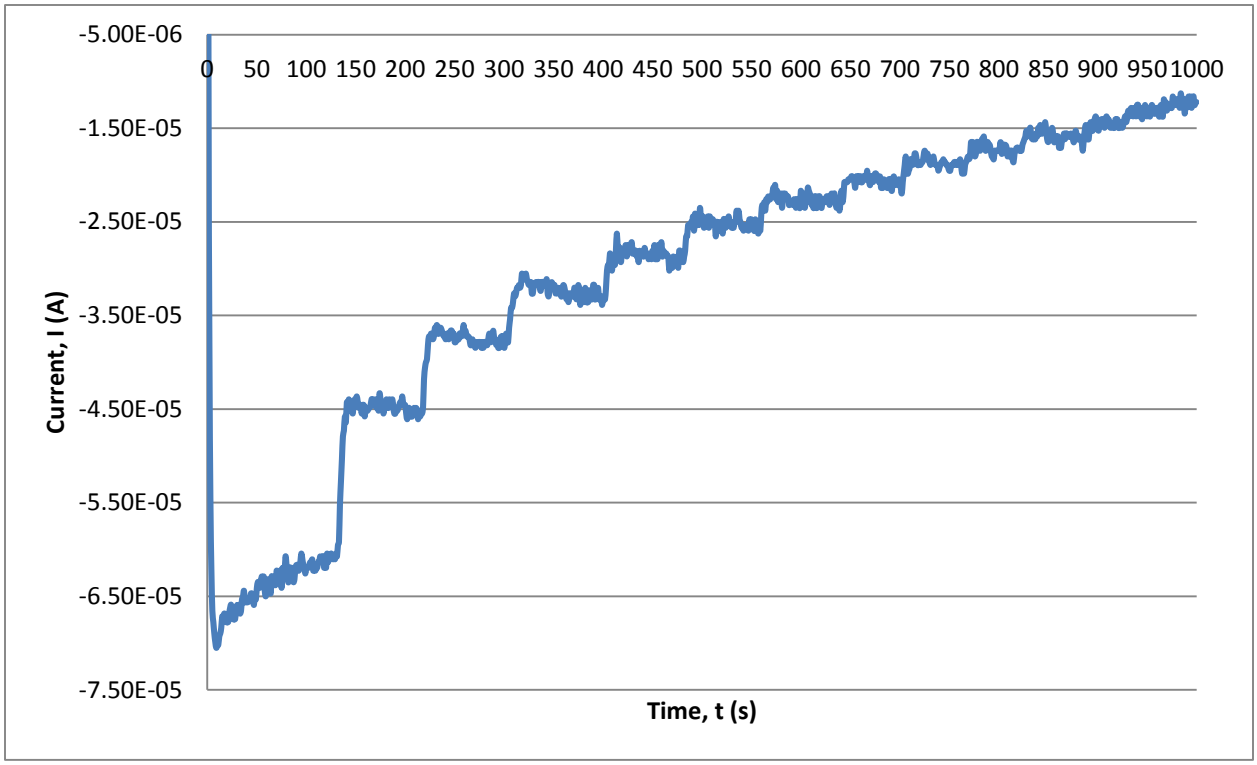

Figure 33. Amperometry of GCE #1 in 0.01M PBS, then 0.1mL of 1M glucose in 0.01M PBS is gradually added to the solution, trial 2

From the above experiment, it can be concluded that glassy carbon electrode modified with Pt nano particles deposited on multi-walled carbon nanotubes is sensitive to glucose though it fails to detect glucose in 0.1M PBS solution, which is questionable. More research should be conducted to investigate this behavior, and find a solution to the problem.

Figures 32 and 33 show that the relationship between corresponding current and bulk concentration forms a straight line, which is expected due to the Randle-Sevcik relationship. Again, this data confirms the proper functionality of the electrode, thus, its promising potential in the field as well.

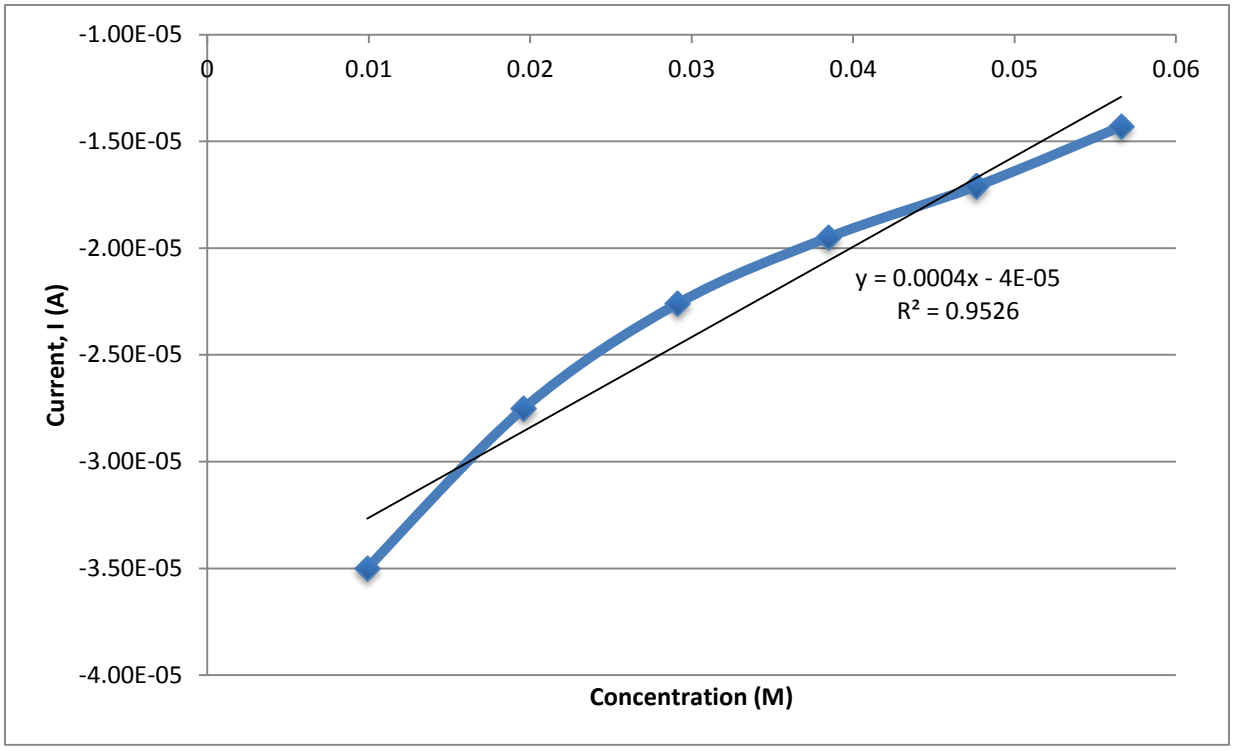

Figure 35. Correlation between current and concentration

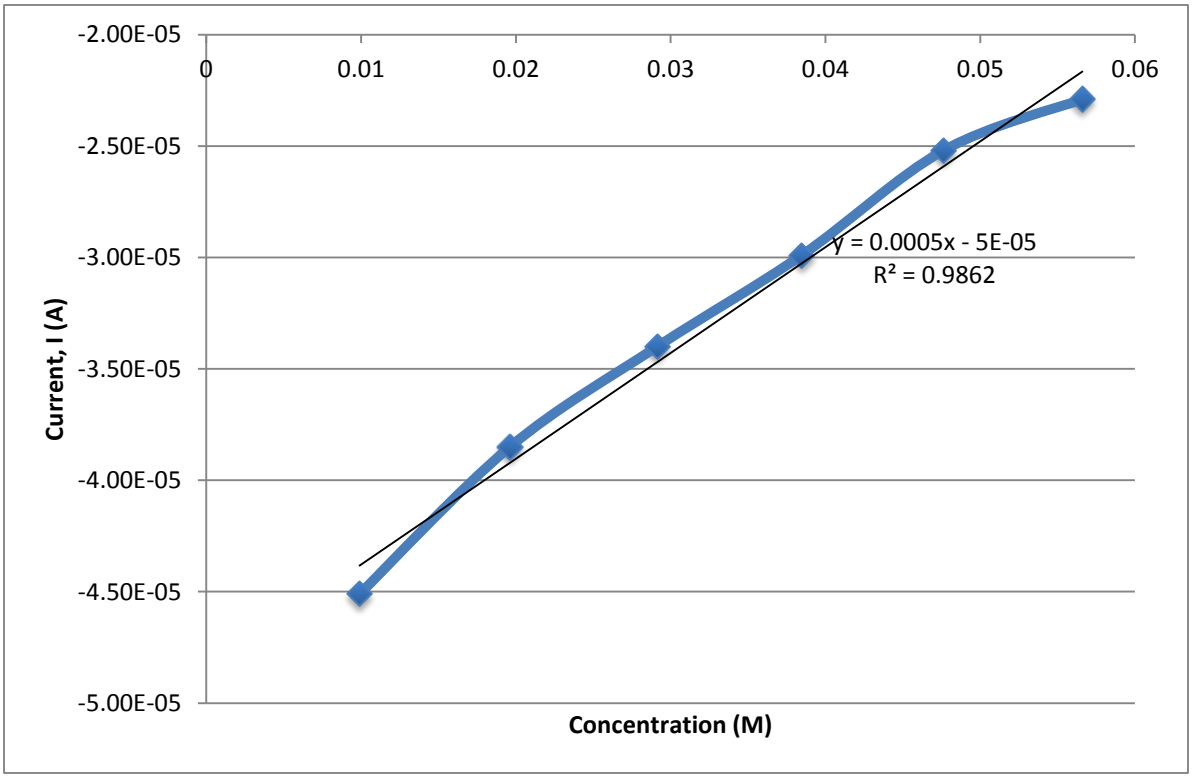

Figure 34. Correlation between current and concentration obtained from data from Figure 44

Part V. Conclusion and Recommendations

This Major Qualifying Project aims to investigate the performance of modified glassy carbon electrode in the detection of glucose. In the first part, glassy carbon electrode is coated with multi-walled carbon nanotubes. Voltammetry and amperometry are applied to study whether this modified electrode is capable of detecting the presence of glucose in 0.1M PBS solution. The concentration of glucose varies from 0.1mM to 10mM. Despite the high glucose concentration, this modified electrode fails to detect glucose since there are no peak present in the generated voltammogram. Lactate is also used as an analyte, but similar results are obtain, meaning this modified electrode does not detect lactate either. Yet, it is confirmed that the electrode is functioning properly. This confirmation is made due to the fact that as the bulk concentration increases, the current increases as well. Moreover, the amperometry also validates this statement.

After ensuring that glassy carbon electrode coated with multi-walled carbon nanotubes is not capable of detecting glucose, the electrode is now modified with Pt nanoparticles deposited on multi-walled carbon nanotubes. Two methods, electrochemical and chemical, are applied to coat the electrode and the voltammetry indicates that the electrode is successfully coated with Pt nanoparticles deposited on multi-walled carbon nanotubes using the chemical method. Similar procedures as above are used to test the electrode's sensitivity toward glucose. Again, no peak is observed in the resulting voltammogram. However, in the experiment where 0.5mL of 50mM glucose additions each time in 0.1M PBS, the amperometry does show the step function as expected. Each time 0.5mL of 50mM glucose is added, the overall glucose concentration increases, thus, the current should increase as well, creating a step function graph. The result successfully coincides with the expectation, suggesting that this modified electrode is not only stable but also sensitive toward glucose. This finding is extremely helpful as it indicates that Pt nanoparticles deposited on multi-walled carbon nanotubes is a promising material for non-enzymatic biosensor.

However, the question remains that if the modified electrode is sensitive toward glucose, why is there no peak in the voltammogram? Due to the time limit of this project, this question has not yet been solved. For future work, it is suggested to use glassy carbon electrode modified with Pt nanoparticles deposited on multi-walled carbon nanotubes and test it using

solutions with even higher concentration of glucose. Also, different electrodes can be tested as well, such as platinum electrode, gold electrode, etc. The resulted step-function amperometry is a very concrete evidence that this modified electrode will be a potential candidate for enzymatic glucose sensor.

Bibliography

Abrahamson, J., P. G. Wiles and B. L. Rhoades. "Structure of carbon fibres found on carbon arc anodes." *Carbon* 37.11 (1999): 1873-1874. 27 July 2014.

Babu, Satheesh. *Development of Non-enzymatic Electrochemical Glucose Biosensors and Glucometer*. 1 January 2012. 2 June 2014.

Balasubramanian, K., M. Burghard and K. Kern. "Carbon nanotubes: electrochemical modification." Schwarz, J. A., C. I. Contescu and K. Putyera. *Dekker encyclopedia of nanoscience and nanotechnology*. New York: Marcel Dekker, 2004. 28 August 2014.

Balasubramanian, Kannan and Marko Burghard. "Biosensors based on carbon nanotubes." *Anal Bioanal Chem* (2006): 452-468. 1 August 2014. <http://www.fkf.mpg.de/49009/kk417.pdf>.

Bianchi, Roberta, et al. "A Nonenzymatic Biosensor based on Platinum Electrodes." *American Chemical Society* 30 (2014): 11568. 2 August 2014.

Day, T. M., et al. *J Am Chem Soc* 127 (2005): 10639-10647. 14 September 2014.

Donaldson, K., R. Aitken and L. Tran. "Carbon nanotubes: a review of their properties in relation to pulmonary toxicology and workplace safety." *Toxicological Sciences* 92 (2006): 15-22. 2 August 2014.

Gao, M., L. Dai and G. G. Wallace. *Electroanalysis* 15 (2003): 1089-1094. 20 August 2014.

Hrlekar, R., et al. "Carbon nanotubes and its applications: a review." *Asian Journal of Pharmaceutical and Clinical Research* 2.4 (2009): 17-27. 27 July 2014.

Kissinger, P. T. and W. R. Heineman. "Cyclic Voltammetry." *Journal of Chemical Education* (1983): 702. 28 June 2014.

Li, J., et al. *Nano Lett* 3 (2003): 597-602. 7 August 2014.

—. *J Phys Chem B* 106 (2002): 9299-9305. 28 August 2014.

Meyyappan, M., et al. "Carbon nanotube growth by PECVD: a review." *Plasma Sources Science and Technology* 12.2 (2003): 205-216. 30 July 2014.

Newman, JD and SJ Setford. "Enzymatic Biosensors." *Mol Biotechnol* 32 (2006): 249. 25 July 2014.

Prevention, Centers for Disease Control and. *2014 National Diabetes Statistics Report*. 24 October 2014. 17 November 2014.

Skoog, D., F. Holler and S. Crouch. "Principle of Instrumental Analysis." (2007). 25 June 2014.

Tang, H., et al. *Annal Biochem* 331 (2005): 29-35. 10 August 2014.

Toghill, Kathryn E. and Richard G. Compton. "Electrochemical Non-enzymatic Glucose Sensors: A Perspective and an Evaluation." *International Journal of Electrochemical Science* (2010): 1246-1301. Document.

Vasil'ev, Y. B., O. A. Khazova and N. N. Nikolaeva. *J. Electroanal. Chem. Interfacial Electrochem.* (1985): 127.

Wang, Guangfeng, et al. "Non-enzymatic electrochemical sensing of glucose." (2012): 163. 17 July 2014.

Wang, J., R. P. Deo and M. Musameh. "Electroanalysis." (2003): 1830-1834.

Zhao, Zhiwei and Helong Jiang. "Enzyme-based Electrochemical Biosensors." Zhao, Zhiwei and Helong Jiang. *Biiosensors*. Shanghai: In Tech, 2010. 298.

Zittel, H. E. and F. J. Miller. "A Glassy-Carbon Electrode for Voltammetry." *Analytical Chemistry* (1965): 200-203. Document. 20 July 2014. <http://pubs.acs.org/doi/abs/10.1021/ac60221a006>.

Appendix

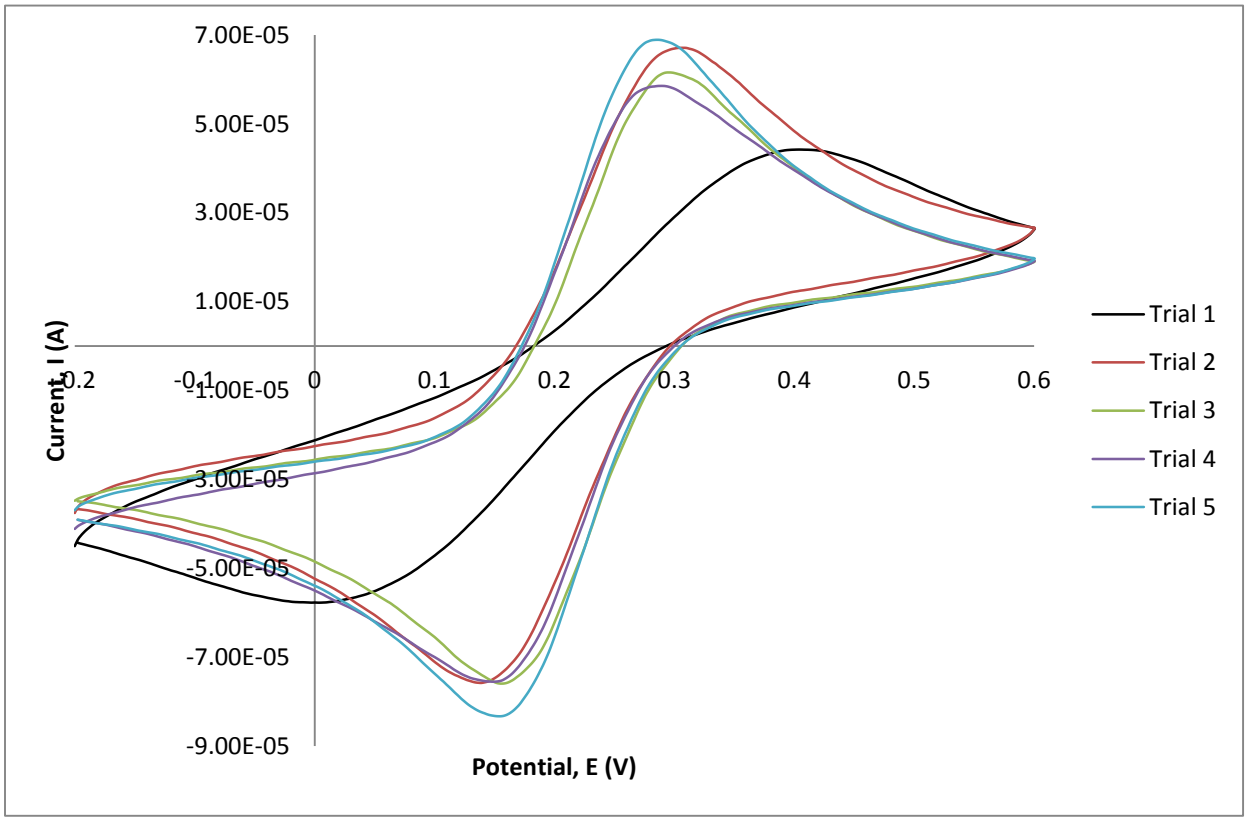

Figure 36. Cyclic voltammogram of unmodified GCE #2 in K3Fe(CN)6

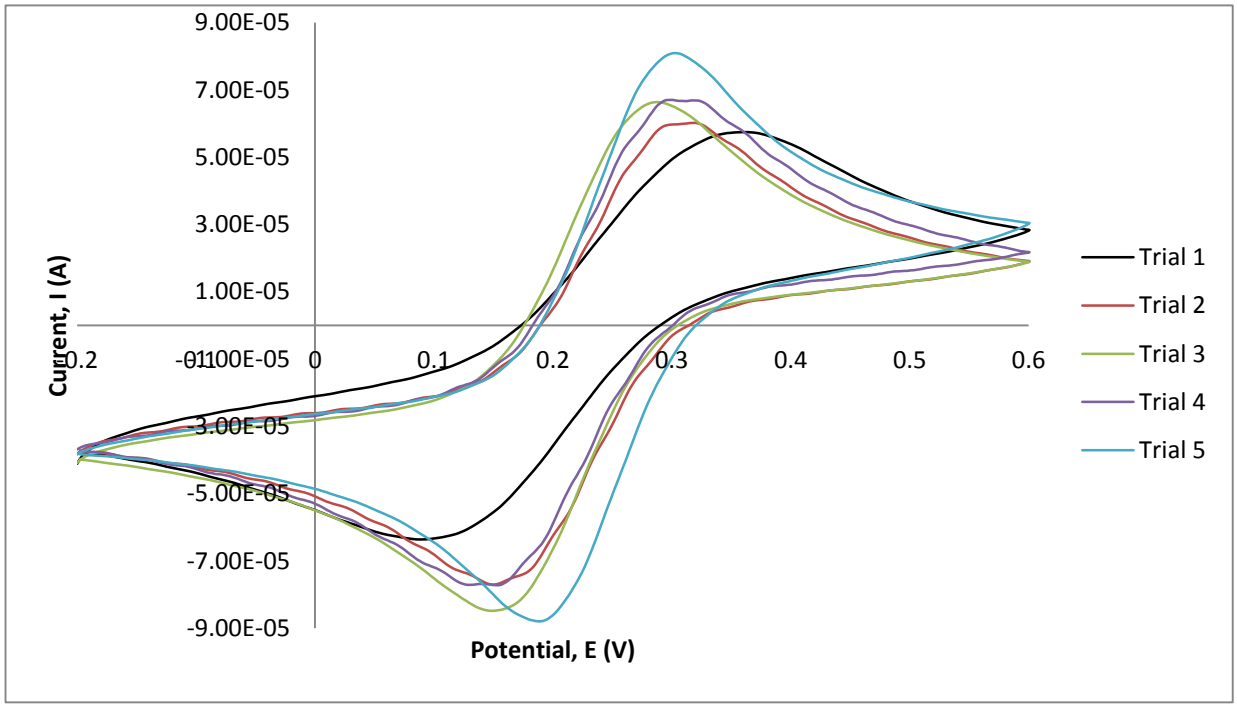

Figure 37. Cyclic voltammogram of unmodified GCE #1 in $K_3Fe(CN)_6$

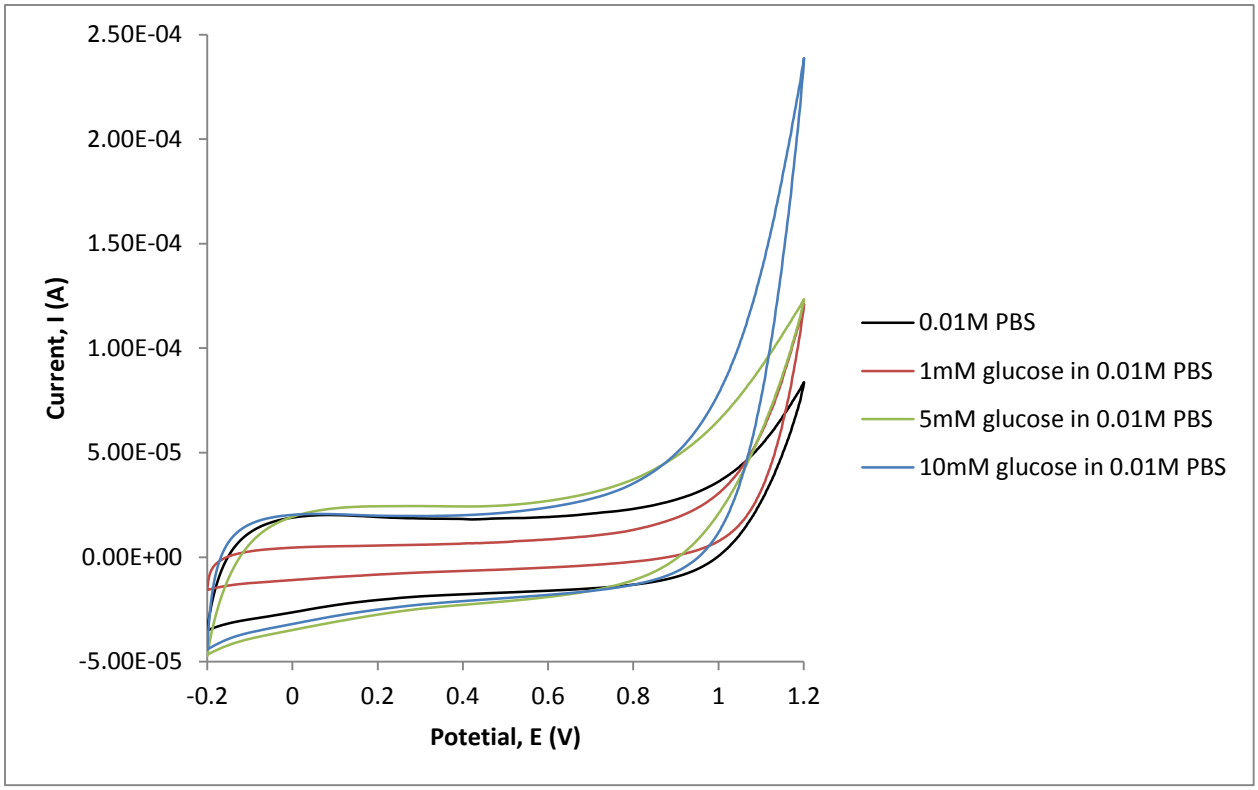

Figure 39. Cyclic voltammogram of GC-MWCNTs electrode #2 in solutions with various glucose concentrations in 0.01M PBS, scanned at 0.01V/s

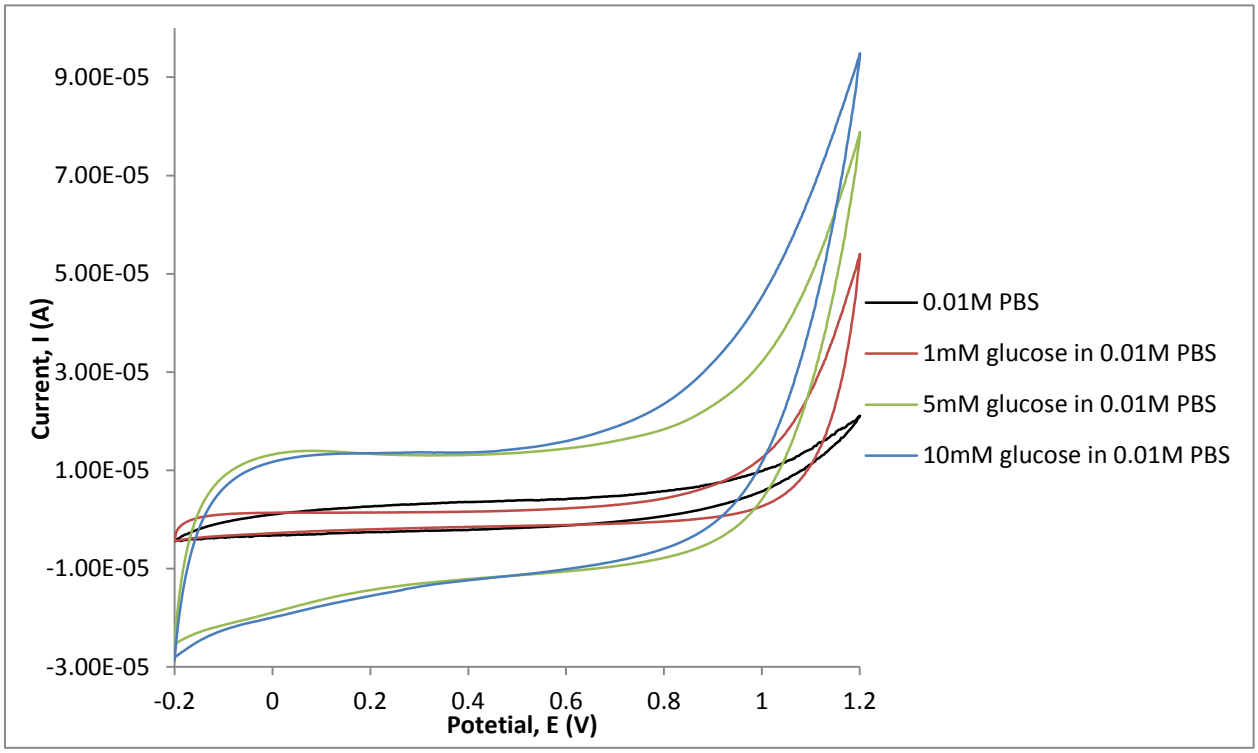

Figure 38. Cyclic voltammogram of GC-MWCNTs electrode #1 in solutions with various glucose concentrations in 0.01M PBS, scanned at 0.01V/s

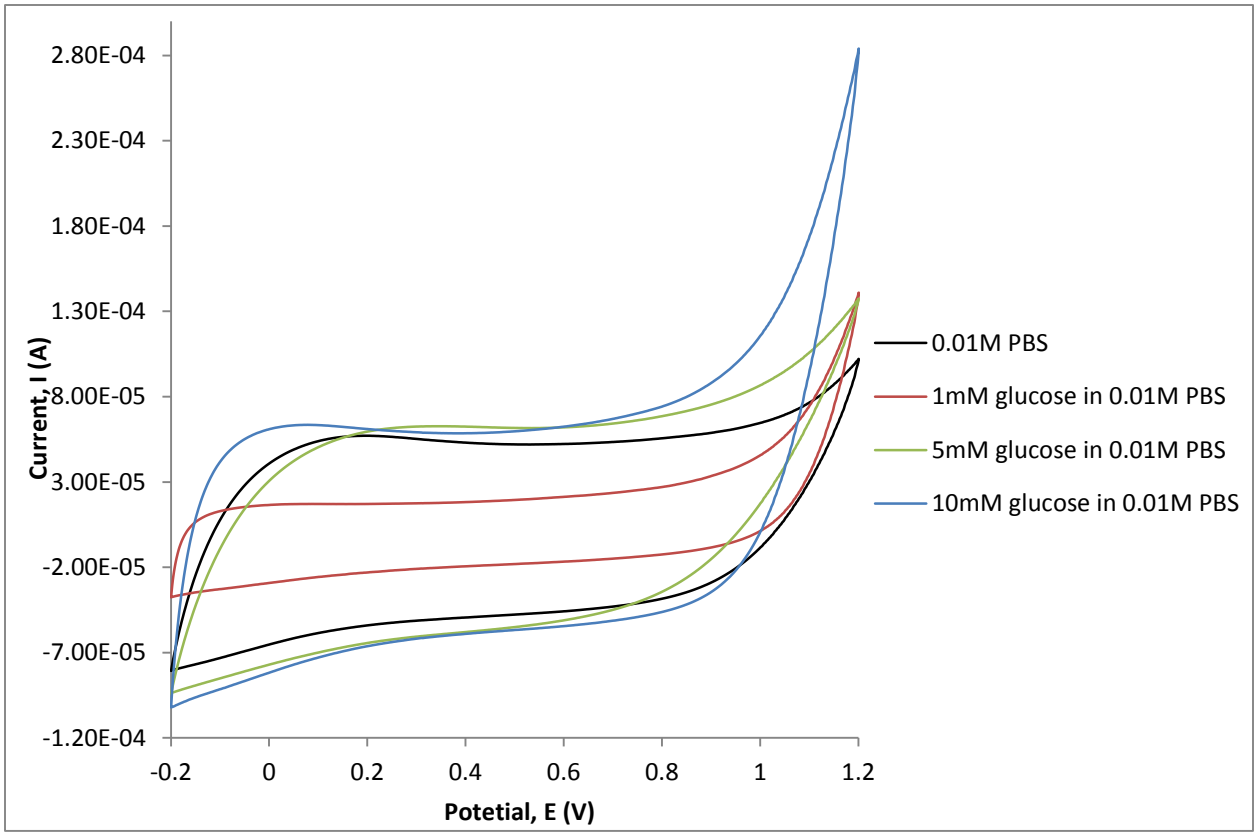

Figure 41. Cyclic voltammogram of GC-MWCNTs electrode #2 in solutions with various glucose concentrations in 0.01M PBS, scanned at 0.03V/s

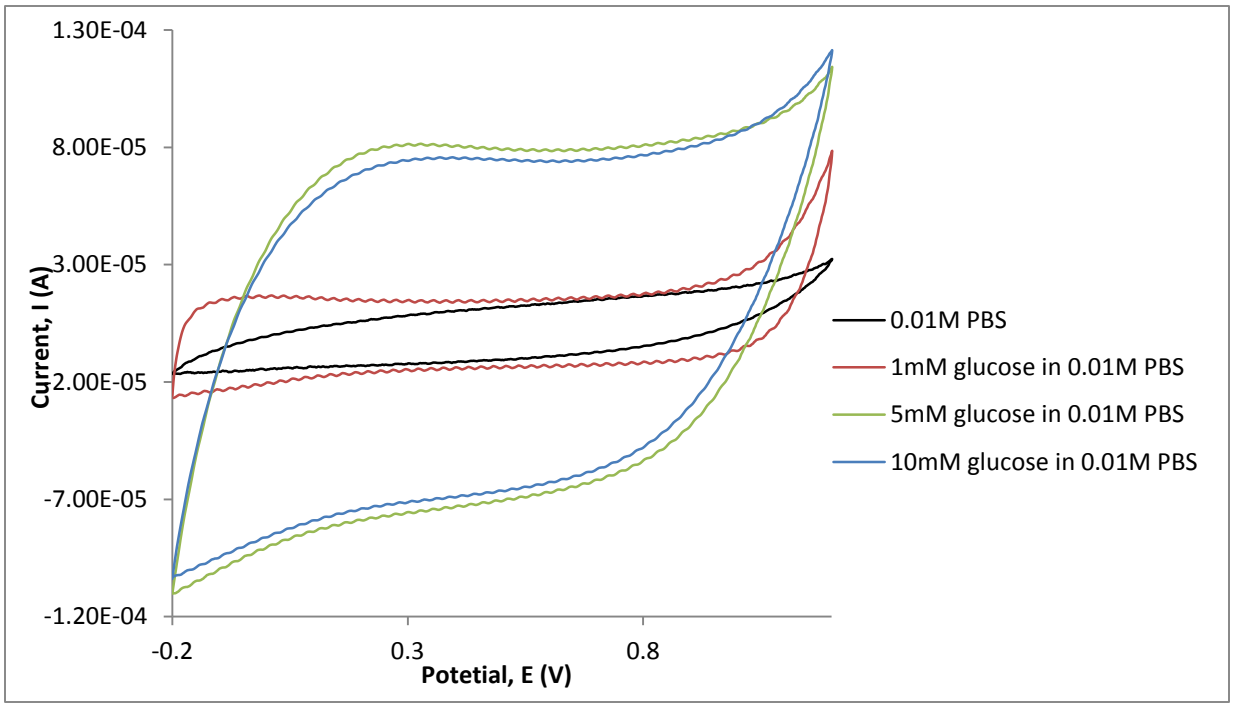

Figure 40. Cyclic voltammogram of GC-MWCNTs electrode #1 in solutions with various glucose concentrations in 0.01M PBS, scanned at 0.07V/s

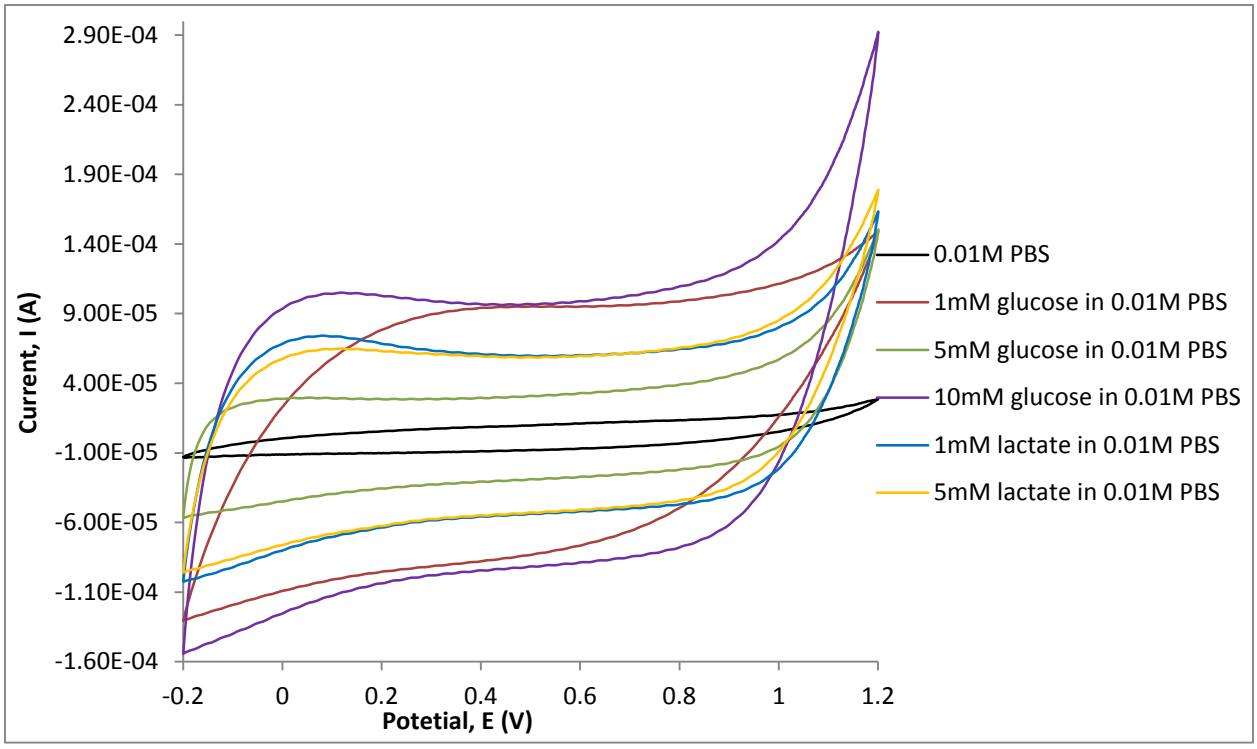

Figure 42. Cyclic voltammogram of GC-MWCNTs electrode #2 in solutions with various glucose and lactate concentrations, scanned at 0.05V/s

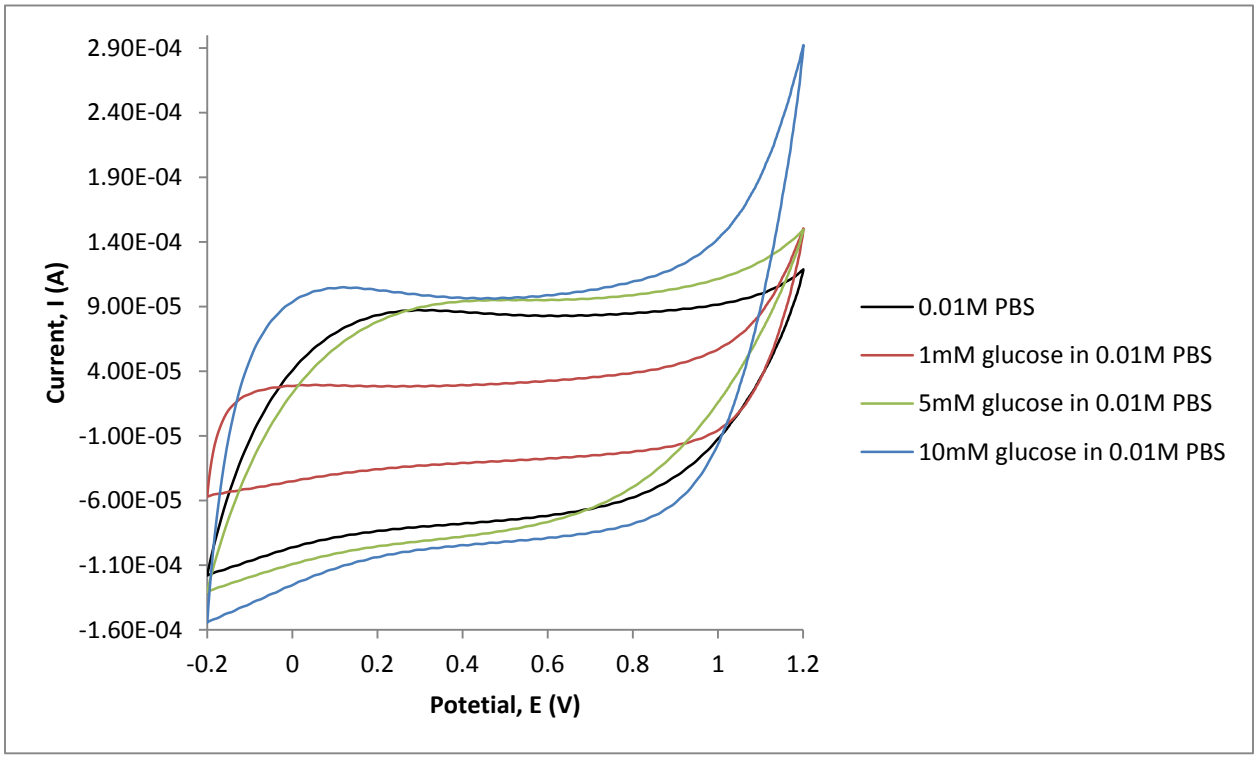

Figure 43. Cyclic voltammogram of GC-MWCNTs electrode #2 in solutions with various glucose concentrations in 0.01M PBS, scanned at 0.05V/s

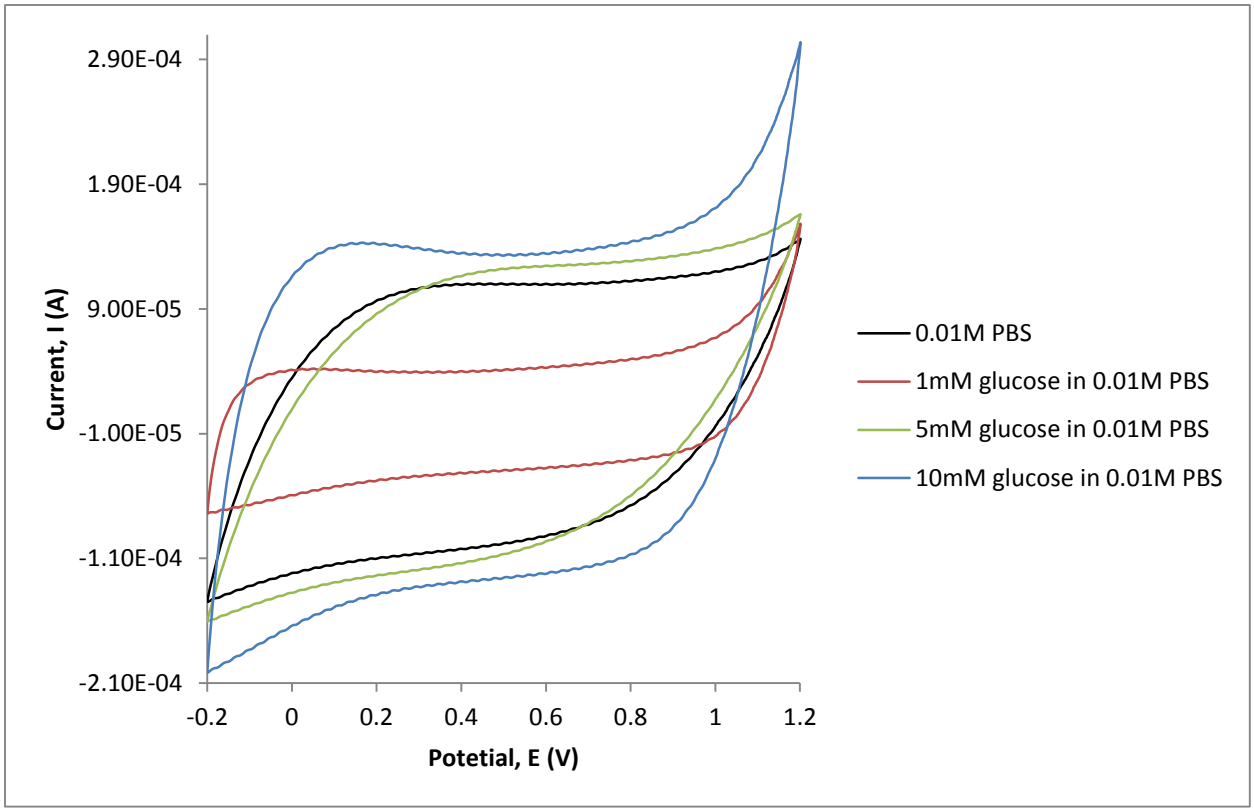

Figure 44. Cyclic voltammogram of GC-MWCNTs electrode #2 in solutions with various glucose concentrations in 0.01M PBS, scanned at 0.07V/s

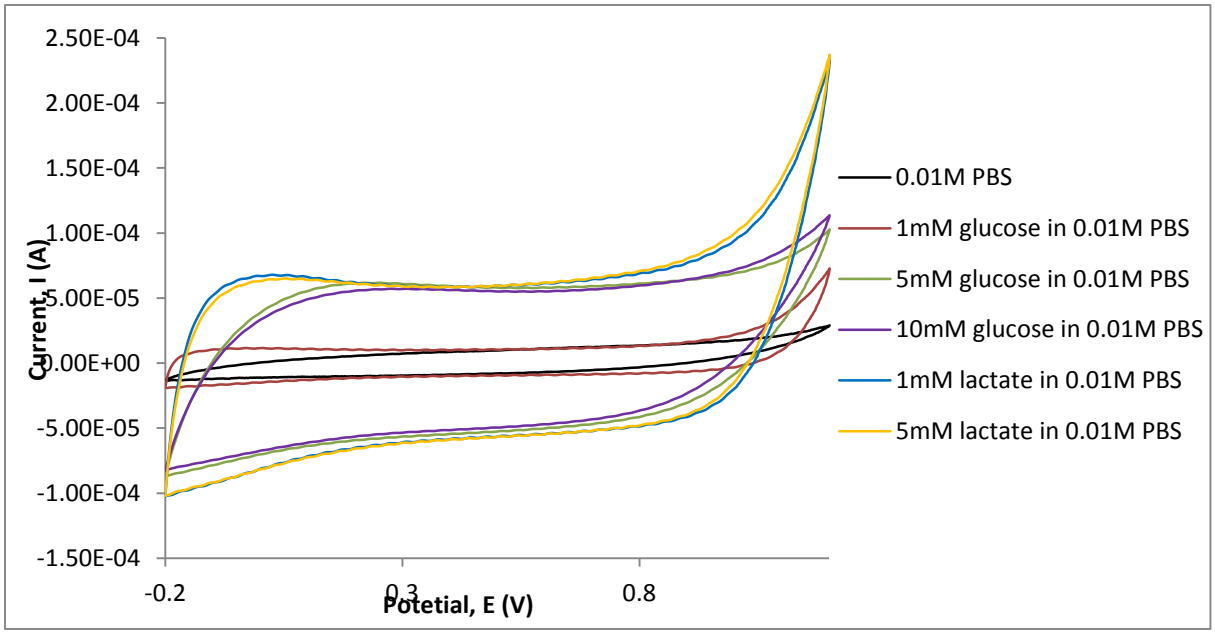

Figure 45. Cyclic voltammogram of GC-MWCNTs electrode #1 in solutions with various glucose and lactate concentrations, scanned at 0.05V/s

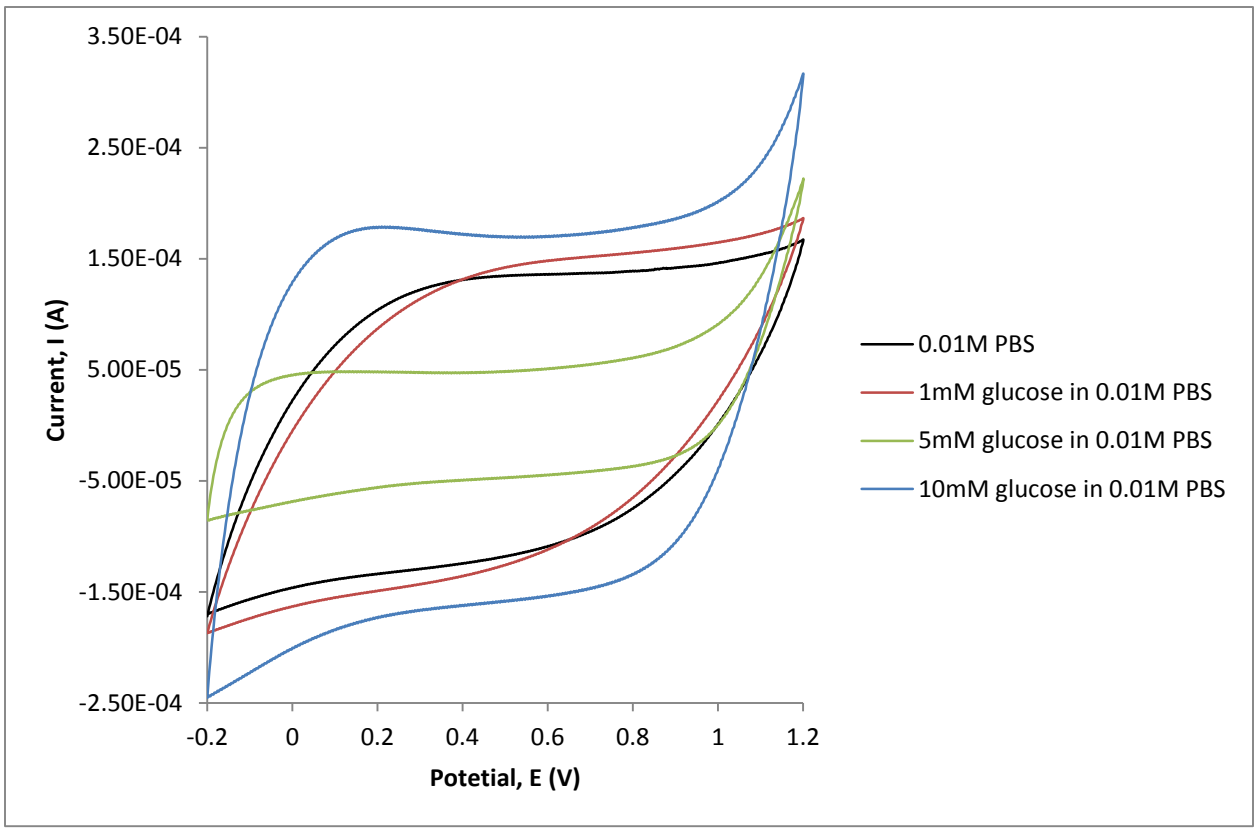

Figure 47. Cyclic voltammogram of GC-MWCNTs electrode #2 in solutions with various glucose concentrations in 0.01M PBS, scanned at 0.09V/s

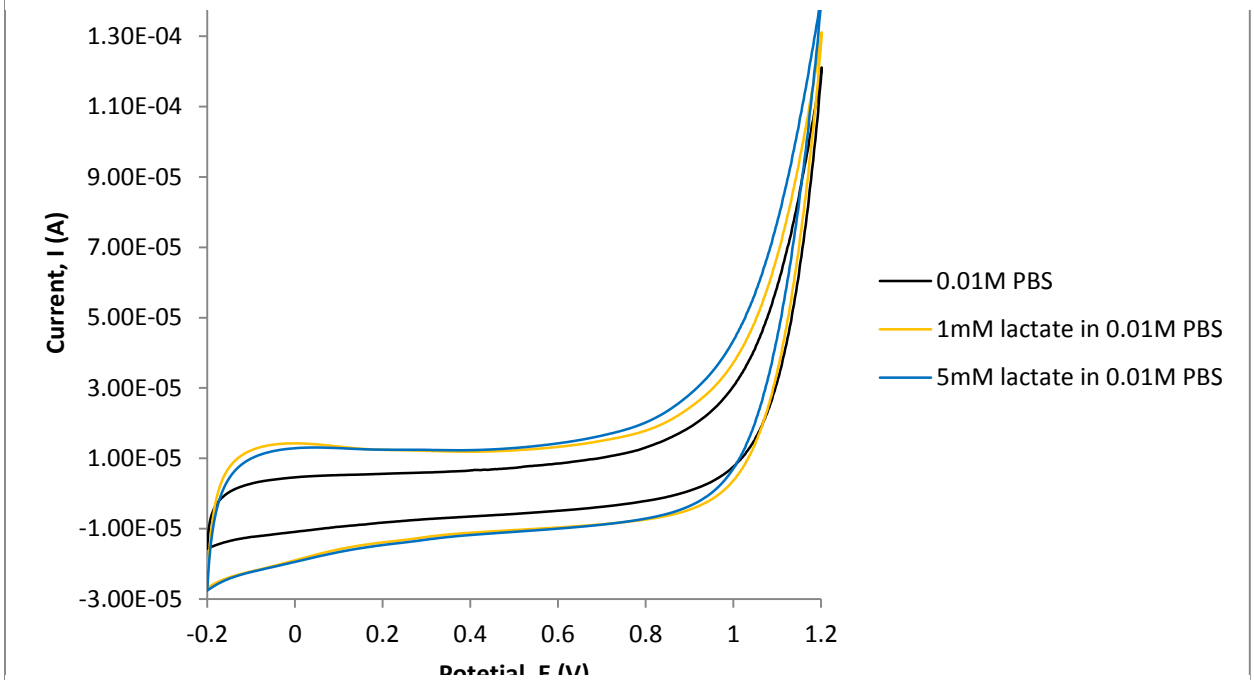

Figure 46. Cyclic voltammogram of GC-MWCNTs electrode #1 in solutions with various lactate concentrations in 0.01M PBS, scanned at 0.01V/s

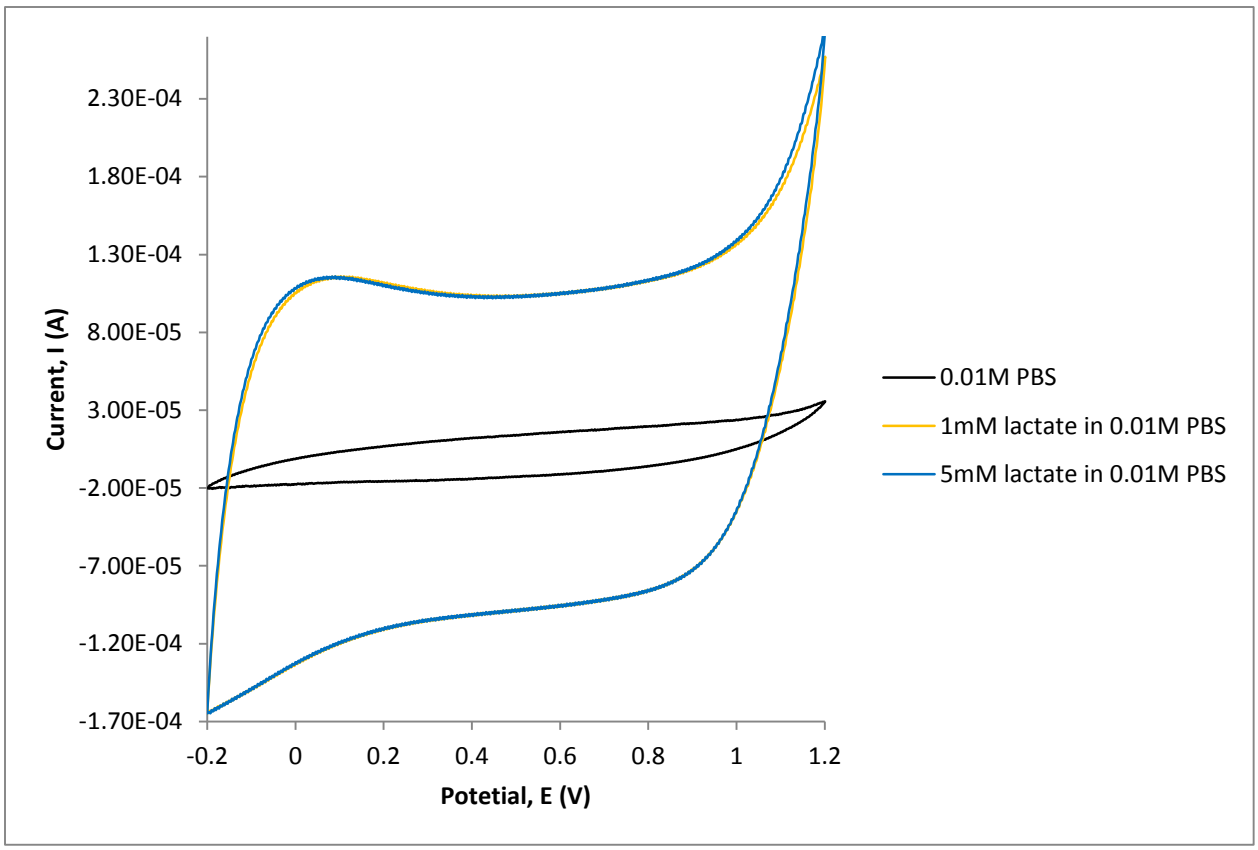

Figure 49. Cyclic voltammogram of GC-MWCNTs electrode #2 in solutions with various lactate concentrations in 0.01M PBS, scanned at 0.01V/s

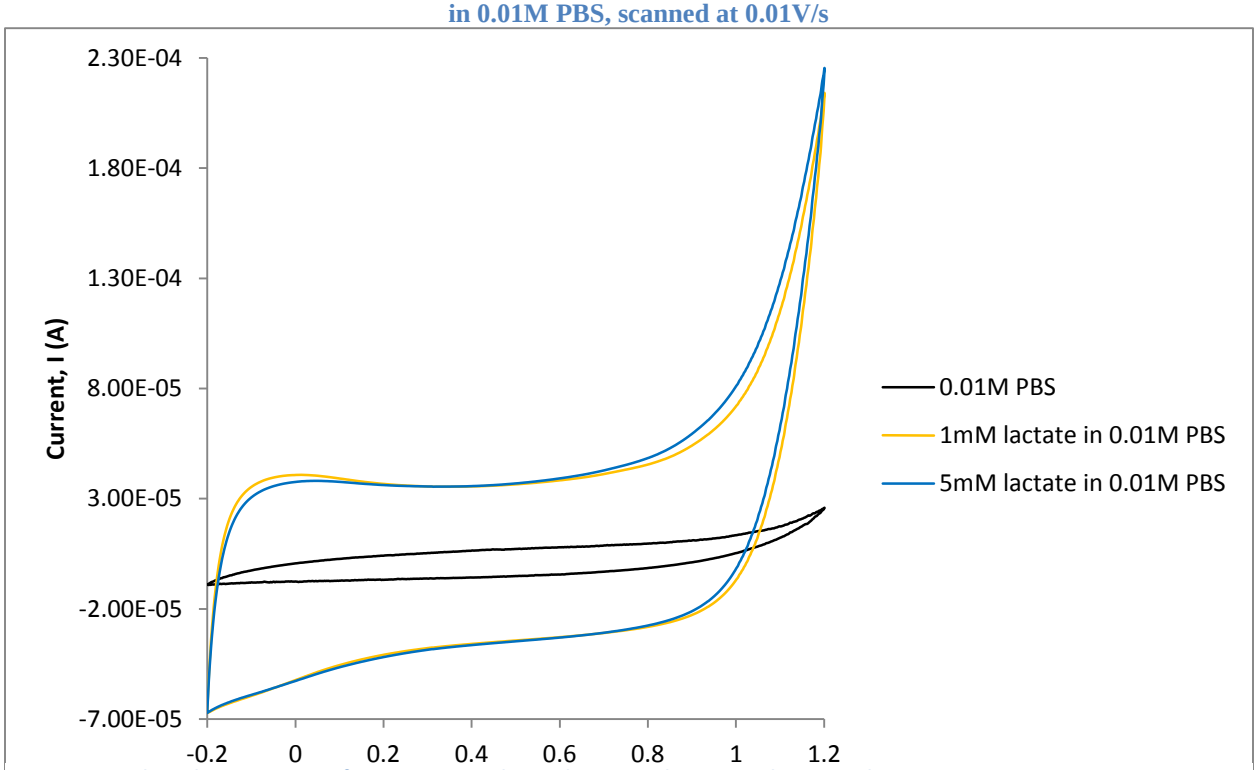

Figure 48. Cyclic voltammogram of GC-MWCNTs electrode #1 in solutions with various lactate concentrations in 0.01M PBS, scanned at 0.03V/s

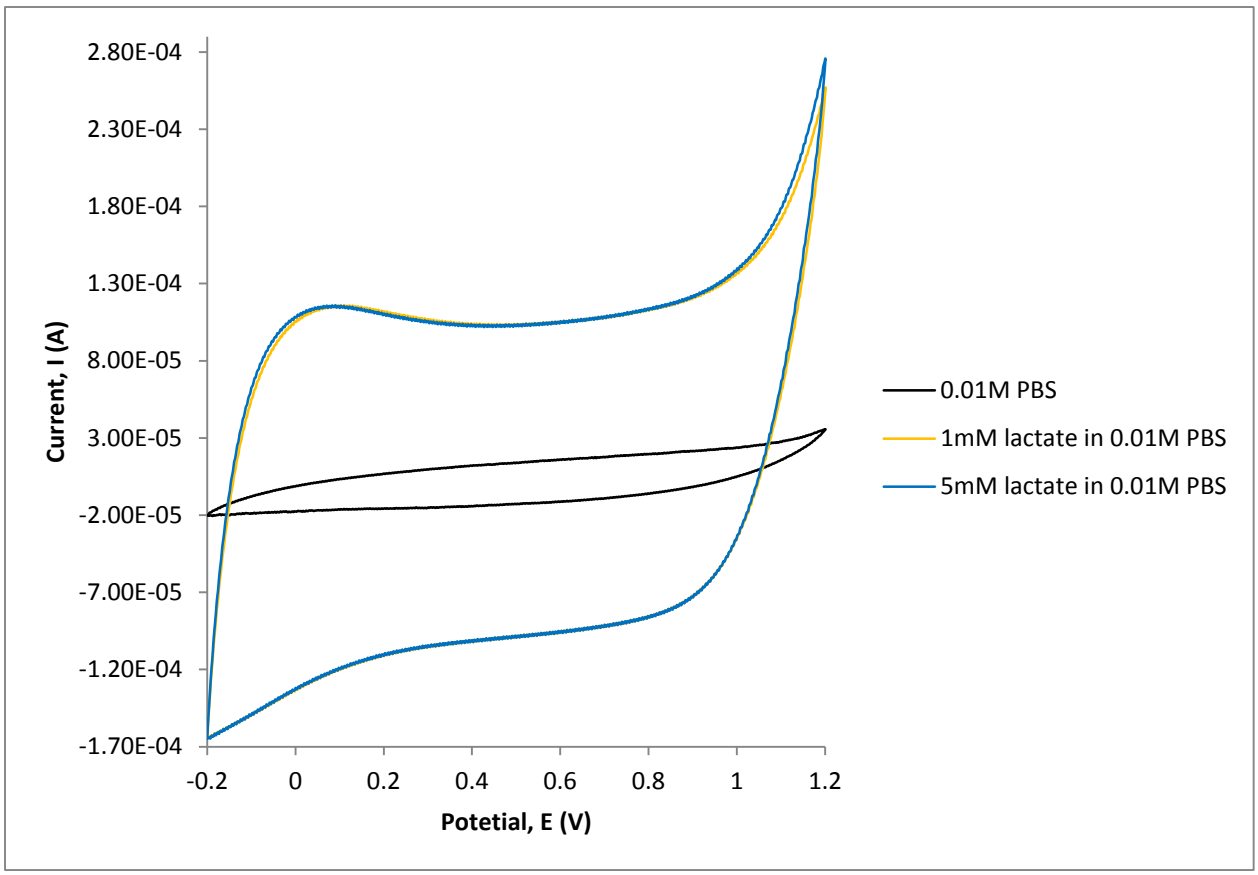

Figure 50. Cyclic voltammogram of GC-MWCNTs electrode #1 in solutions with various lactate concentrations in 0.01M PBS, scanned at 0.05V/s

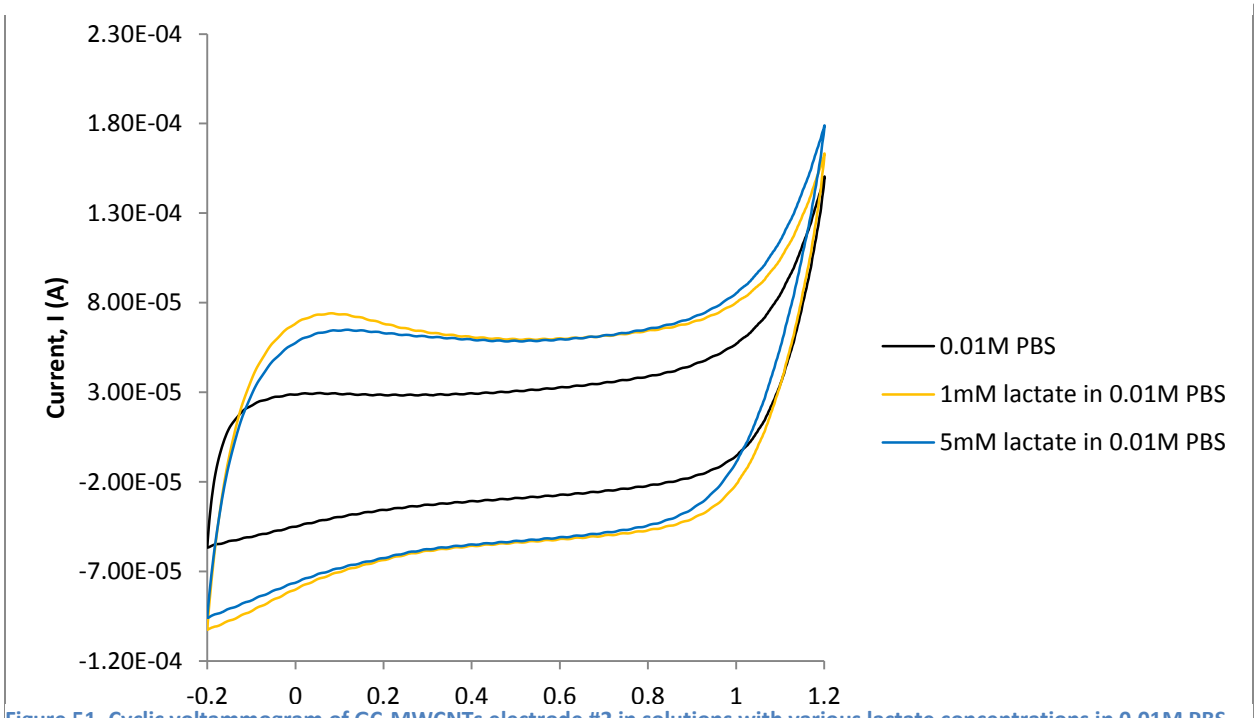

Figure 51. Cyclic voltammogram of GC-MWCNTs electrode #2 in solutions with various lactate concentrations in 0.01M PBS, scanned at 0.05V/s

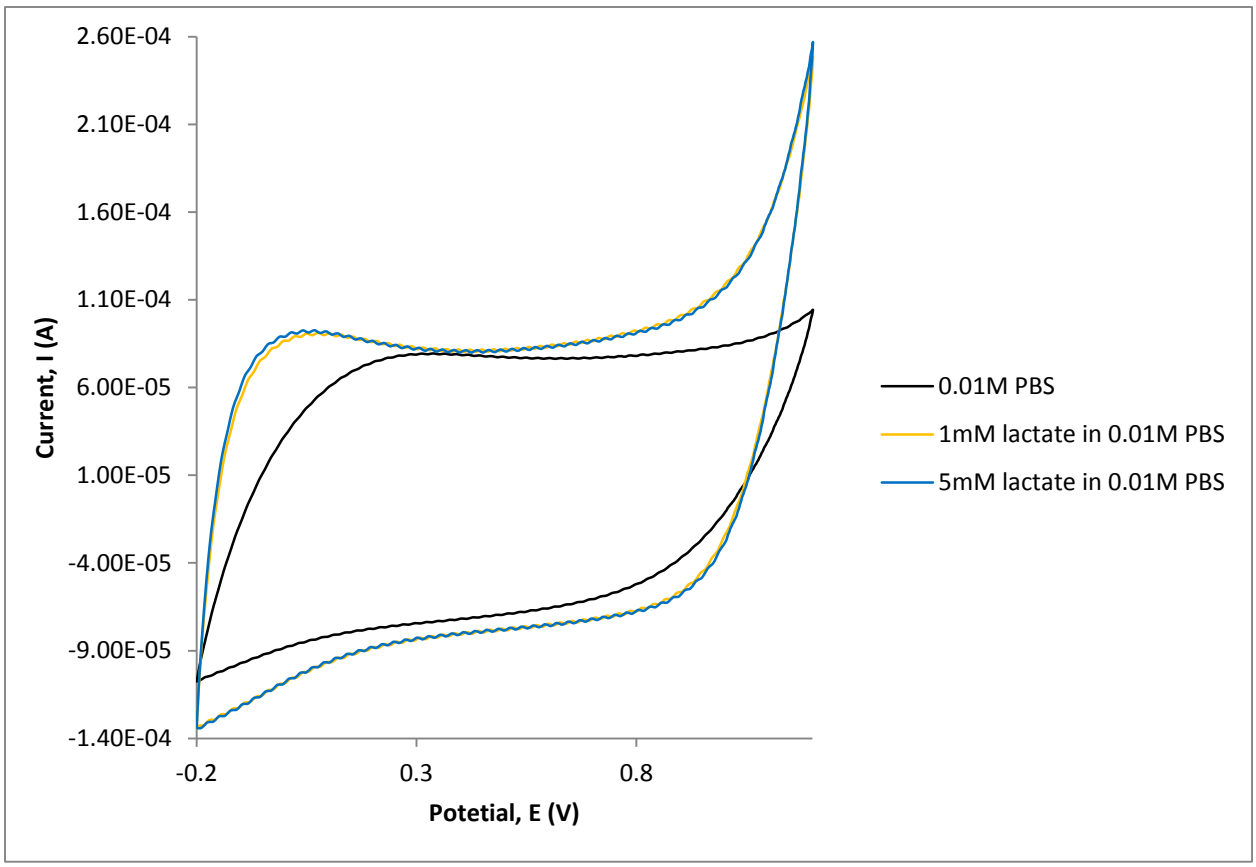

Figure 53. Cyclic voltammogram of GC-MWCNTs electrode #1 in solutions with various lactate concentrations in 0.01M PBS, scanned at 0.07V/s

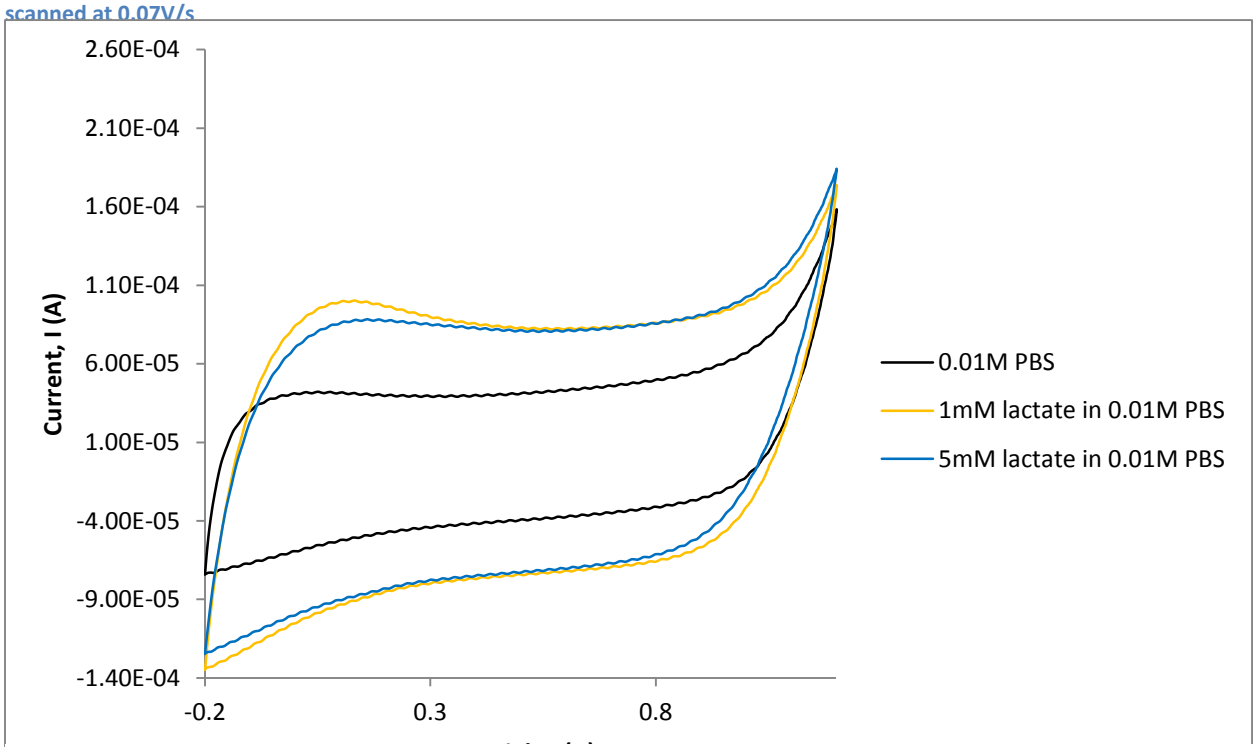

Figure 52. Cyclic voltammogram of GC-MWCNTs electrode #2 in solutions with various lactate concentrations in 0.01M PBS, scanned at 0.07V/s

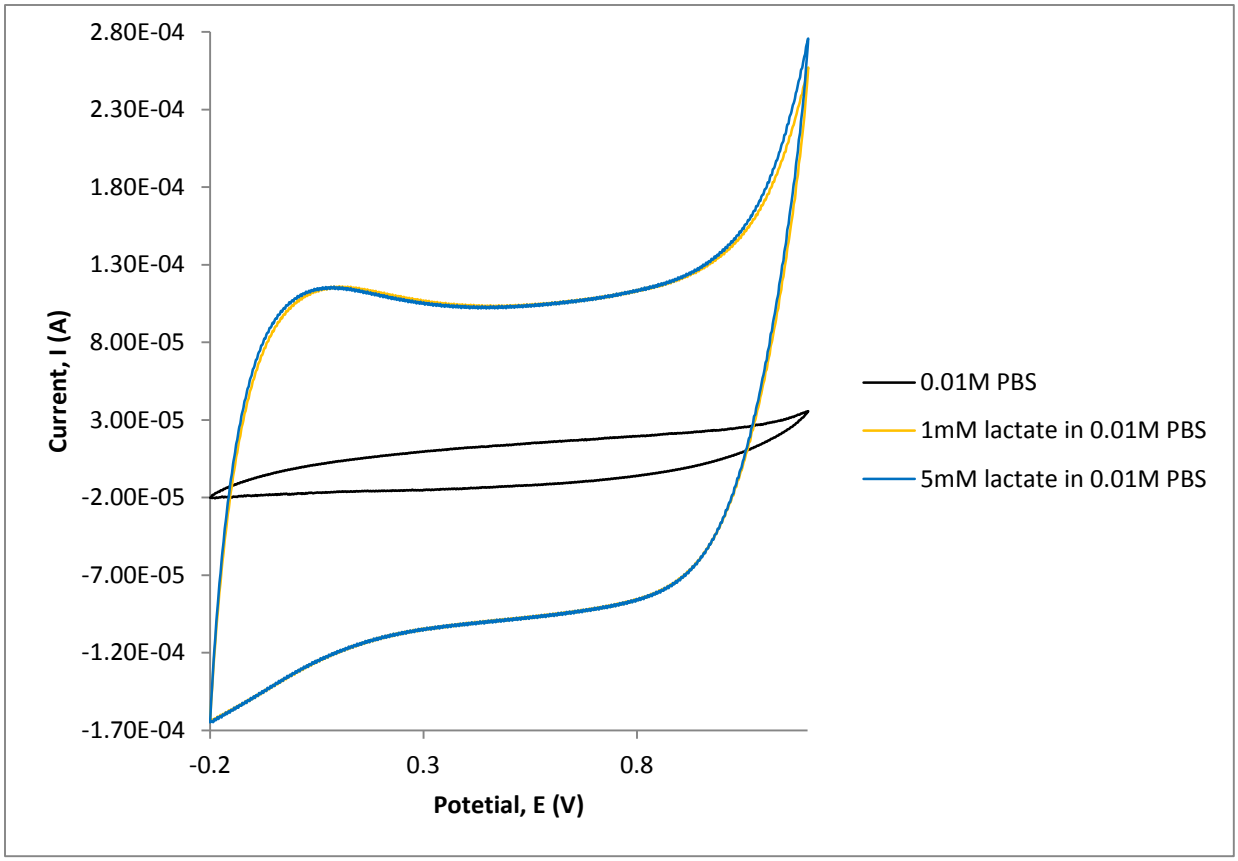

Figure 55. Cyclic voltammogram of GC-MWCNTs electrode #1 in solutions with various lactate concentrations in 0.01M PBS, scanned at 0.09V/s

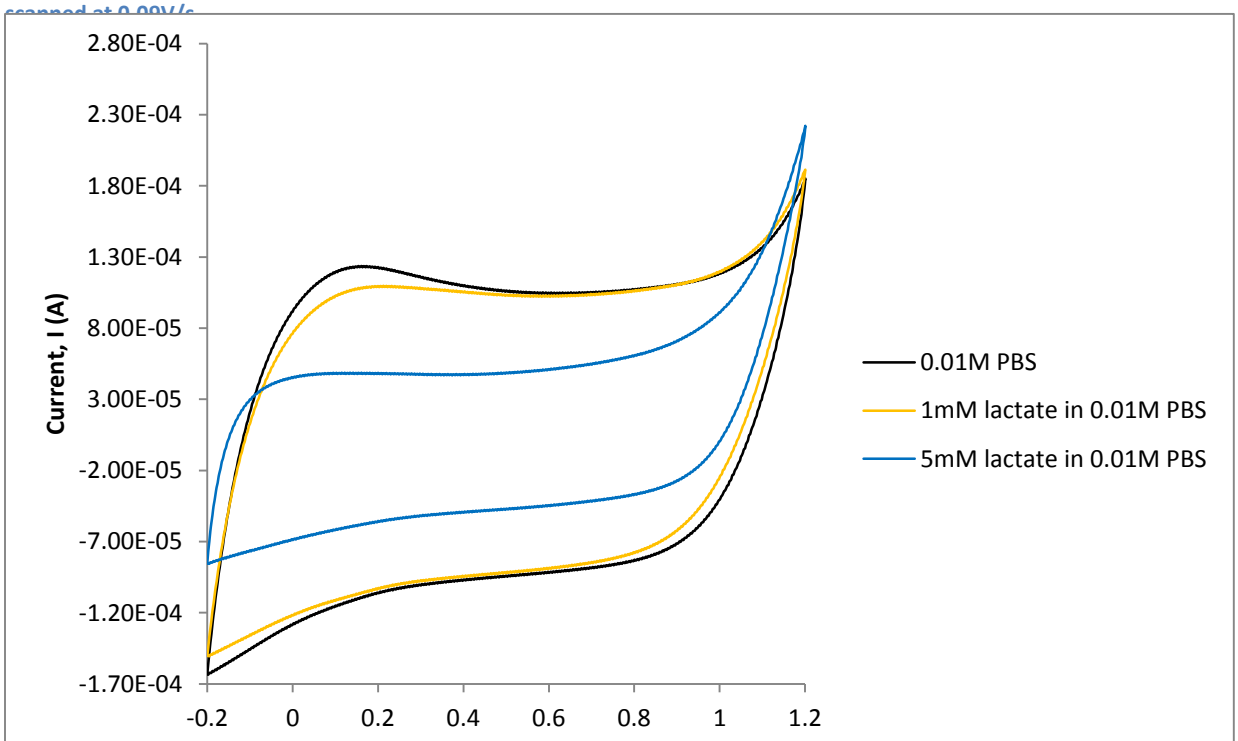

Figure 54. Cyclic voltammogram of GC-MWCNTs electrode #2 in solutions with various lactate concentrations in 0.01M PBS, scanned at 0.09V/s

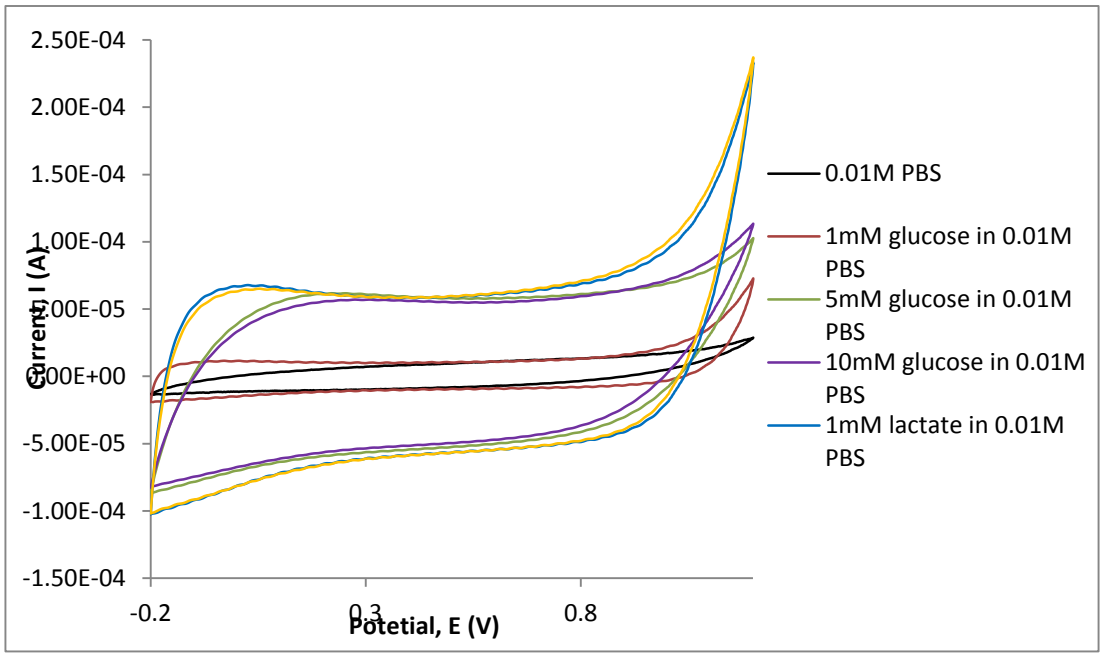

Figure 57. Cyclic voltammogram of GC-MWCNTs electrode #1 in solutions with various glucose and lactate concentrations, scanned at 0.05V/s

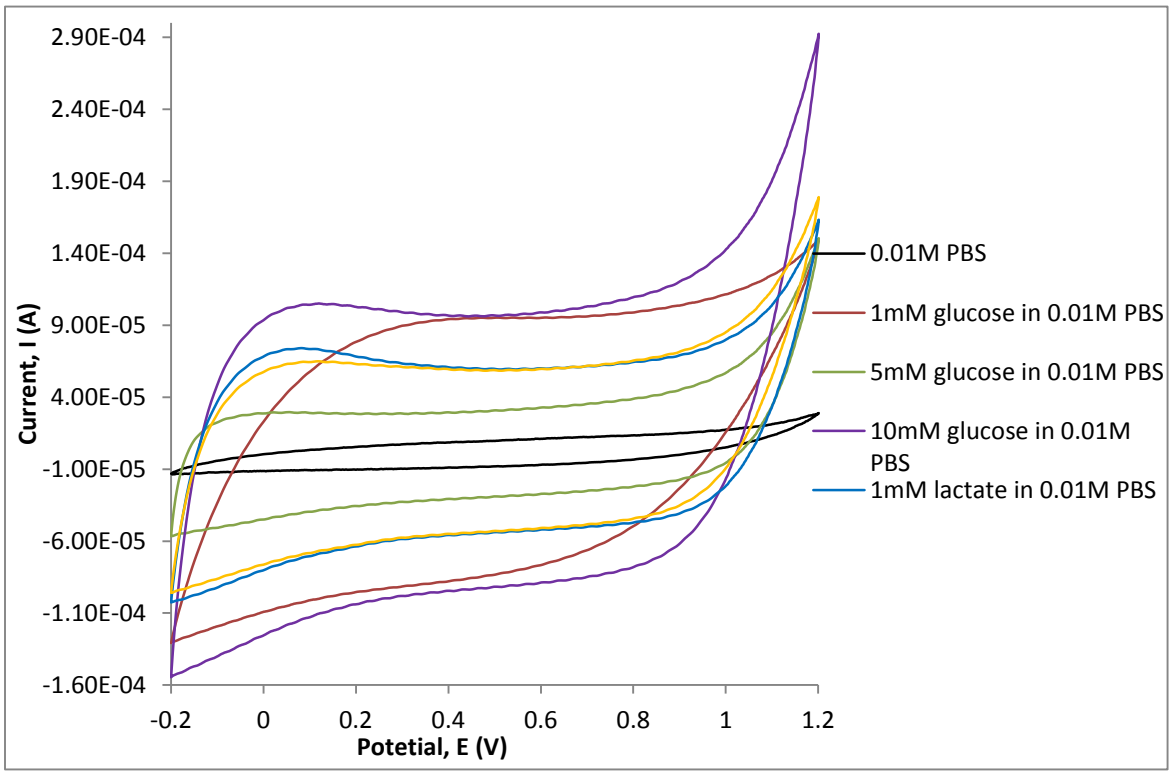

Figure 56. Cyclic voltammogram of GC-MWCNTs electrode #2 in solutions with various glucose and lactate concentrations, scanned at 0.05V/s

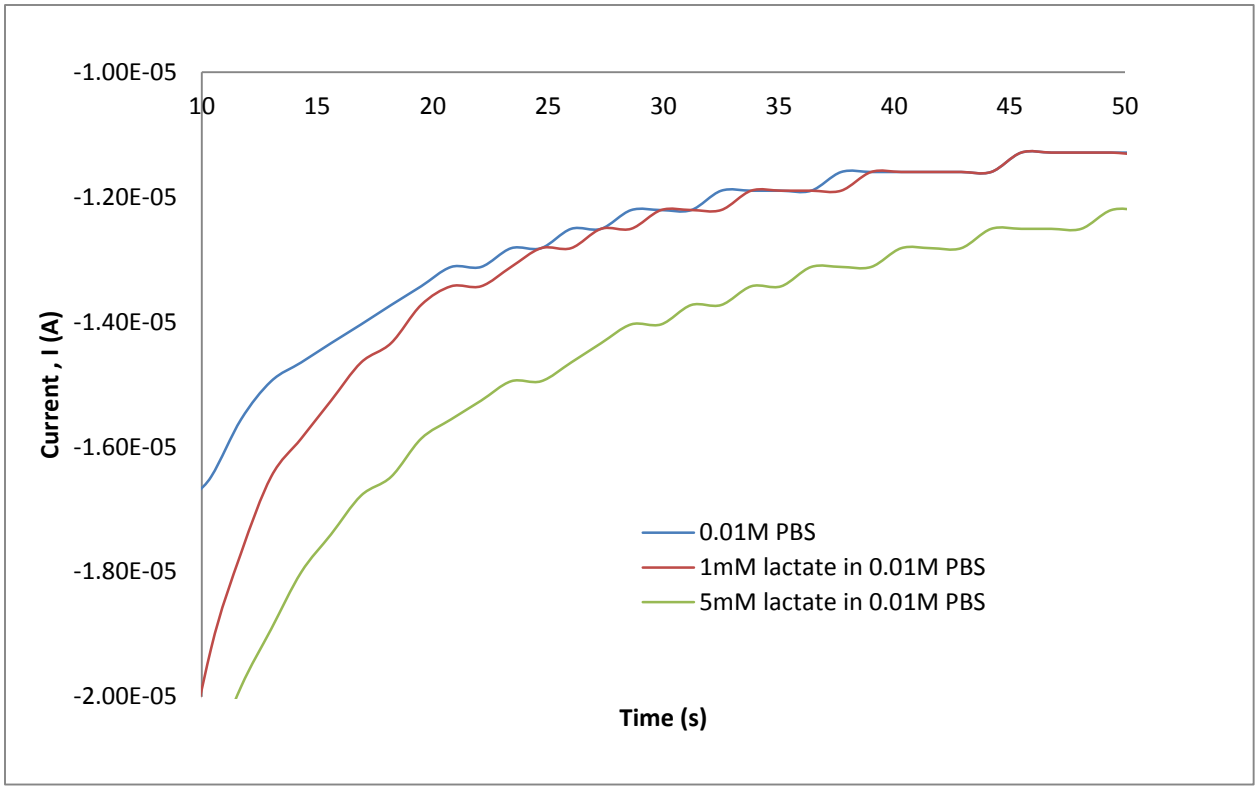

Figure 59. Amperometry of GC-MWCNTs electrode #1 in solutions with various glucose concentrations in 0.01M PBS

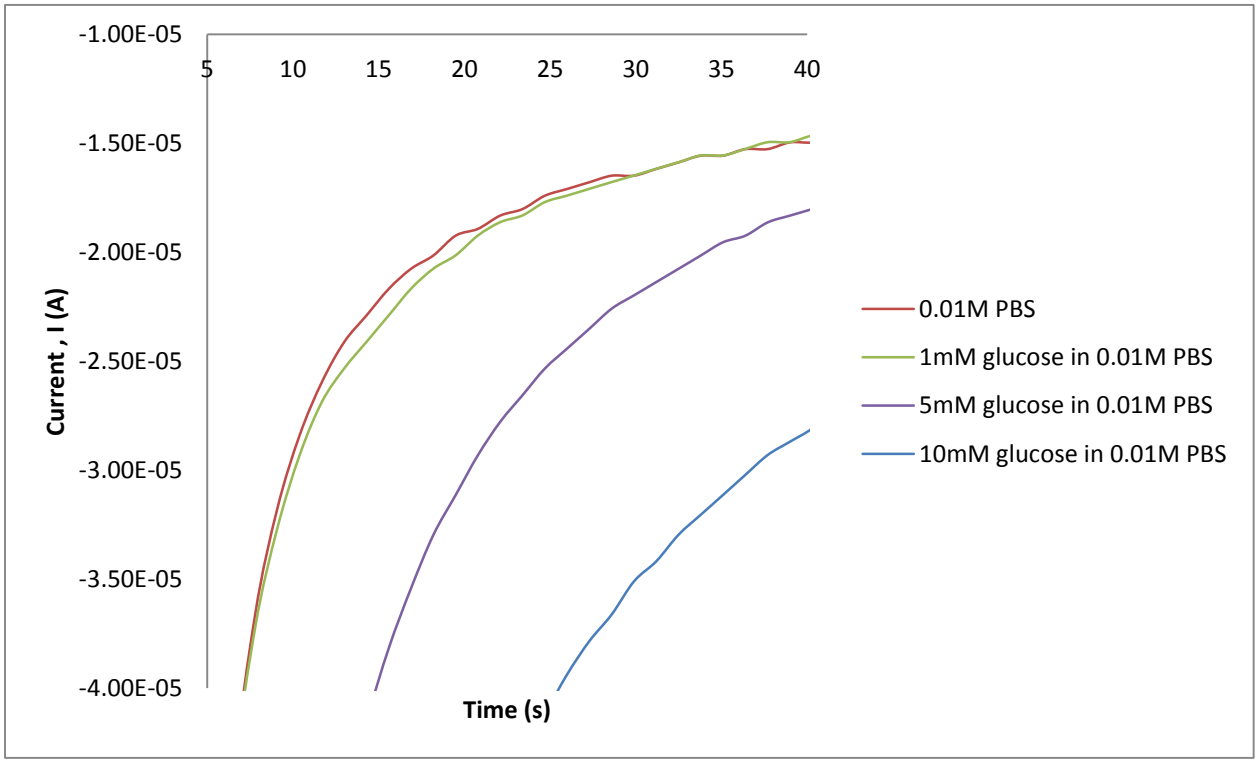

Figure 58. Amperometry of GC-MWCNTs electrode #2 in solutions with various lactate concentrations in 0.01M PBS

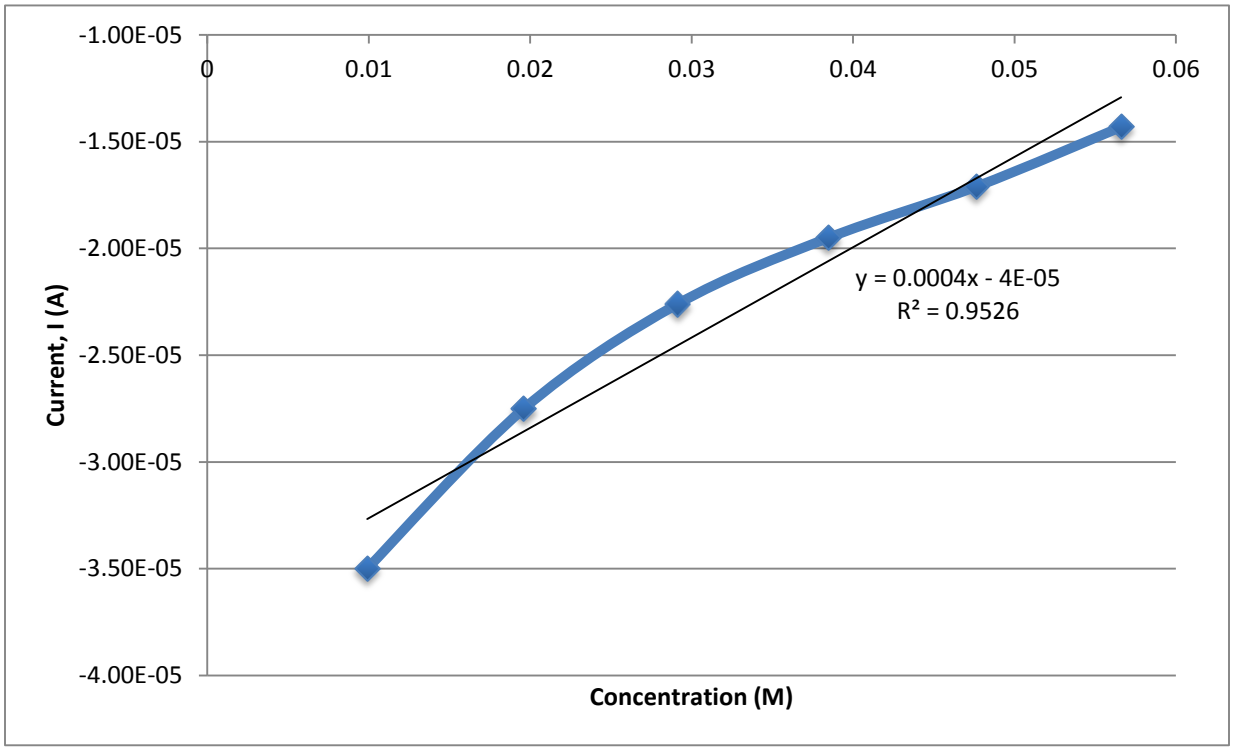

Figure 61. Correlation between current and concentration

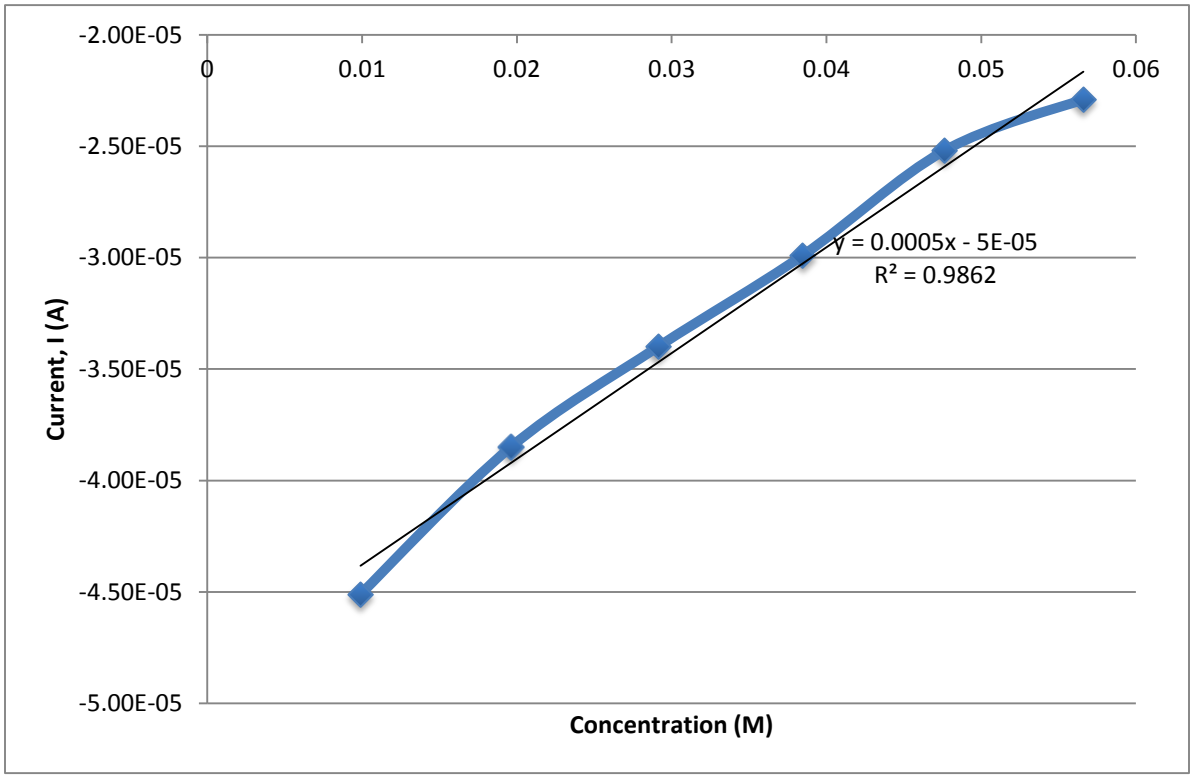

Figure 60. Correlation between current and concentration obtained from data from Figure 44

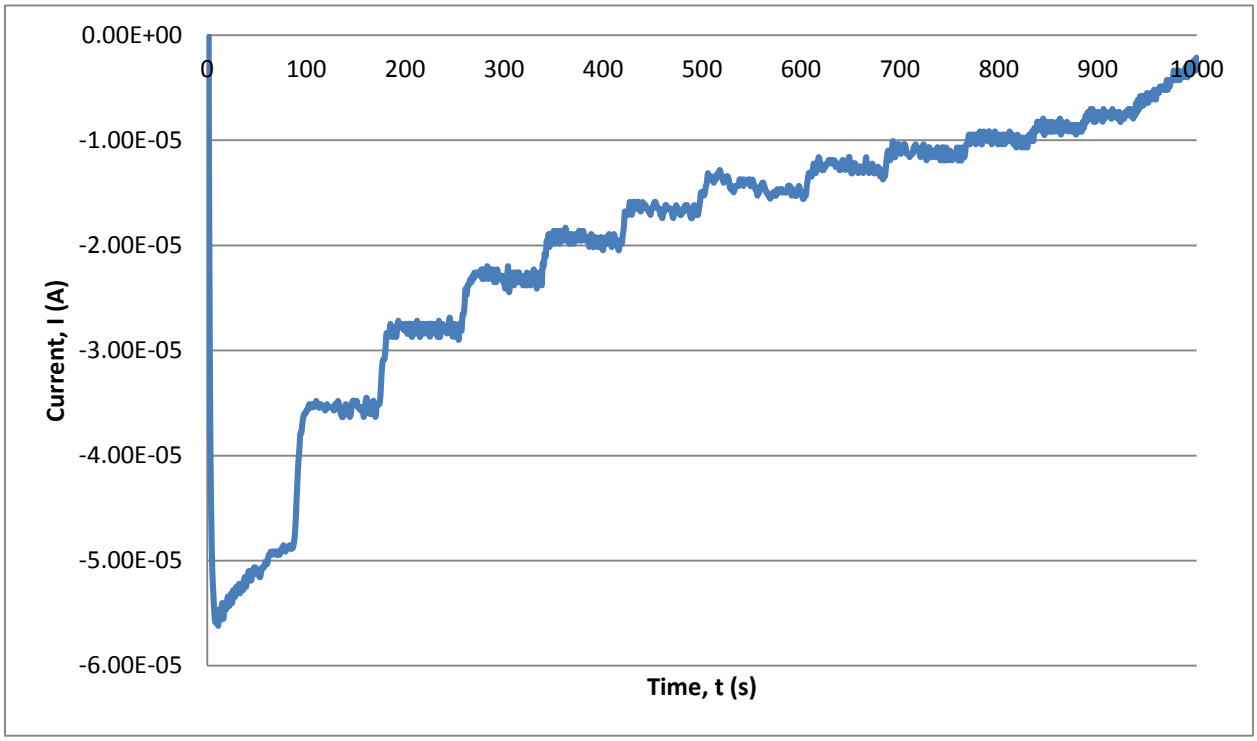

Figure 63. Amperometry of GCE #1 in 0.01M PBS, then 0.1mL of 1M glucose in 0.01M PBS is gradually added to the solution, trial 1

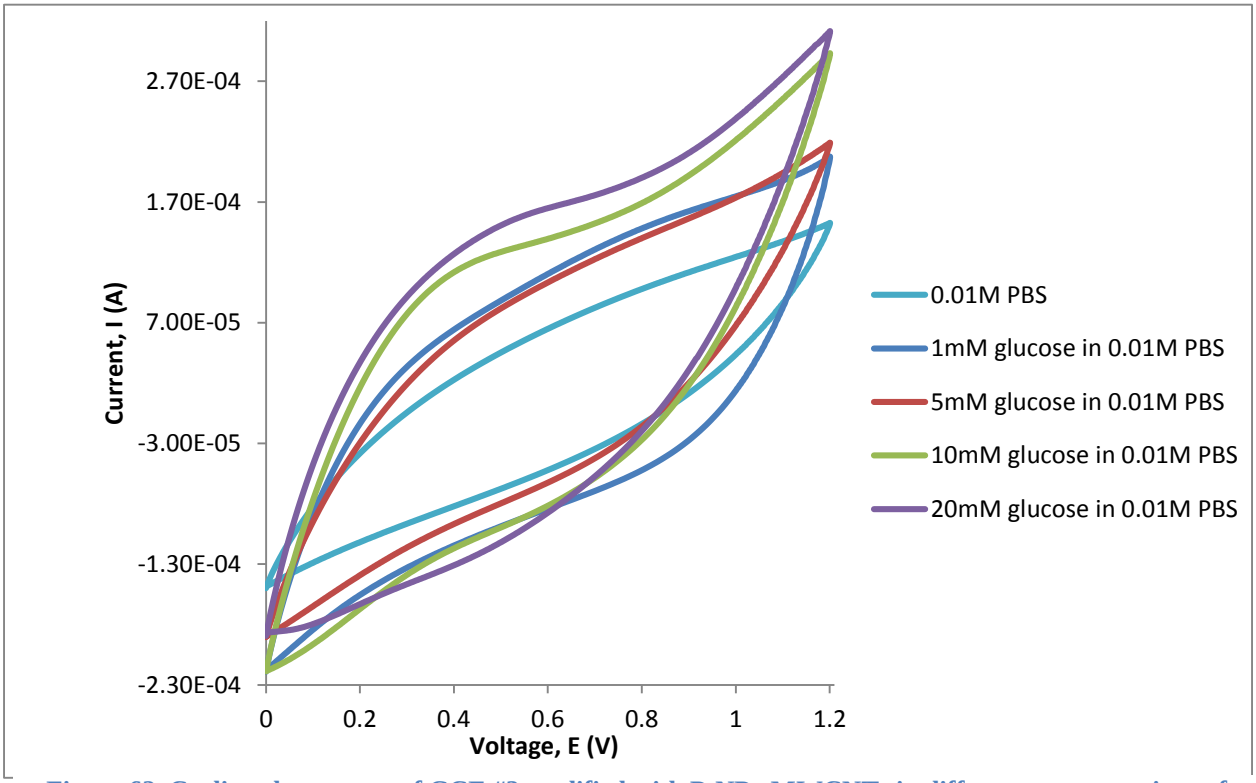

Figure 62. Cyclic voltammetry of GCE #3 modified with PtNPs-MWCNTs in different concentrations of glucose in 0.01M PBS

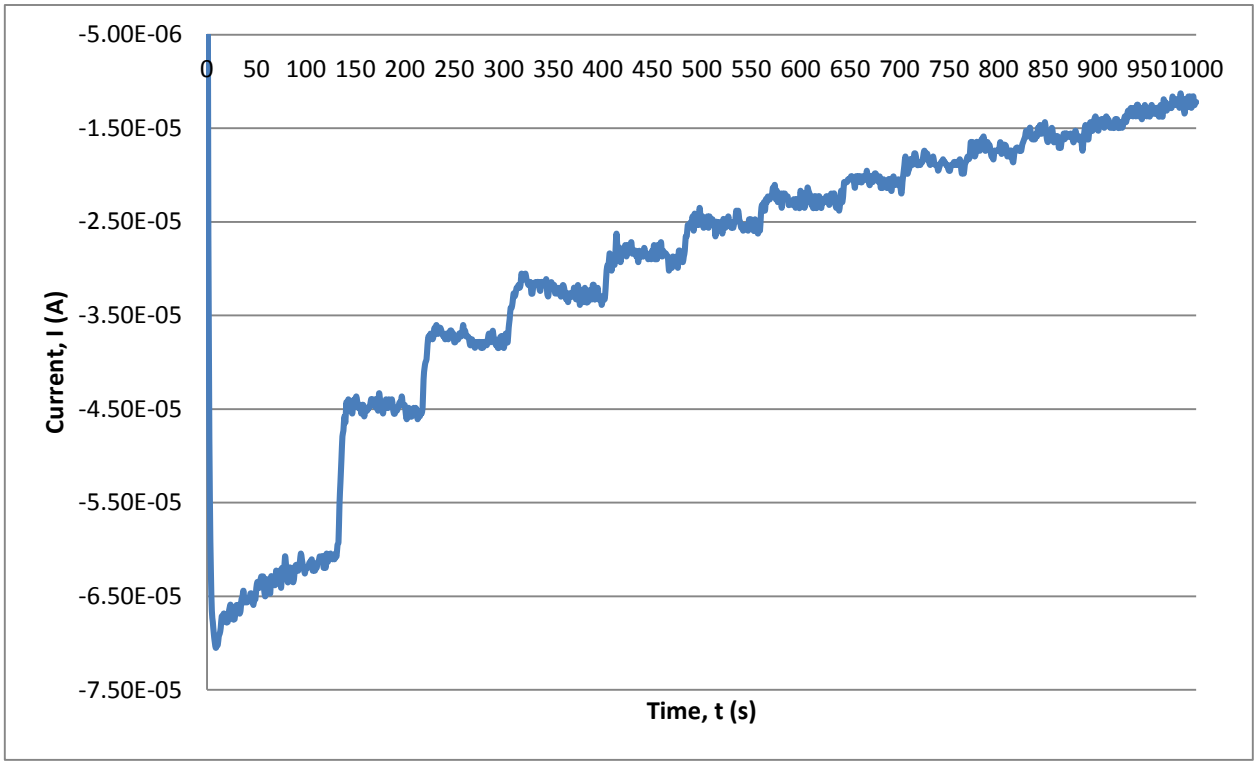

Figure 64. Amperometry of GCE #1 in 0.01M PBS, then 0.1mL of 1M glucose in 0.01M PBS is gradually added to the solution, trial 1

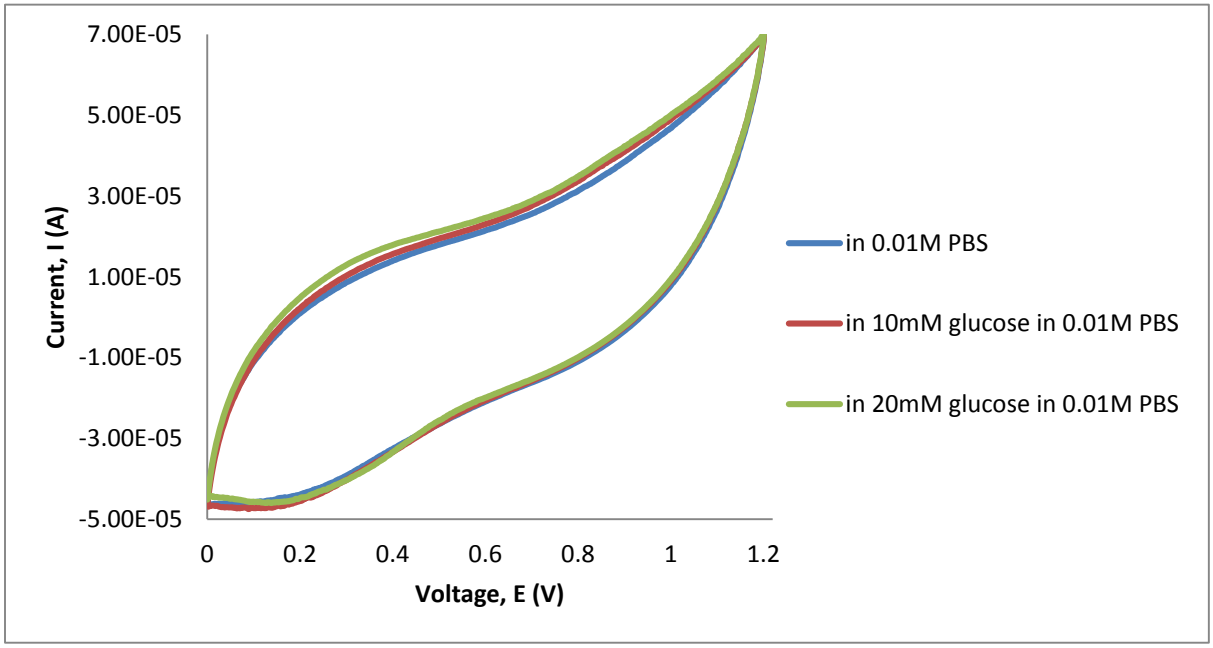

Figure 65. Cyclic voltammetry of GCE #1 with two distinct layers in other electrolytes after chemical deposition of Pt nanoparticles is performed

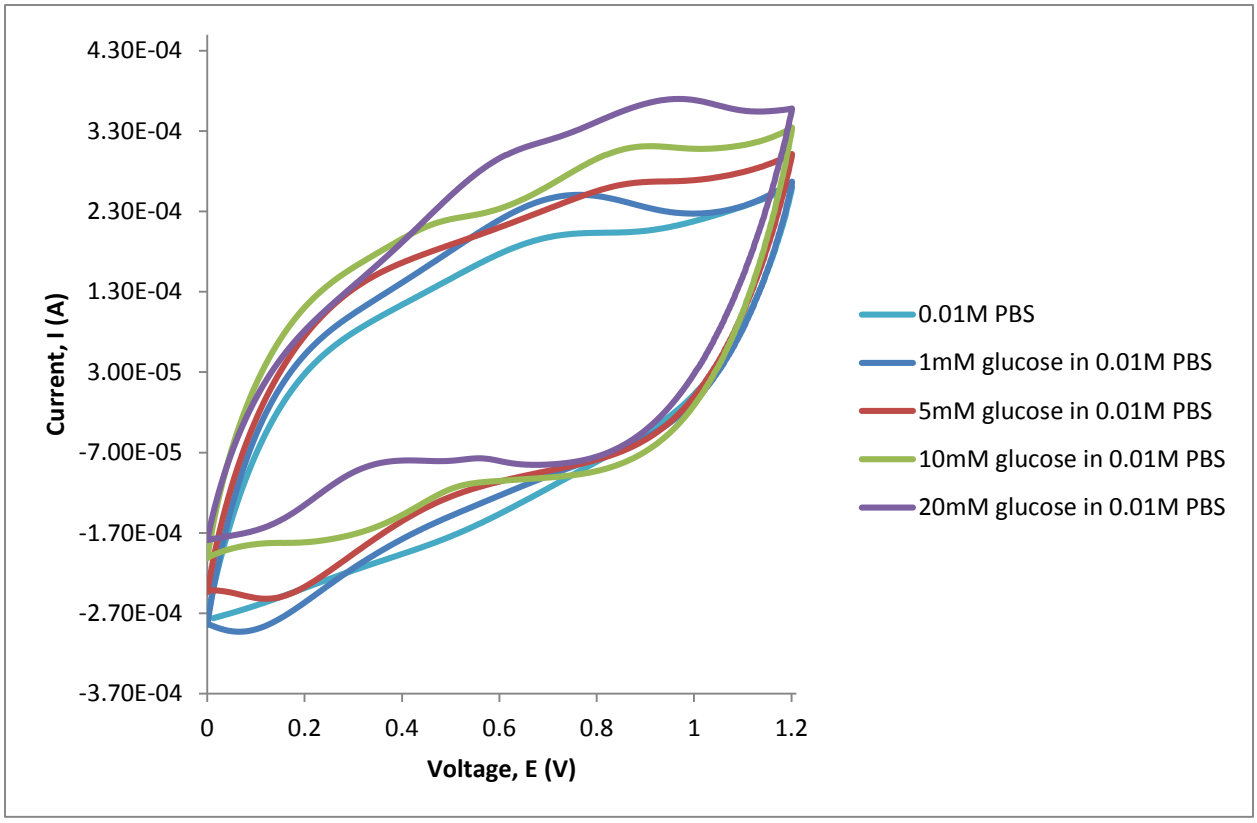

Figure 67. Cyclic voltammetry of GCE #1 modified with PtNPs-MWCNTs in different concentrations of glucose in 0.01M PBS, trial 1

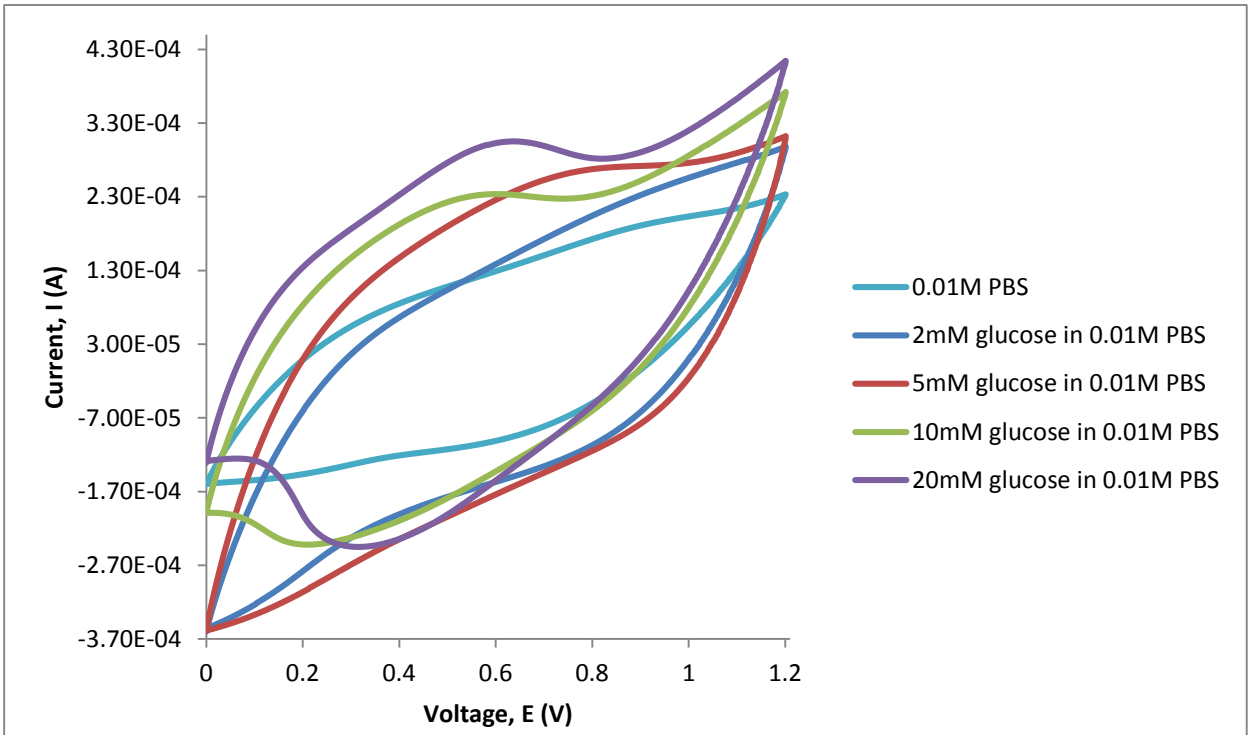

Figure 66. Cyclic voltammetry of GCE #1 modified with PtNPs-MWCNTs in different concentrations of glucose in 0.01M PBS, trial 2